The Abdus Salam
International Centre for Theoretical Physics

United Nations
Educational, Scientific and
Cultural Organization

IAEA
International Atomic Energy Agency

1936-46

Advanced School on Synchrotron and Free Electron Laser Sources and their Multidisciplinary Applications

7 - 25 April 2008

Andrea Locatelli
Elettra, Sincrotrone Trieste

Strada Costiera 11, 34014 Trieste, Italy - Tel. +39 040 2240 111; Fax +39 040 224 163 - sci_info@ictp.it, www.ictp.it

Methodology of LEEM-XPEEM and applications

Andrea Locatelli

MOTIVATIONS

Why do we need photoelectron microscopy?

- To combine SPECTROSCOPY and MICROSCOPY to characterise the structural, chemical and magnetic properties of surfaces, interfaces and thin films
- Applications in diverse fields such as surface science, catalysis, material science, magnetism but also geology, soil sciences, biology and medicine.

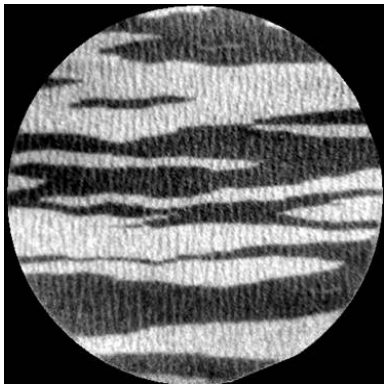

Magnetic state

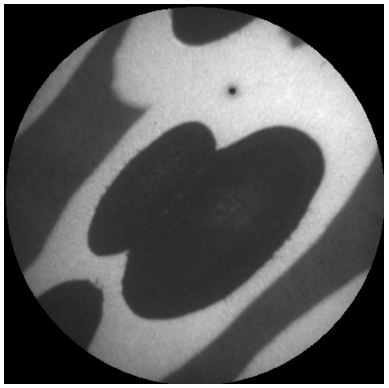

Composition maps

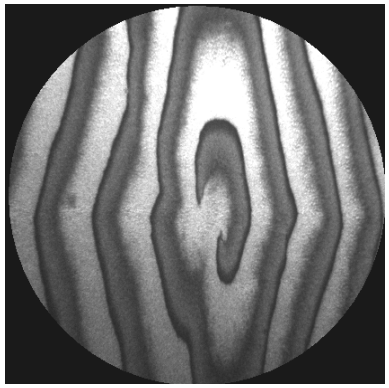

Surface reactions

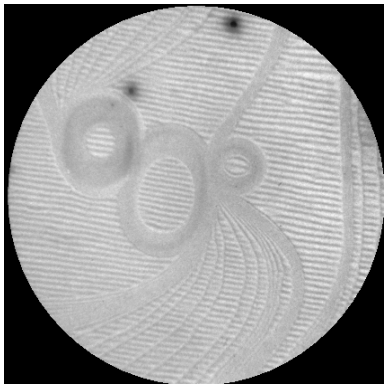

Self-organisation

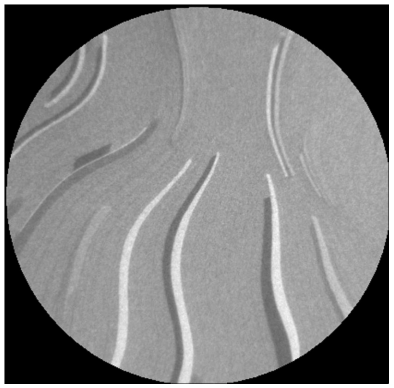

Thin film growth

Application fields

- Materials and surface sciences
  - Magnetism *(magnetic imaging, magnetic dynamics)*
  - Catalysis *(oxide growth, transport phenomena)*
  - Semiconductors *(electro-migration)*
  - Nanostructures *("there is a lot of room at the bottom",…,„SAM, self-organisation, ….)*
- Biological and medical sciences *(cell in cultures, dynamical process in cells, nano-structural genomics i.e. relation protein cplx. To DNA)*
- Earth and planetary sciences *(geology, micrometeorites, micro-fossiles, inter-planetary dust particles)*
- Environmental and soil sciences *(soil colloids, clays, organics colloids)*
- Archeometry
- New applications …. (quickly developing field!)

Outlook

- Introduction on PEEM and SPEM
- Spectroscopic methods
- Instrumental
- Comparison XPEEM-SPEM
- LEEM
- Chemical imaging
- Magnetic Imaging
- Time resolved Magnetic Imaging

1. SPECTROSCOPIC METHODS

X-ray photoelectron microscopy: methods

- Scanning photo emission electron microscopy (SPEM)

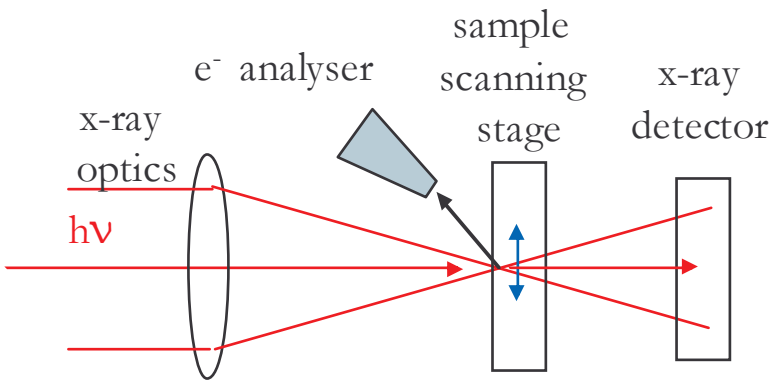

Scanning → indirect imaging
Sequential detection

Lateral resolution is determined by diffractive optics (diffraction limited)
90 nm at state of art

- X-ray photo emission electron microscopy (XPEEM)

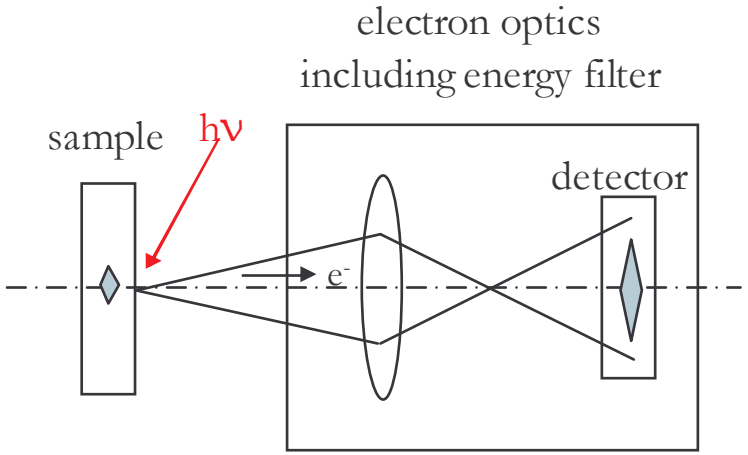

Direct imaging
Parallel detection

Lateral resolution is determined by electron optics (10-50 nm)
With aberration correction: few nm

X-ray photoelectron microscopy: methods

- Scanning photo emission electron microscopy (SPEM)

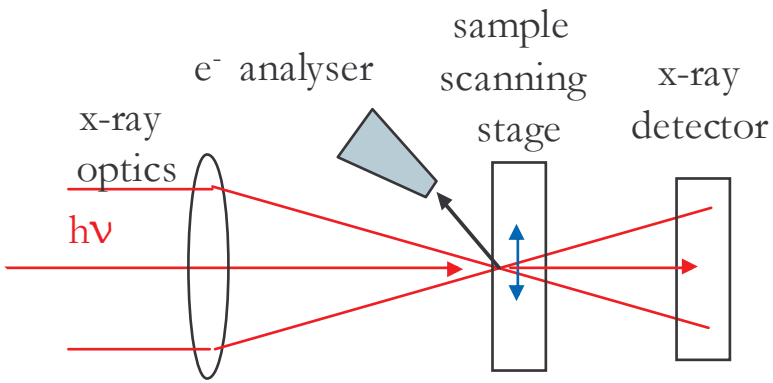

Excellent spectroscopic ability (100 meV or better)

- Combination with TXM
- Limited use in dynamic processes
- Sensitive to out of plane magnetisation
- High vacuum (but high press. SPEM exists!)

- X-ray photo emission electron microscopy (XPEEM)

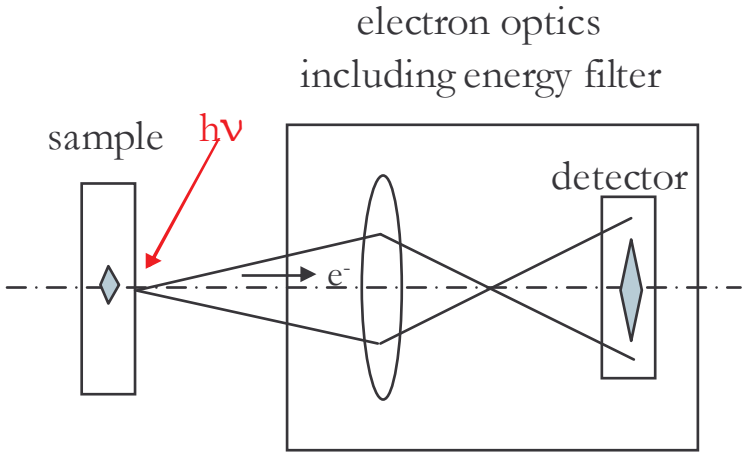

- Intermediate spectroscopic ability (200 meV)
- Combination with LEEM/LEED
- Dynamic processes ok!
- Sensitive in plane magnetisation!
- Vacuum better than $1 \cdot 10^{-5}$ mbar

Lateral resolution performance

- SPEM: Fresnel zone plate

$$\delta_m = \sqrt{\delta_i^2 + \delta_g^2 + \delta_c^2} =$$

$$= \sqrt{(1.22\,\Delta r/m)^2 + \left(\sigma\frac{q}{p}\right)^2 + \left(2r\frac{\Delta E}{E}\right)^2}$$

intrinsic ZP resolution (from Rayleigh criterion) — **demagnified source** — **chromatic aberration**

↓

small outermost zone — **small source size** — **monochromatic beam**

e.g. Δr=100 nm and typical beamline
δ_i=122 nm
δ_g= 30 μm² × 8 mm/3 m=80 nm
δ_c=100 μm × 0.2eV/500eV=40 nm

δ=150 nm, best90 nm, future 50 nm!

- PEEM:
  - Objective lens and contrast aperture determine lateral resolution

Approximate resolution:

$$d = \sqrt{d_{SP}^2 + d_{CH}^2 + d_D^2}$$

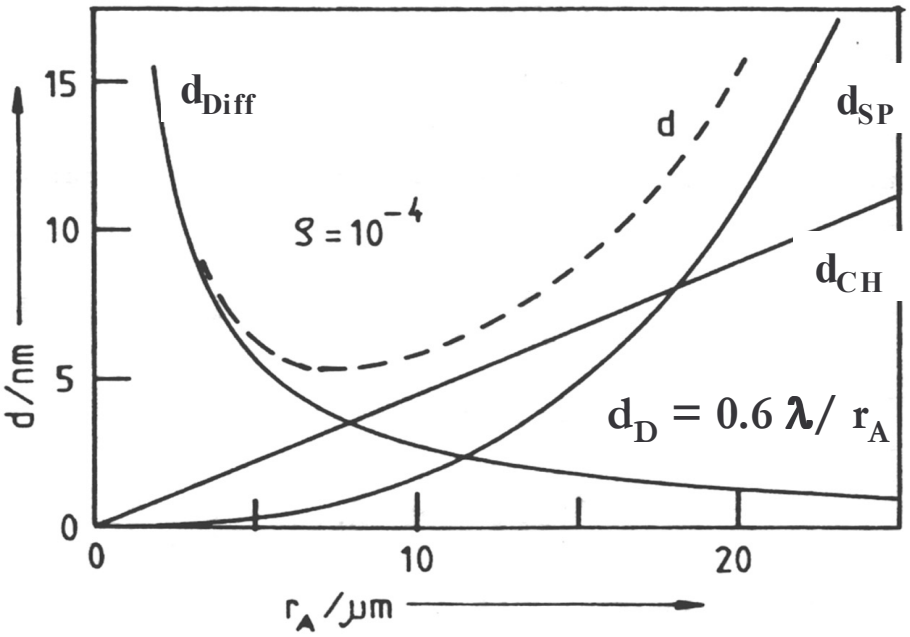

XPEEM performance

Lateral resolution

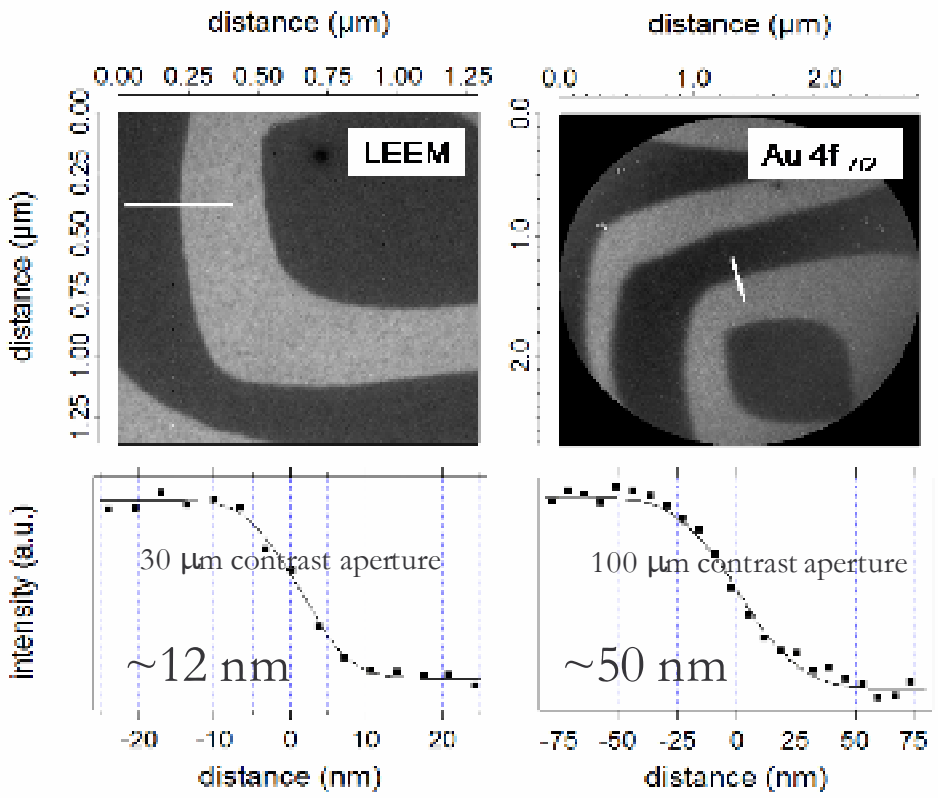

Au/W(110)

Step flow growth at 700 C

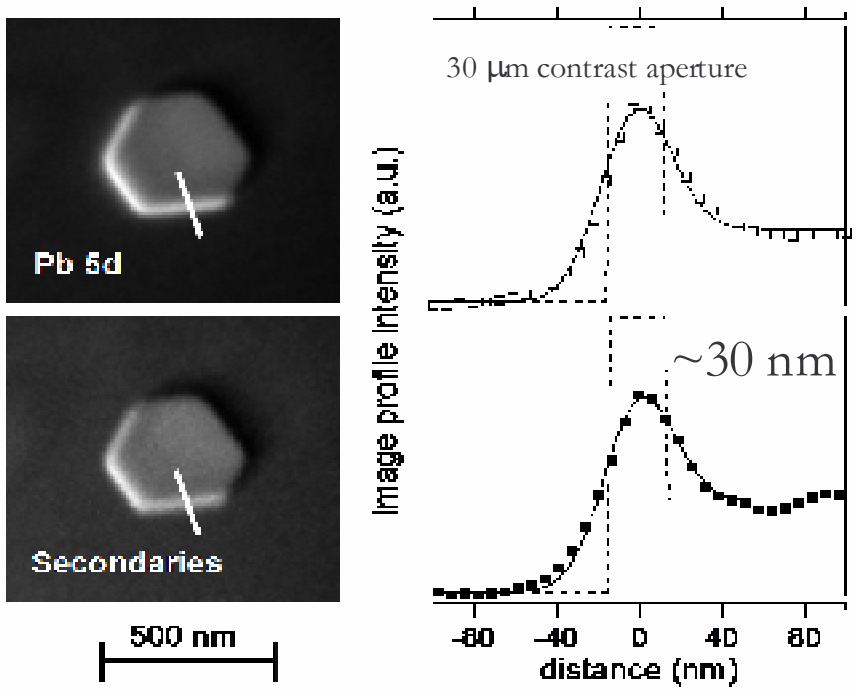

Pb island = wetting layer on W(110)

Latest Results of the SMART microscope @BESSY

Atomic steps on Au(111),
LEEM 16 eV, FoV = 444 nm x 444 nm
(18.09.06)

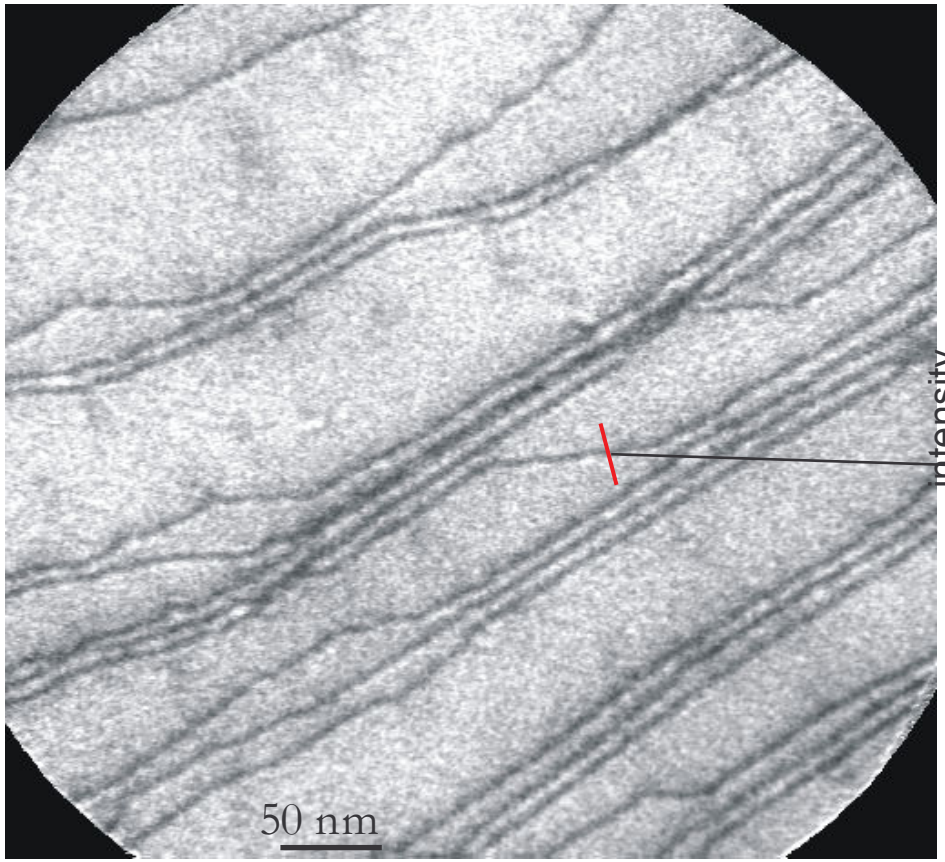

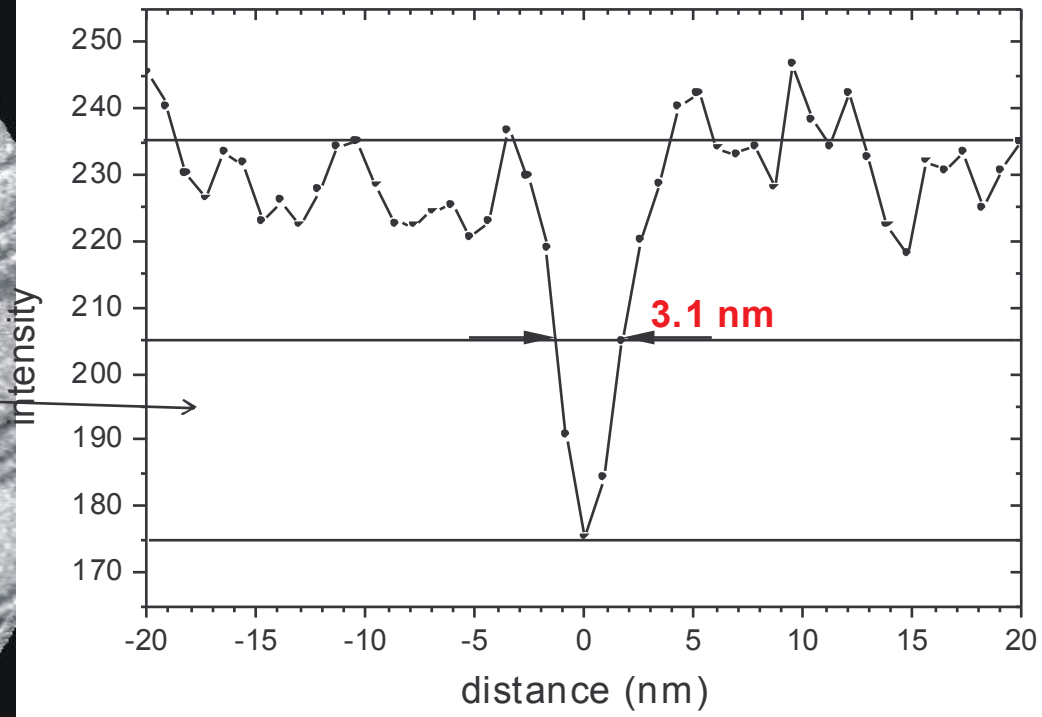

Courtesy of Th. Schmidt et al.; 5th Int. Conf. LEEM/PEEM, Himeji, 15.-19. Oct. 2006

Instrument performance: energy resolution

Energy resolution of SPELEEM @ Elettra

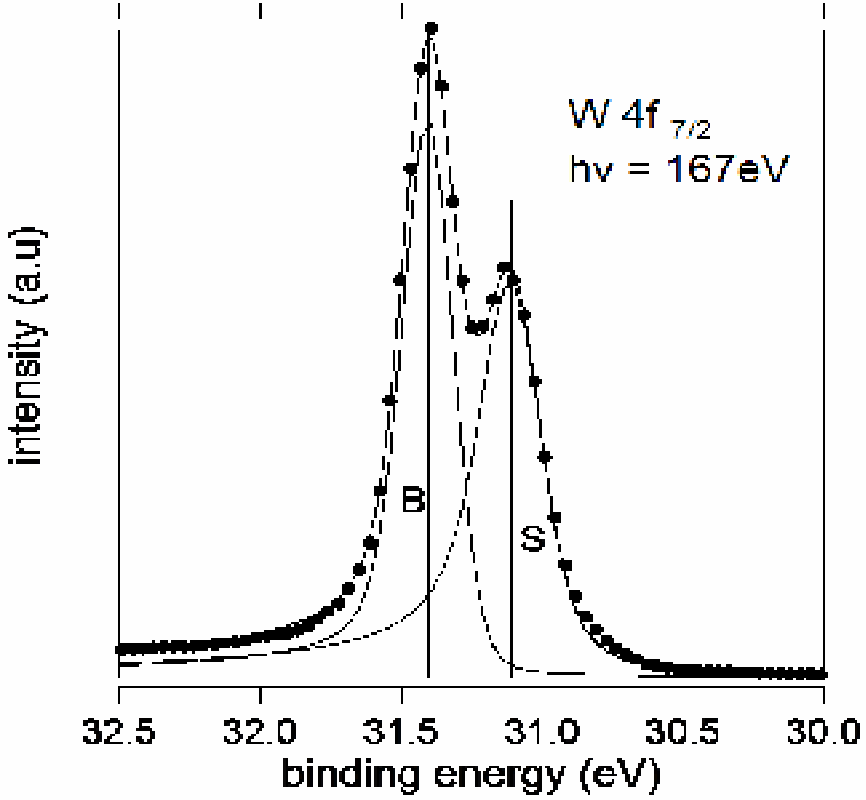

clean W(110)

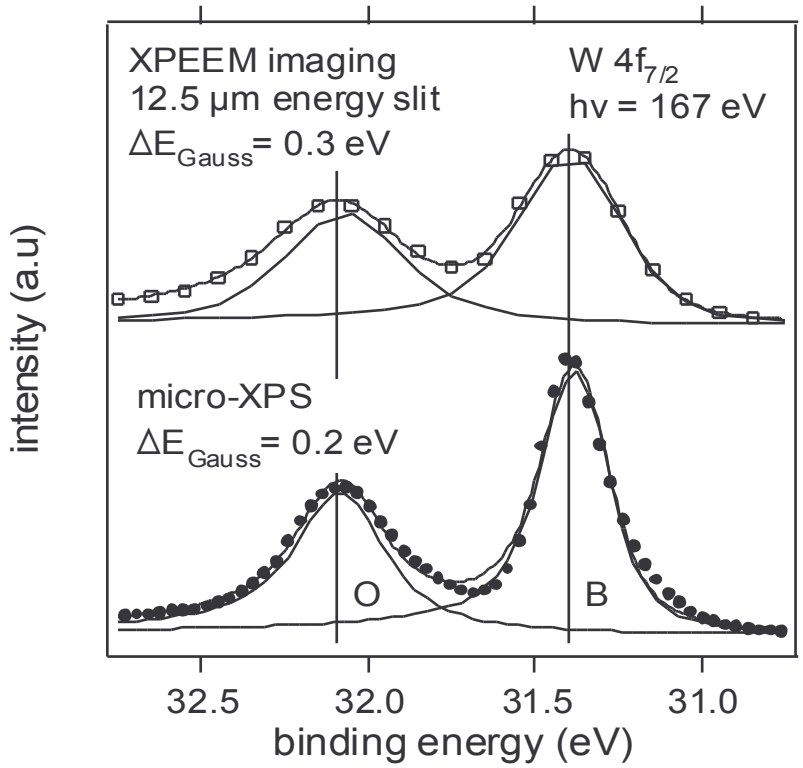

oxidised W(110)

The spectroscopic ability of SPEM is superior to that of PEEM, because the SPEM can exploit the full potential of multi-channel hemispherical energy analyzers developed for laterally averaged x-ray photoelectron spectroscopy.

Spectroscopic modes

1	UV threshold microscopy	photoelectrons	with
2	XPS, UPS:	"	energy
3	Auger Spectroscopy:	Auger electrons AE	filter

4 XAS, XANES, XMCD, XMLD: Secondary electrons SE

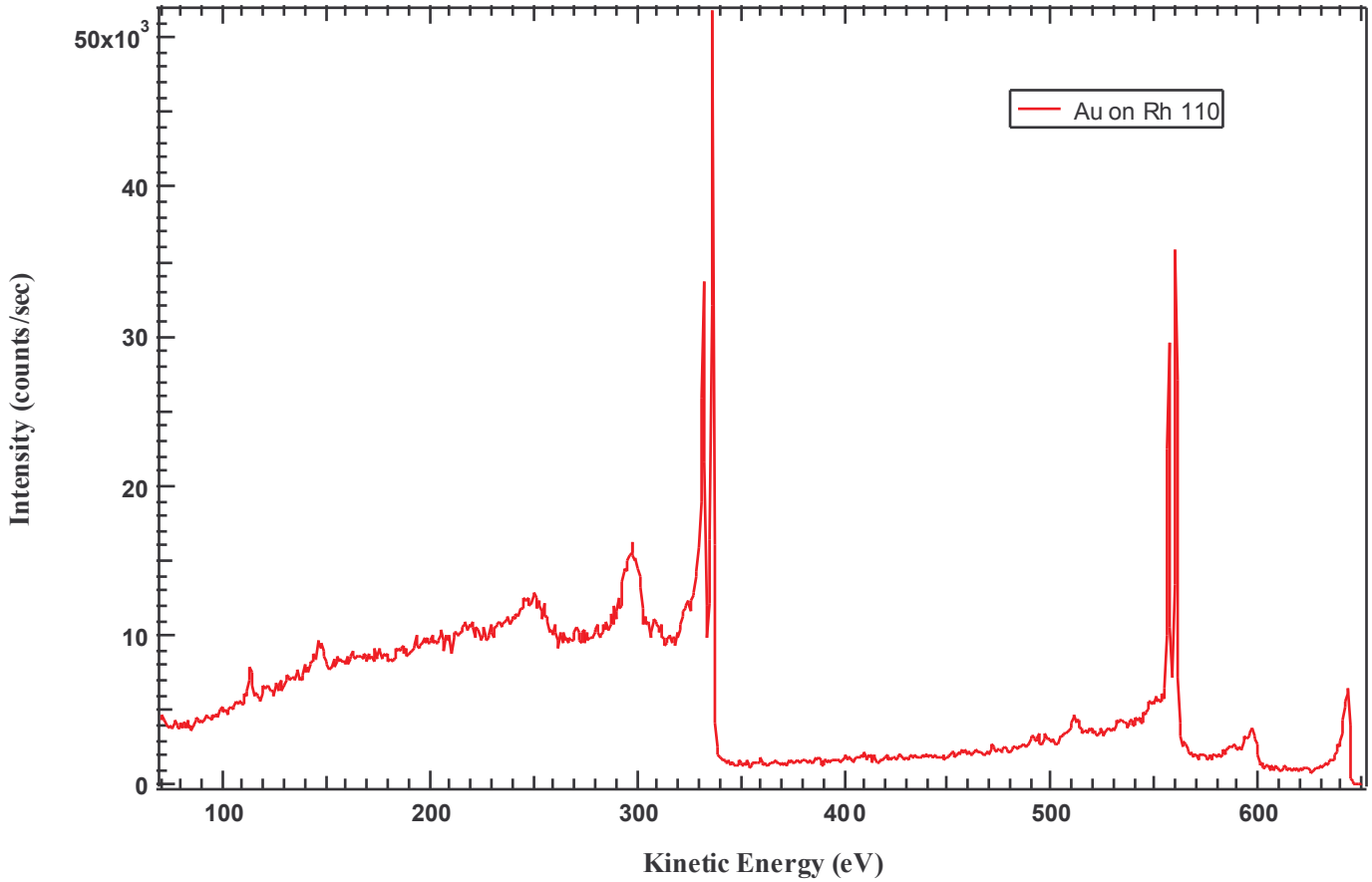

XPEEM: sampling depth

Inelastic mean free path ("universal curve") determines sampling depth

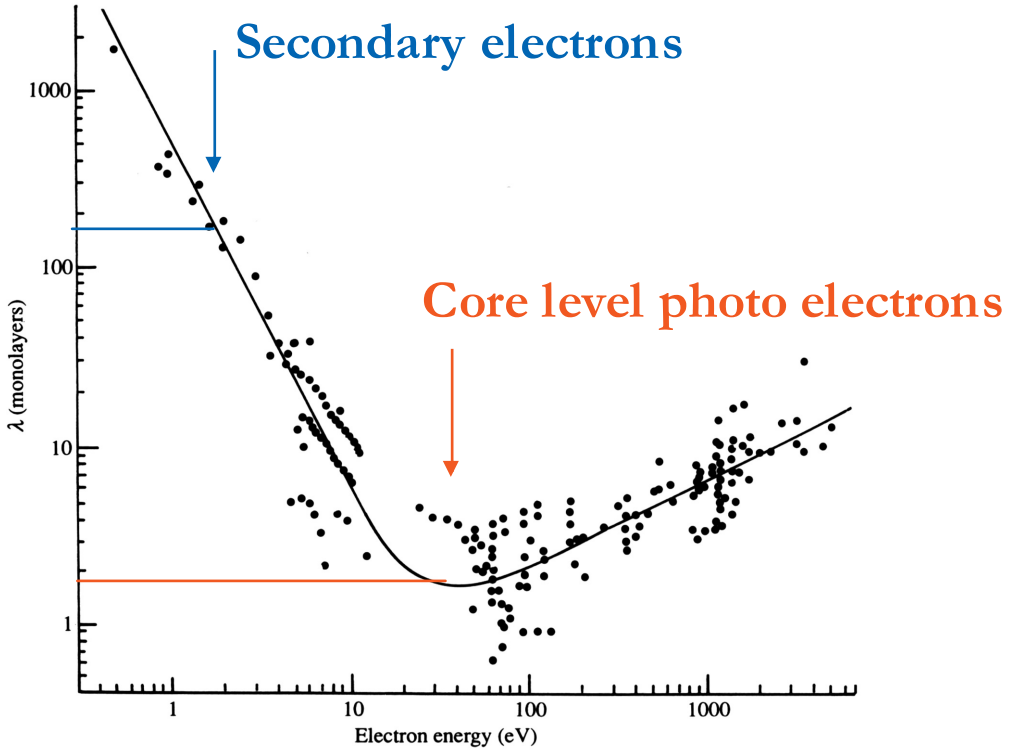

XAS, XANES, XMCD, XMLD can probe thin films and buried interfaces to max. depth of ~5nm

Sensitivity to the topmost surface layers, especially at K. E. 50-150 eV

Principal spectroscopies implemented by SPEM and PEEM

- XAS (XANES, XMLD, XMCD)
  - Elemental sensitivity.
  - Sensitivity to emitter (site location, valence state, bond orientation, nearest-neighbour)
  - Magnetic sensitivity
  - Buried layer and interfaces accessible
  - NO ENERGY FILTER NEEDED IN PEEM

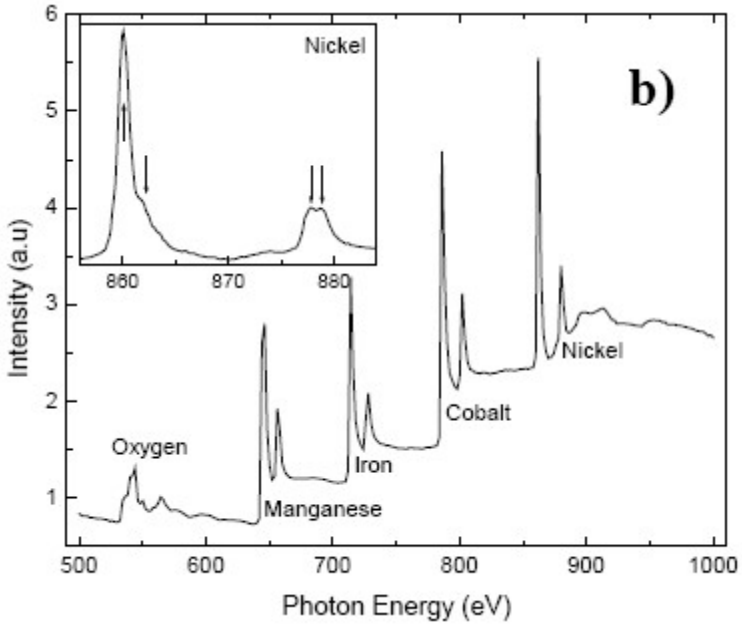

resonances arise from transitions from core levels into unoccupied valence states via excitation processes occurring during the filling of the core holes.

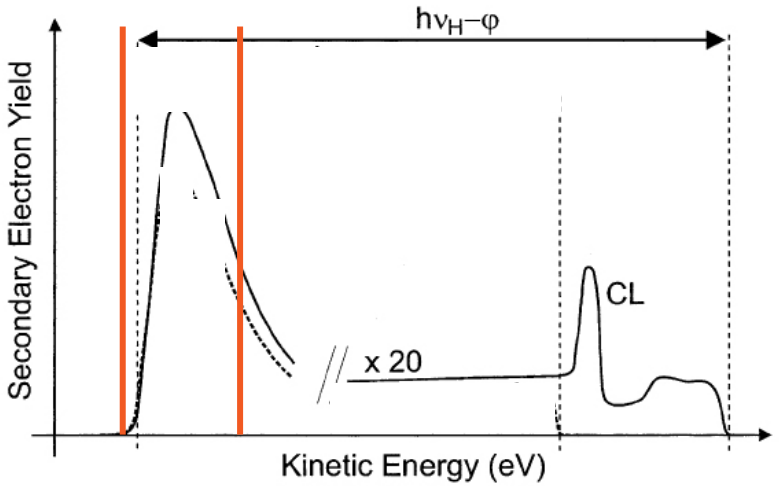

Principal spectroscopies implemented by SPEM and PEEM

- XPS and UPS
  - Elemental and chemical sensitivity, surface core level shifts.
  - Valence band: LOCAL electronic structure (micro-ARPES);
  - Sensitivity to local structure (micro-XPD).
  - High surface sensitivity
  - Energy filter needed in PEEM

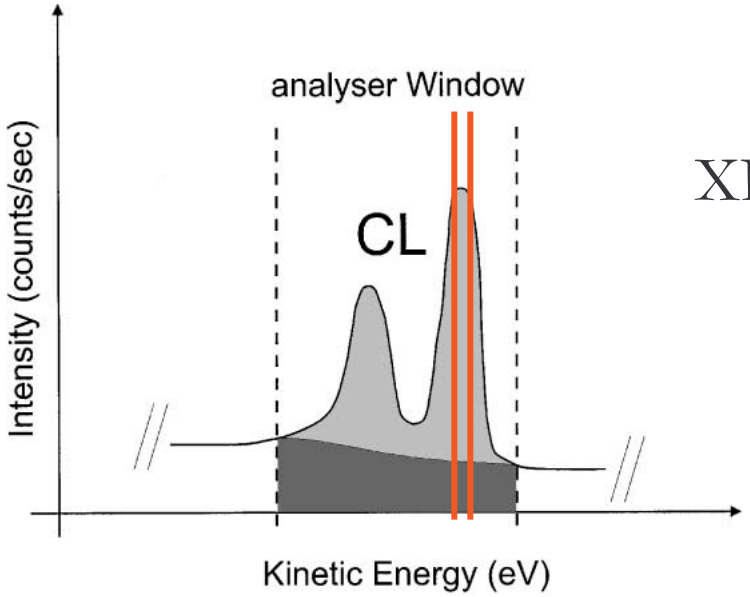

XPS mode: hν const
hν in / e^- out

Reviews on spectromicroscopy

- [1.1] Gunther S, Kaulich B, Gregoratti L, Kiskinova M 2002 *Prog. Surf. Sci.* **70** 187–260.
- [1.2] Bauer E and Schmidt T, 2003 *"Multi-Method High Resolution Surface Analysis with Slow Electrons"* in: High Resolution Imaging and Spectroscopy of Materials, Eds. Ernst F. and Ruehle M. (Springer, Berlin Heidelberg 2003) 363-390.
- [1.3] Bauer E 2001 *J. Electron Spectrosc. Relat. Phenom.* **114-116** 976-987.
- [1.4] Bauer E 2001 J. Phys.: Condens. Matter **13** 11391-11405.

References on XPEEM and LEEM instrumentation

- [2.1] Tonner B P, Harp G R 1988 *Rev. Sci. Instrum.* **59** 853.
- [2.2] Swiech W et al 1997 *J. Electr. Spectr. Relat. Phenom.* **84** 171.
- [2.3] Kleineberg U et al 1999 *J. Electr. Spectr. Relat. Phenom.* **103** 931.
- [2.4] Chmelik J et al 1983 *Optik* **83**, 155.
- [2.5] Cruise D R 1964 *J. Appl. Phys.* **35** 3080.
- [2.6] Bauer E, *1991Ultramicroscopy* **36** 52.
- [2.7] Bauer E, Koziol C, Lilienkamp G, Schmidt Th 1997 *J. Electron Spectrosc. Relat. Phenom.* **84** 201-209.
- [2.8] Schmidt Th, Heun S, Slesak J, Diaz J., Prince KC, Lilienkamp G, Bauer E 1998 *Surf. Rev. Lett.* **5** 1287-1296.
- [2.9] Locatelli A, Abelle L, Mentes T O, Kiskinova M, Bauer E, 2006 *Surf. Interface Anal.* **38**, 1554-1557.

2. COMBINIG XPEEM with LEEM

The SPELEEM

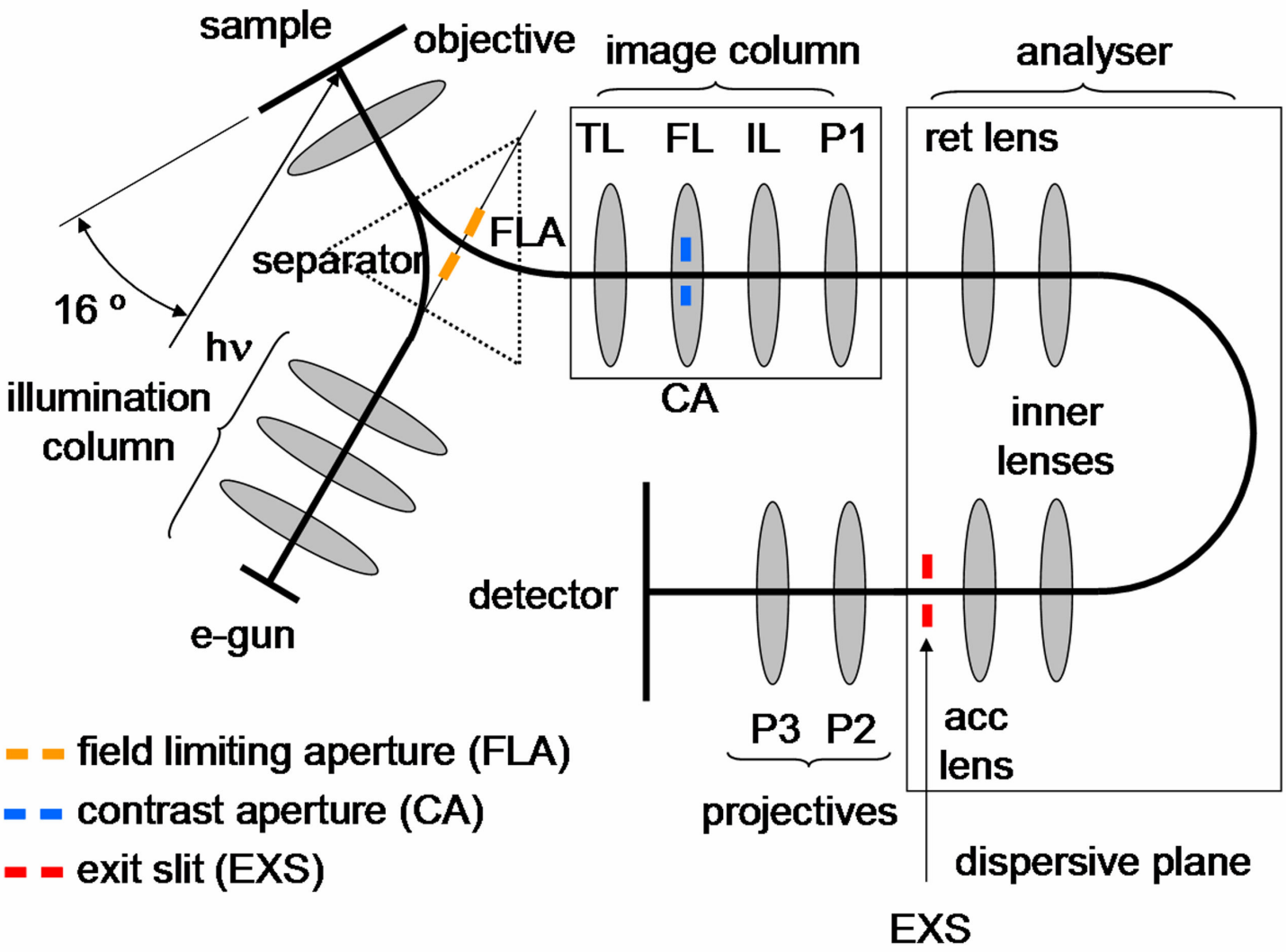
sample
objective
image column
analyser
TL
FL
IL
P1
ret lens
FLA
separator
16 °
hν
illumination
column
CA
inner
lenses
detector
e-gun
P3
P2
acc
lens
projectives
dispersive plane
EXS
field limiting aperture (FLA)
contrast aperture (CA)
exit slit (EXS)

Properties accessible in XPEEM

ELEMENTAL COMPOSITION & CHEMICAL STATE

C1s image of SWCN

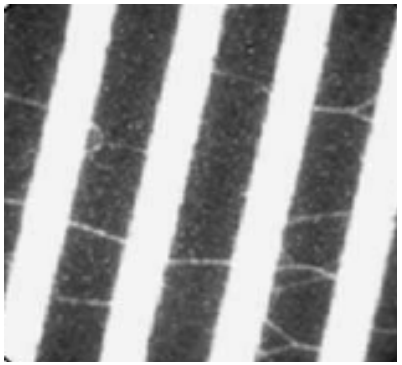

1 μm

S. Suzuki et al,
J. El. Spec Rel. Phenom.
357-360, 144 (2005)

Pb on W110

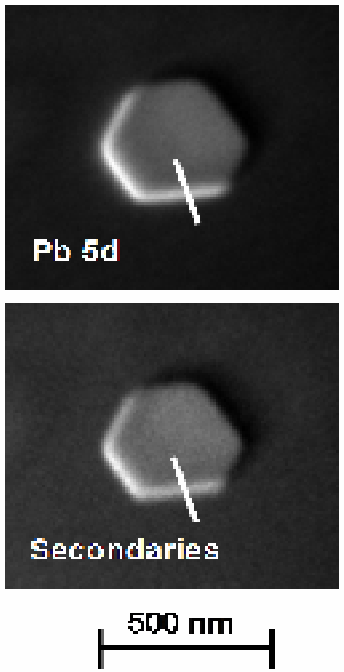

MAGNETIC STATE using XMCD

Co nanodots on Si-Ge

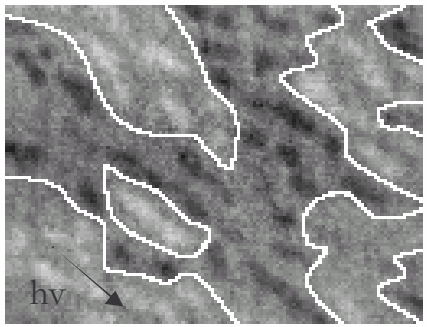

Co - L_3 edge

A. Mulders et al,
Phys. Rev. B 71,
214422 (2005).

patterned structures

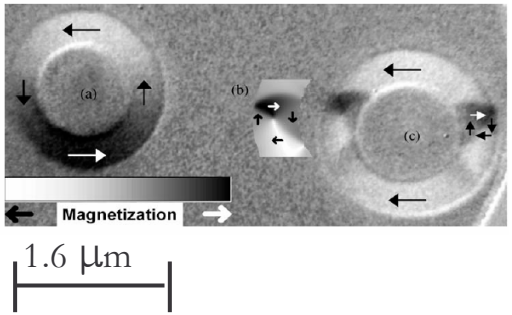

M. Klaeui et al,
Phys. Rev. B 68,
134426 (2003).

SPECTROSCOPY MODE AND PHOTOELECTRON DIFFRACTION ALSO POSSIBLE

Lateral resolution 35 nm in XPEEM; 10 nm in LEEM

What is LEEM? What can LEEM do?

- **LEEM**
  - uses low energy electrons to probe crystalline surfaces at high lateral resolution and video rate imaging. It allows high structure sensitivity.
- **Applications:**
  - dynamic processes at surfaces (thin-film growth, strain relief, etching and adsorption, step dynamics, phase transitions in real time, *in situ*).

www.leem-user.com

Properties not accessible in XPEEM but in LEEM

SURFACE STRUCTURE

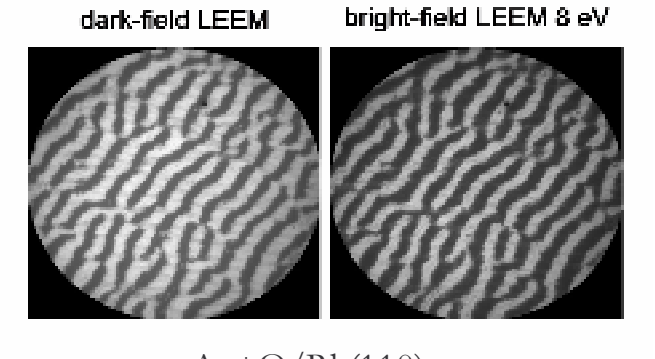

Au+O/Rh(110)

FILM THICKNESS

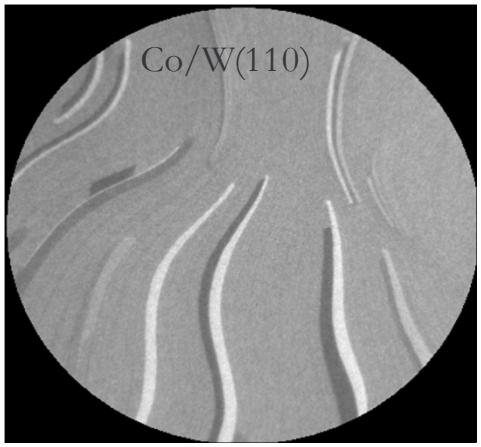

MORPHOLOGY

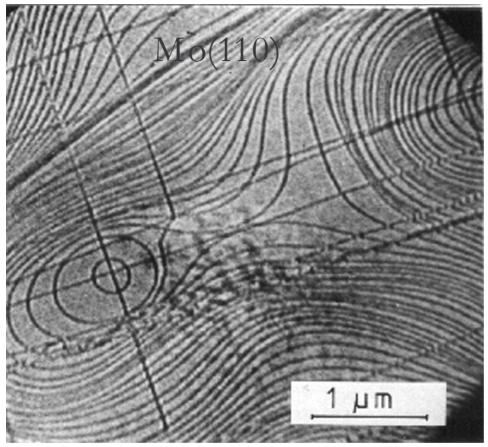

diffraction contrast

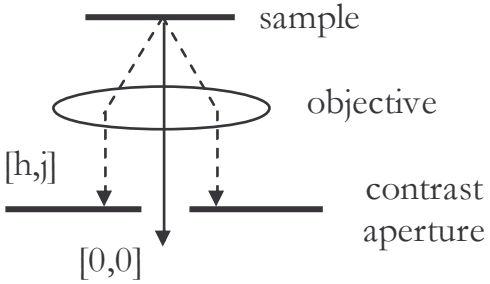

quantum size contrast

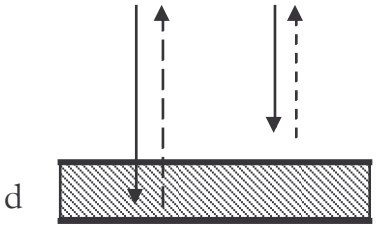

geometric phase contrast

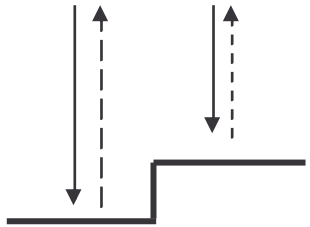

UNIQUE MULTI-TECHNIQUE APPROACH POSSIBLE!

E. Bauer: *Low Energy Electron Microscopy*, Rep. Prog. Phys. 57 (1994) 895-938.

LEEM: darkfield imaging

Domain orientation
Si (001)

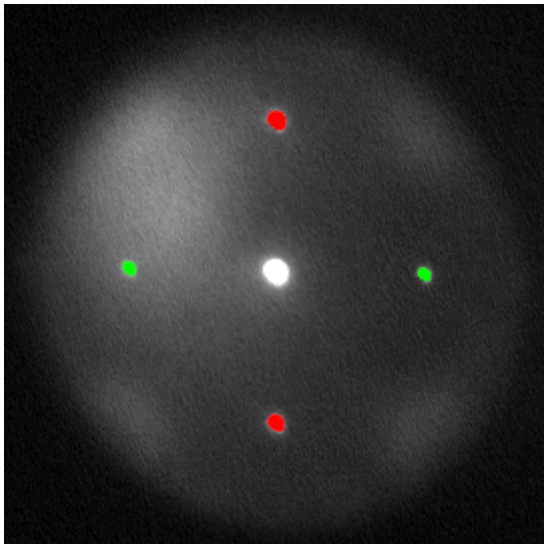

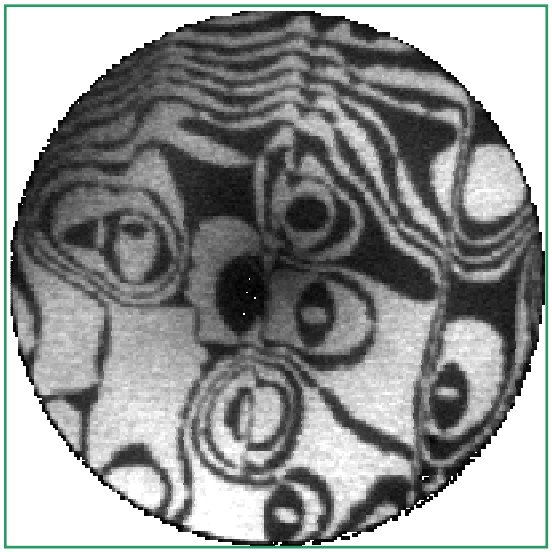

Quantum size contrast in LEEM

- Modulations in reflectivity due to QWR above vacuum level.
- Quantised energy levels
- Characteristic IV spectra
- Reflectivity maxima minima reproduced by the phase-accumulation model (PRB 61, 1804)

$$2k(E)mt + \Phi_C(E) + \Phi_B(E) = 2n\pi,$$

$$m = \frac{[\Phi_C(E) + \Phi_B(E)]/2\pi + \nu}{\kappa(E)/k_{BZ}},$$

Graphite / SiO_2

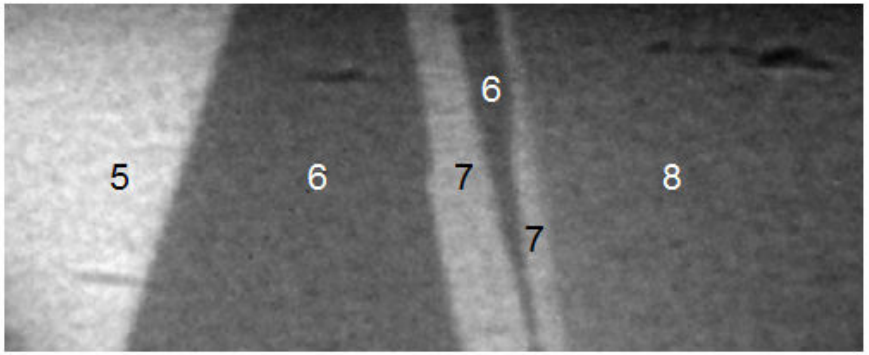

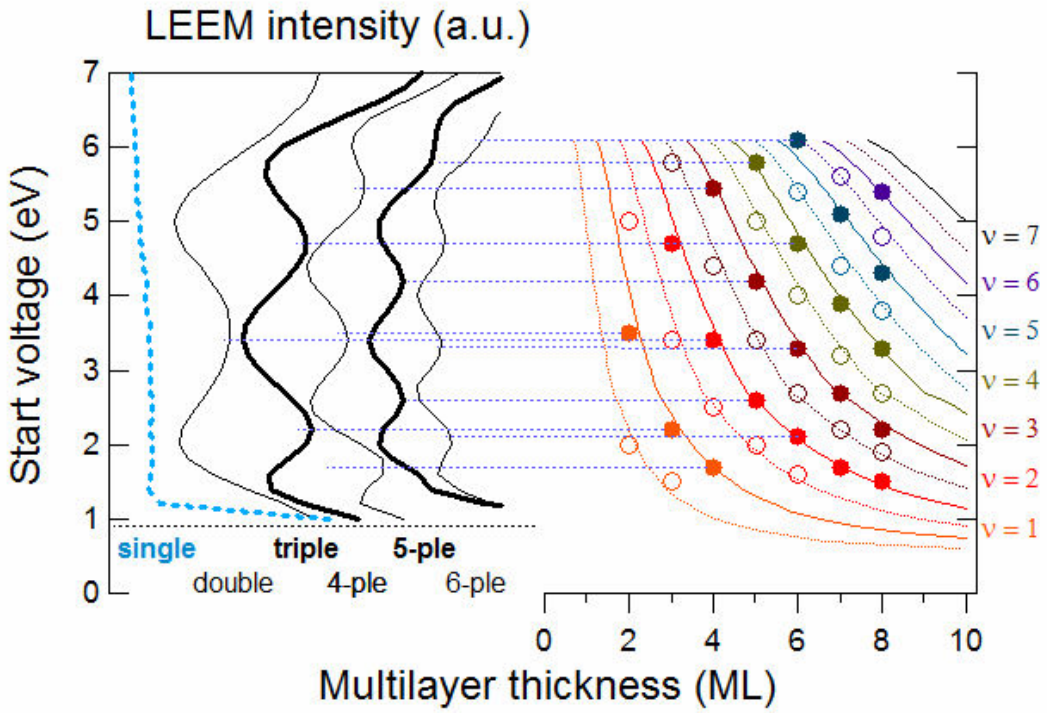

Operating modes - summary:

- **Imaging**
  - XPEEM (energy filtered)
  - LEEM (brightfield and darkfield)
- **Diffraction**
  - micro-XPD (energy filtered)
  - micro-LEED
- **Spectroscopy**
  - micro-XPS (dispersive plane)

UNIQUE MULTI-TECHNIQUE APPROACH INTO ONE AND ONLY ONE INSTRUMENT!!!

3.1 Applications of XPEEM

CHEMICAL IMAGING:

Giant faceting: Au on vicinal Si(001)

Ex.1 – Au/Si(001) faceting

VOLUME 86, NUMBER 22 PHYSICAL REVIEW LETTERS 28 MAY 2001

Spatial Variation of Au Coverage as the Driving Force for Nanoscopic Pattern Formation

Frank-J. Meyer zu Heringdorf,[1,*] Th. Schmidt,[2,†] S. Heun,[2] R. Hild,[1,‡] P. Zahl,[1]
B. Ressel,[2] E. Bauer,[3] and M. Horn-von Hoegen[1,‡]

[1]*Institut für Festkörperphysik, Universität Hannover, Appelstraße 2, 30167 Hannover, Germany*
[2]*ELETTRA, Sincrotrone Trieste, 34012 Basovizza TS, Italy*
[3]*Department of Physics and Astronomy, Arizona State University, Tempe, Arizona 85287*
(Received 9 October 2000)

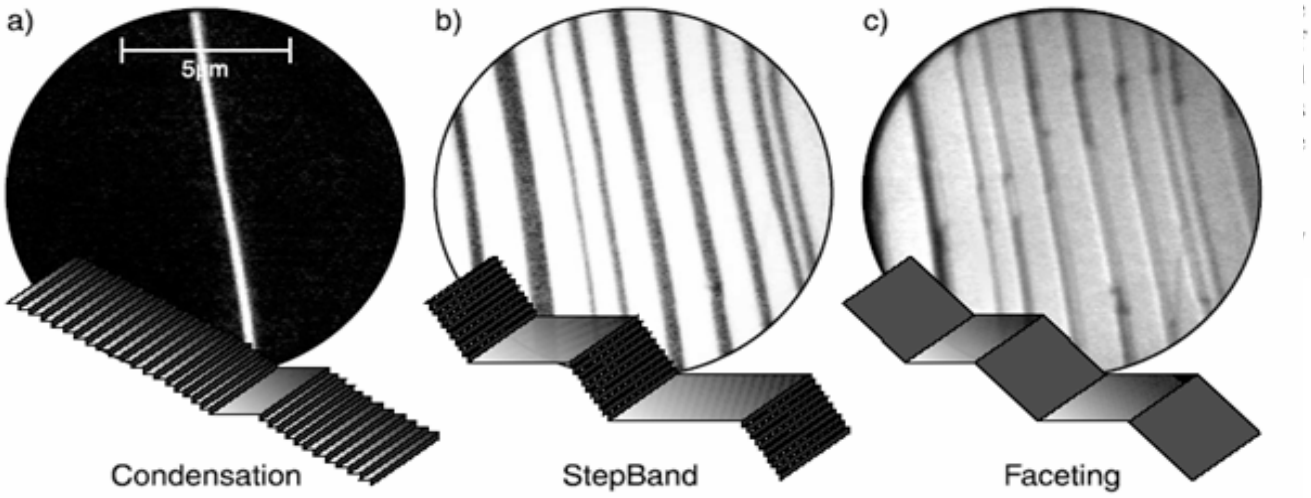

Ex.1 – Au/Si(001) faceting

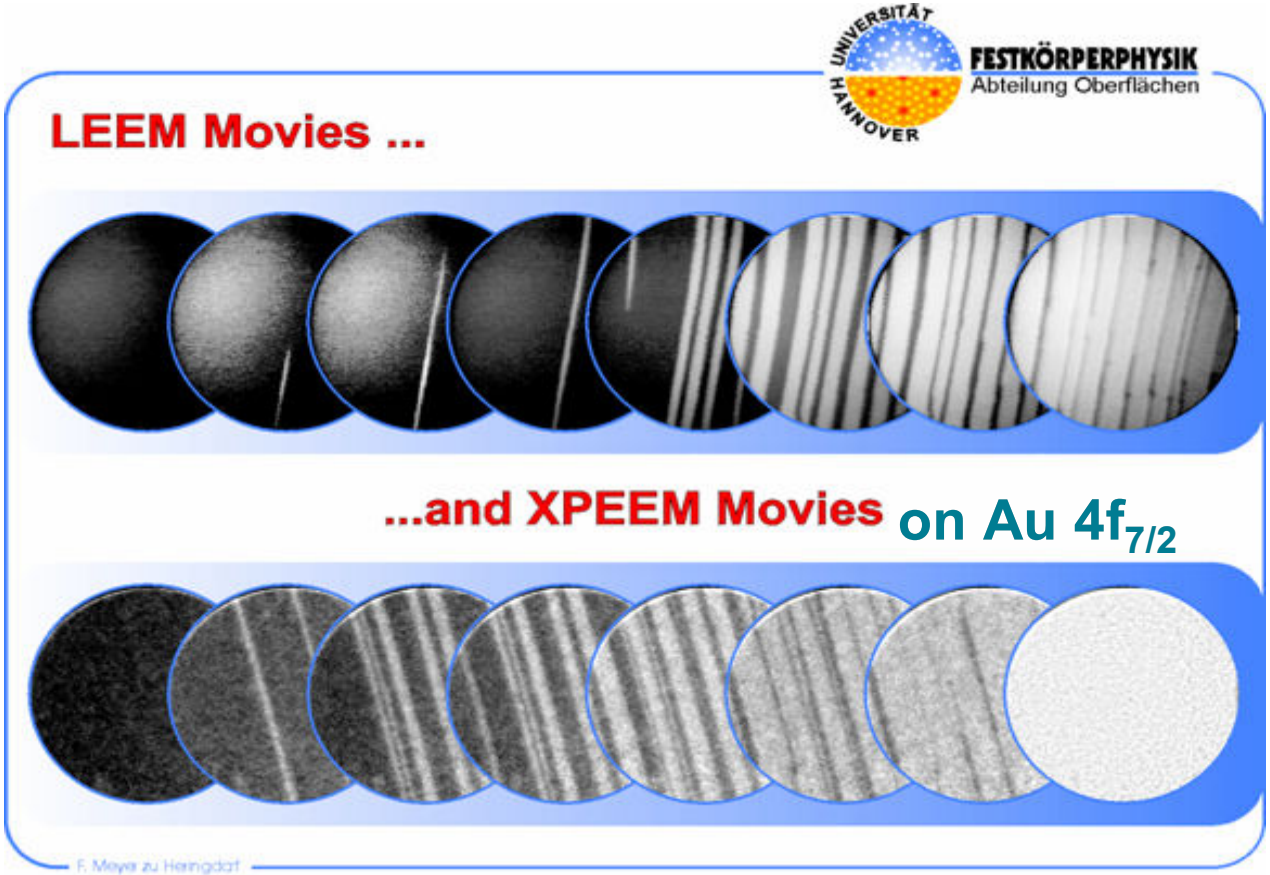

F.-J. Meyer zu Heringdorf, R. Hild, P. Zahl, Th. Schmidt, S. Heun, B. Ressel, E. Bauer, M. Horn-von Hoegen: Elettra News **36** (1999).

Ex.1 – Au/Si(001) faceting

Formation of the Au-rich (5 × 3.2)

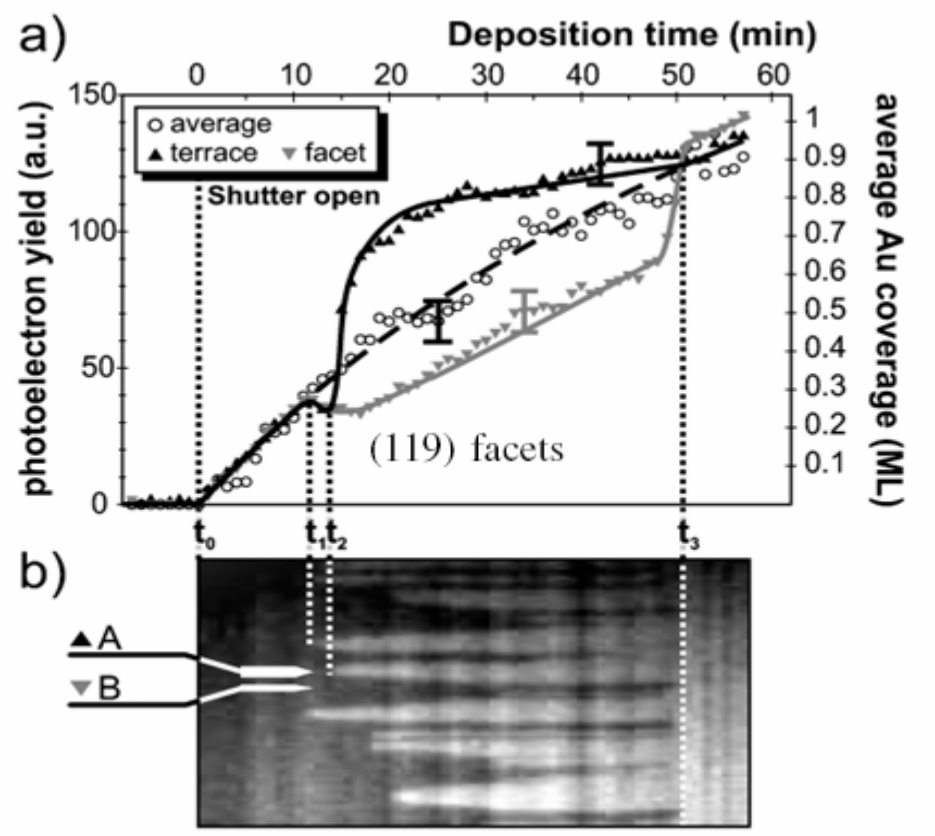

FIG. 3. Temporal evolution of the local Au coverage during faceting. (a) Au $4f_{7/2}$ photoelectron yield over deposition time. Absolute values of Au coverage on the right are calibrated by MEIS [17]. t_0: deposition starts, t_1: a first terrace is formed, t_2: a terrace is formed in the region of interest, t_3: the faceting is complete. (b) Slices from the XPEEM images analyzed in (a) were assembled to a time dependent grey scale representation. The arrows mark terraces analyzed in detail in (a).

3.2 Applications of XPEEM

CHEMICAL IMAGING:

Tuning reactivity

by quantum electron confinement

Mg epitaxial growth

growth is followed *in-situ*
by LEEM

Film thickness is measured by
quantum interference contrast

[001]

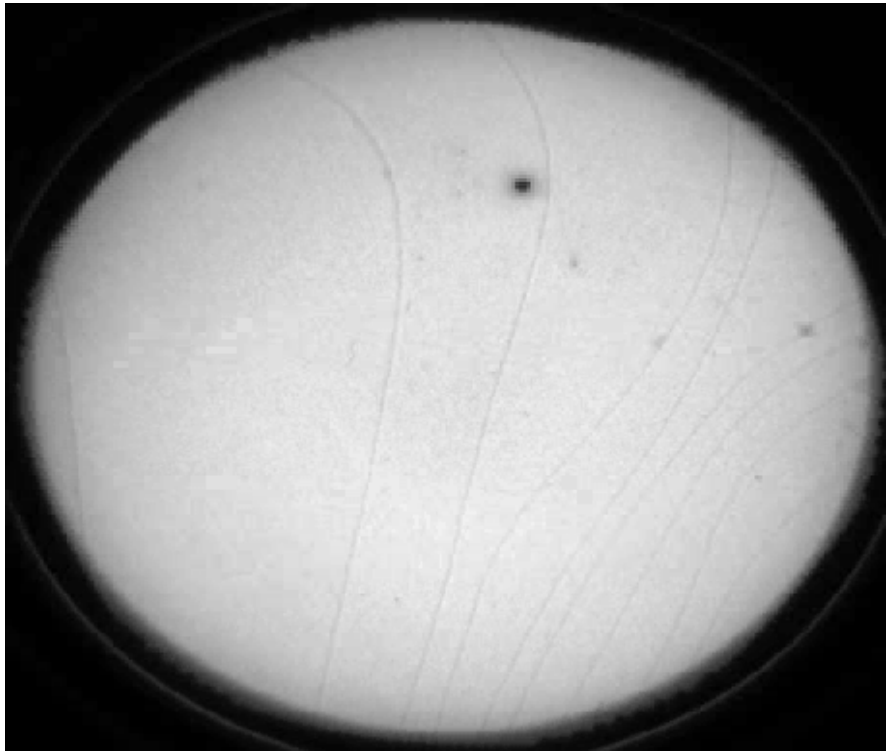

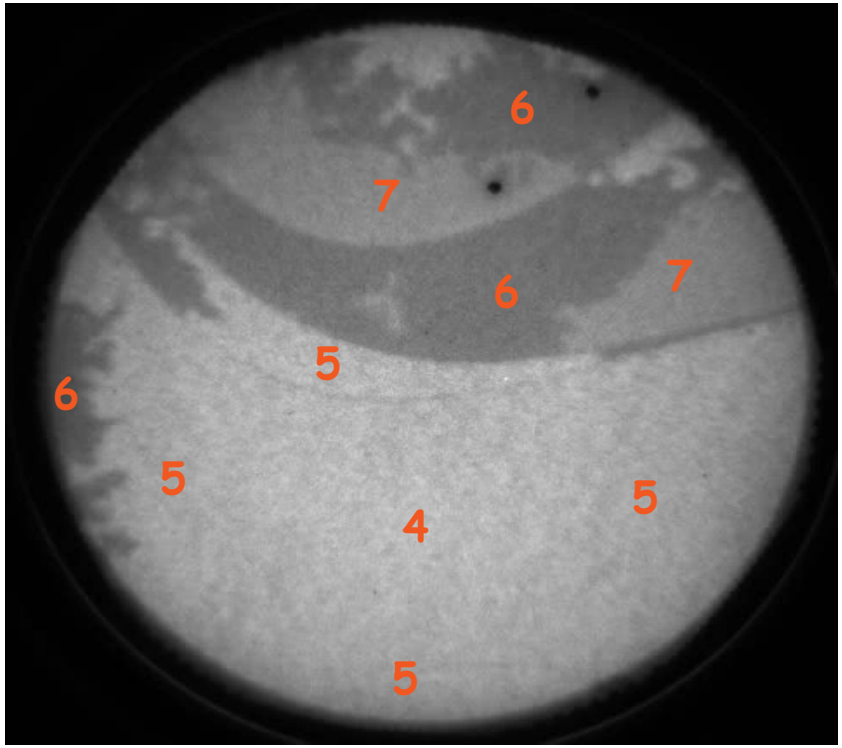

Mg/W(110) dep. 405 K, 0.1ML/min
11.1eV, 5 μm

4 - 7 ML Mg/W(110)
0.1-10.1eV/0.2eV, 5 μm

Electron confinement in Mg thin films

- conduction electrons confined to the Mg film
- only few "quantum-well" states allowed
- modulation of electronic density at E_F

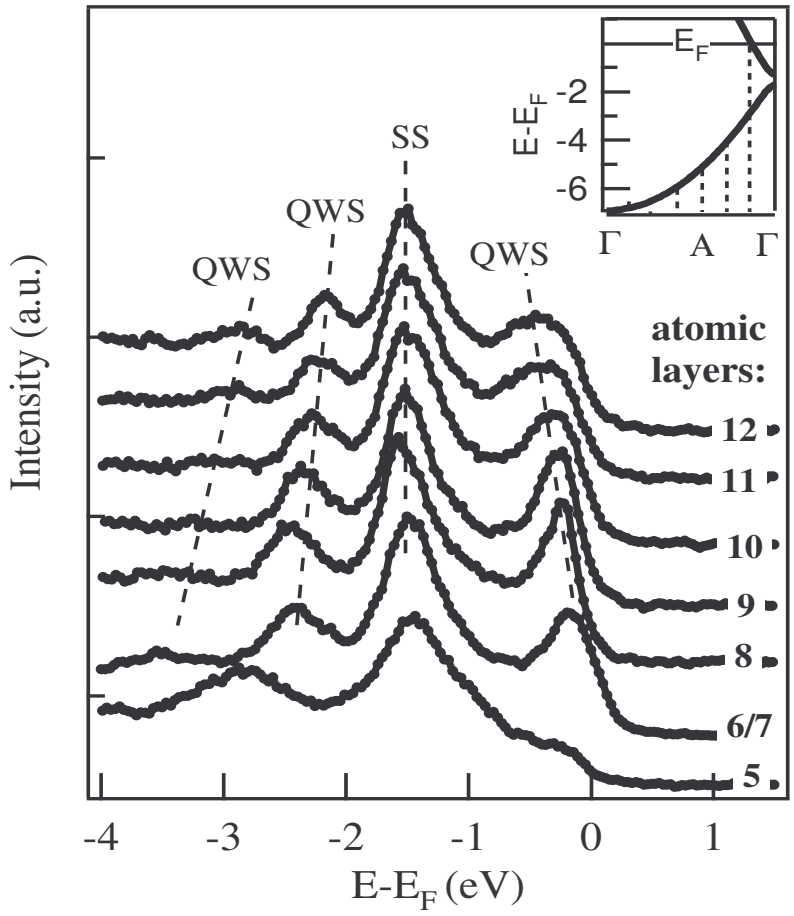

L. Aballe et al, Phys. Rev. Lett. 93, 196103 (2004)

Oxidation of Mg film

- Know from literature:
  - O_2 spontaneous dissociation
  - O goes below surface
  - 2 layers Mg oxidized
  - Coalescence MgO islands

Bungaro et al, PRL 79, 4433 (1997)
Goonewardene et al, Surf. Sci. 501, 102 (2002)

- Micro-XPS: Mg VB reveals oxidation extent

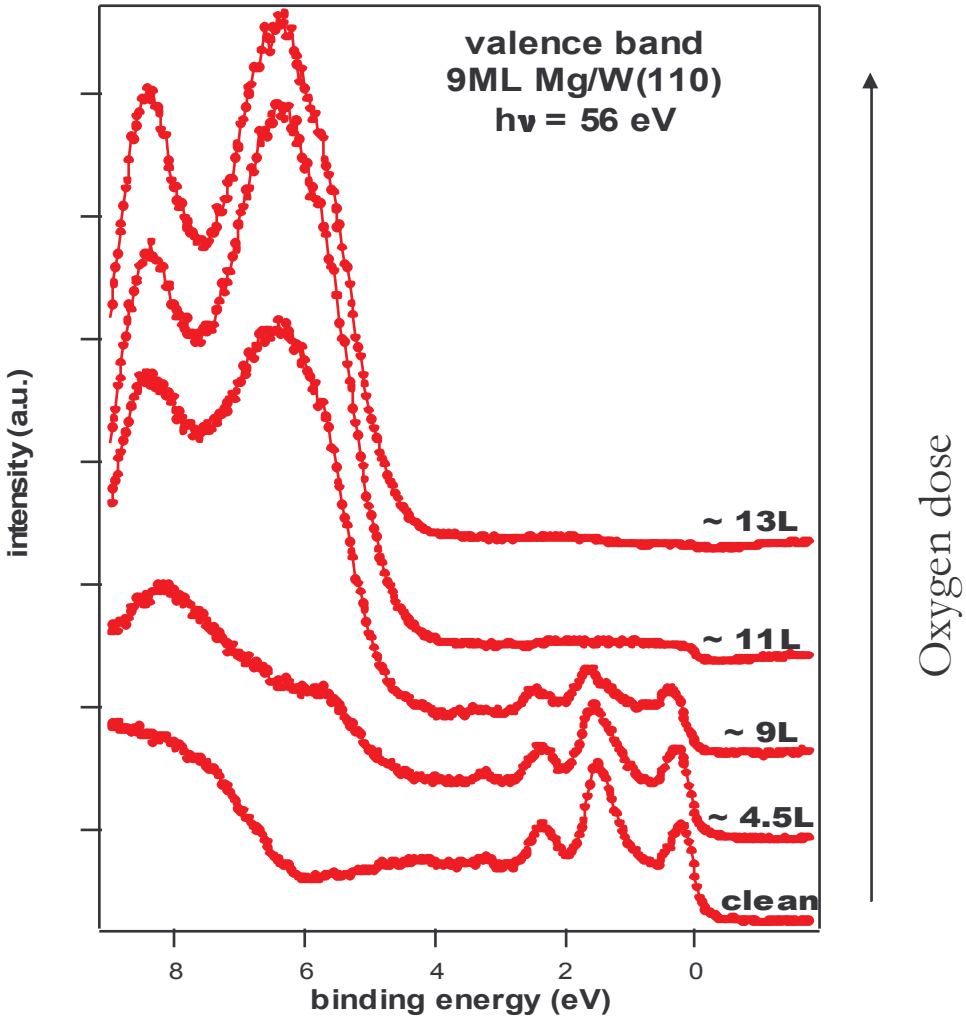

L. Aballe et al, Phys. Rev. Lett. 93, 196103 (2004)

Oxidation of Mg film

- Micro-XPS on Mg 2p reveals oxidation extent
- 2 Mg component
  - bulk/surface Mg
  - Oxide Mg
- Micro-XPS: Mg spectra allow quantitative determination of oxidation extent
  - I_{ox}/I_{tot}

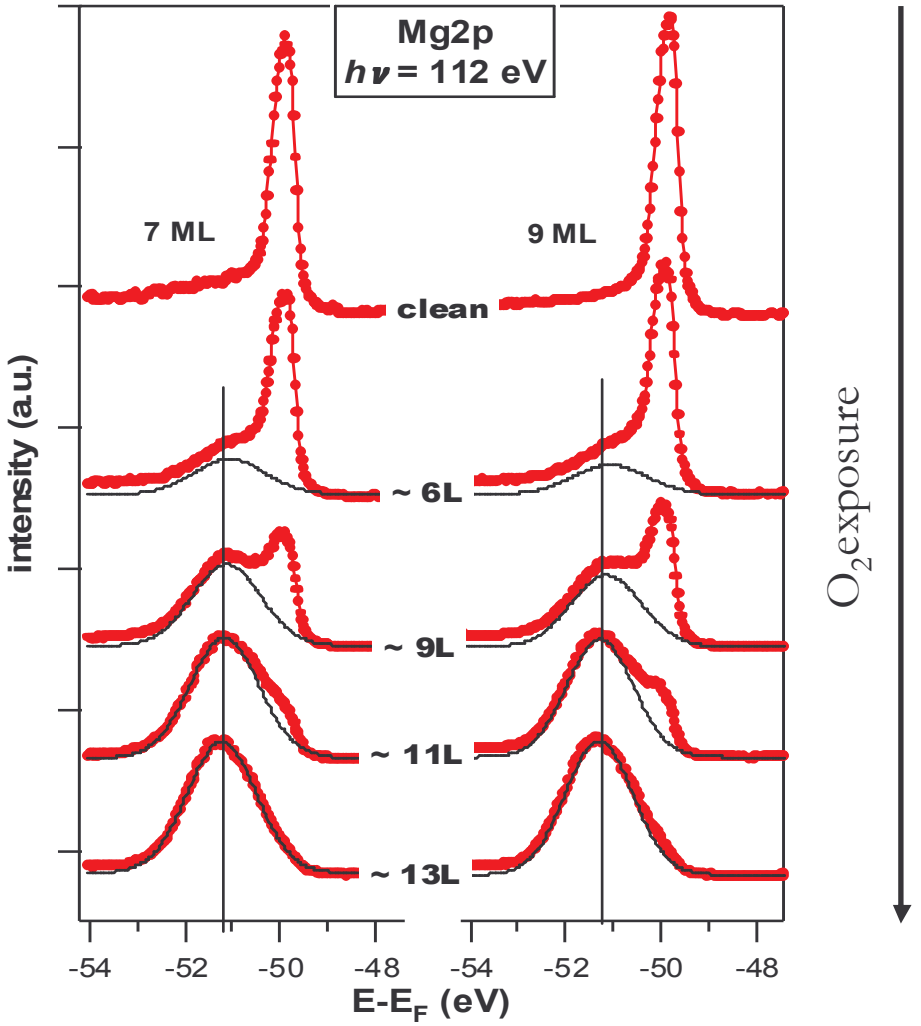

L. Aballe et al, Phys. Rev. Lett. 93, 196103 (2004)

Oxidation of Mg film

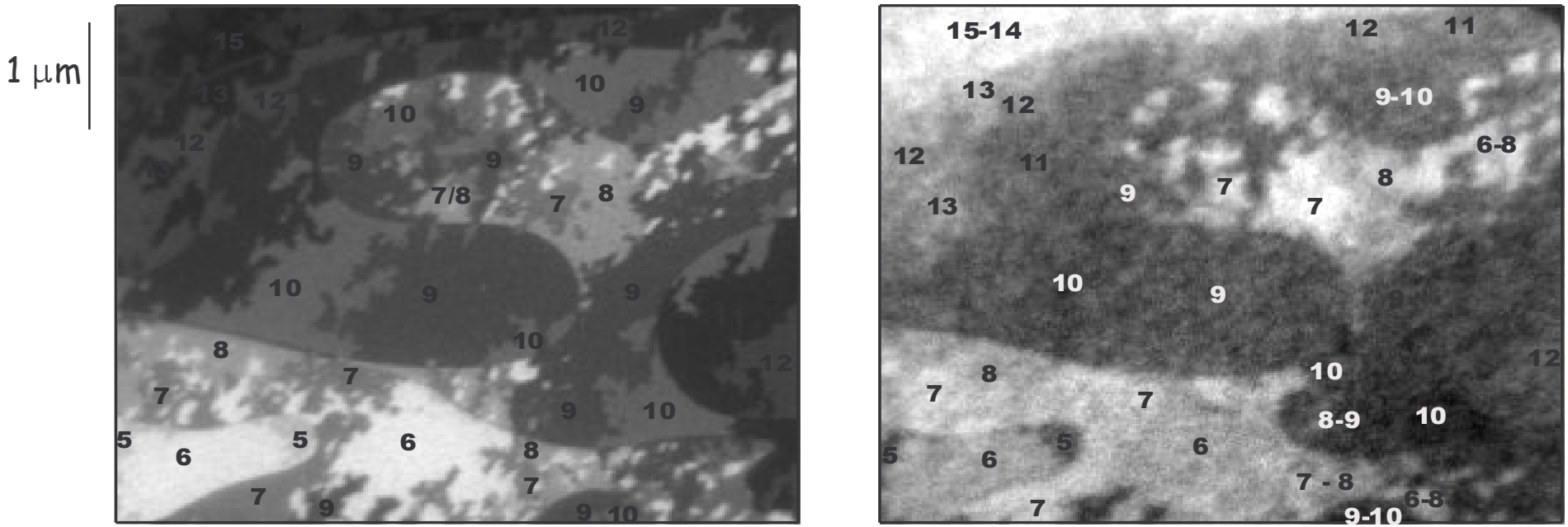

LEEM reveals morphology
atomic thickness

oxide component imaged by XPEEM
reveals chemistry!

→ DOSE OXYGEN →

oxidation rate depends on thickness!!

Oxidation of Mg film

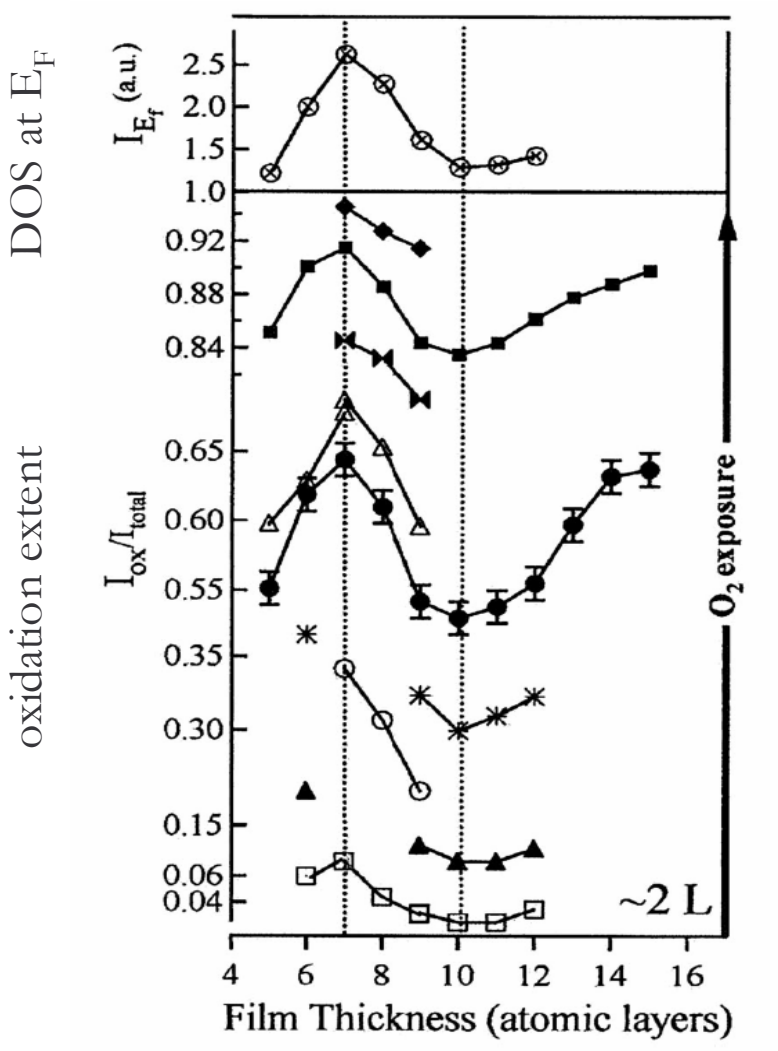

- strong variations in the oxidation extent as a function of film thickness
- The density of *bulk* states at E_F correlated to oxidation extent
- Control on film thickness enables modifying the molecule surface interaction
- Strong theoretical interest!

L. Aballe et al, Phys. Rev. Lett. 93, 196103 (2004)

3.3 Applications of XPEEM

CHEMICAL IMAGING

Reorganisation processes driven by surface chemical reactions

Outlook:

- **Adsorbates Structures Formed during Surface Chemical Reactions**
  - Spatio-temporal reaction-diffusion patterns in presence of spectator species
    - Mass transport phenomena by reaction wavefronts.
    - Surface structural and morphological changes induced by adsorbates
  - Stationary patterns during reactive phase separation
    - Role of "spectator species" (modifiers) in pattern formation
    - Self organisation by chemical reactions: analogy to chemically frozen spinodal decomposition.
    - Links to catalysis and non-linear sciences

Spatio-temporal concentration patterns in surface reactions

Belousov-Zabatinski reaction

(solution of, acidified bromate, malonic acid, ceric salt)

VOLUME 65, NUMBER 24 PHYSICAL REVIEW LETTERS 10 DECEMBER 1990

Spatiotemporal Concentration Patterns in a Surface Reaction: Propagating and Standing Waves, Rotating Spirals, and Turbulence

S. Jakubith, H. H. Rotermund, W. Engel, A. von Oertzen, and G. Ertl
Fritz-Haber-Institut der Max-Planck-Gesellschaft, Faradayweg 4-6, D-1000 Berlin 33, Germany
(Received 25 June 1990)

Pattern formation

in surface chemical reactions

oscillatory oxidation of carbon monoxide on a Pt(110) surface

standing fronts

rotating spirals

target waves

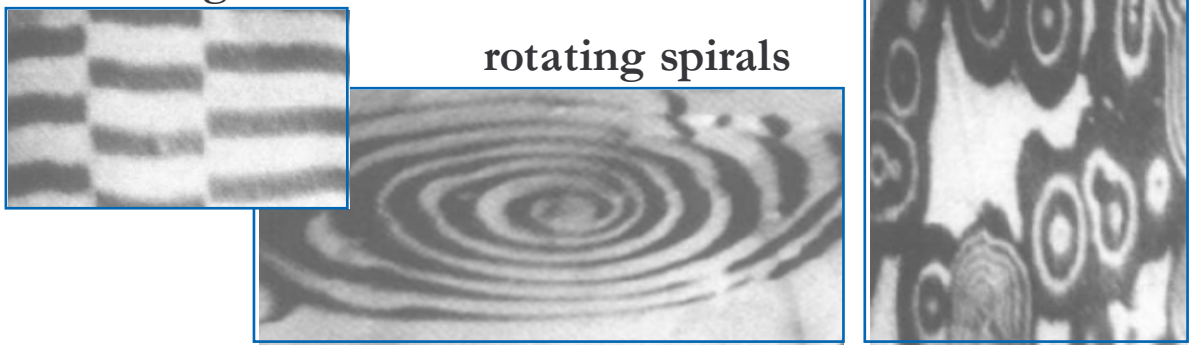

Jakubith et al, PRL 65, 3013 (1990)

Reaction diffusion patterns: NO+H_2 /Rh(110)

- First quantitative measurement of concentration profiles

  Schaak et al Phys. Rev. Lett. **83**, 1882 (1999)

$$H_2 + 2^* \leftrightarrow 2H_{ad},$$
$$NO + * \leftrightarrow NO_{ad},$$
$$NO_{ad} + * \rightarrow N_{ad} + O_{ad},$$
$$2N_{ad} \rightarrow N_2 + 2^*,$$
$$O_{ad} + 2H_{ad} \rightarrow H_2O + 3^*,$$

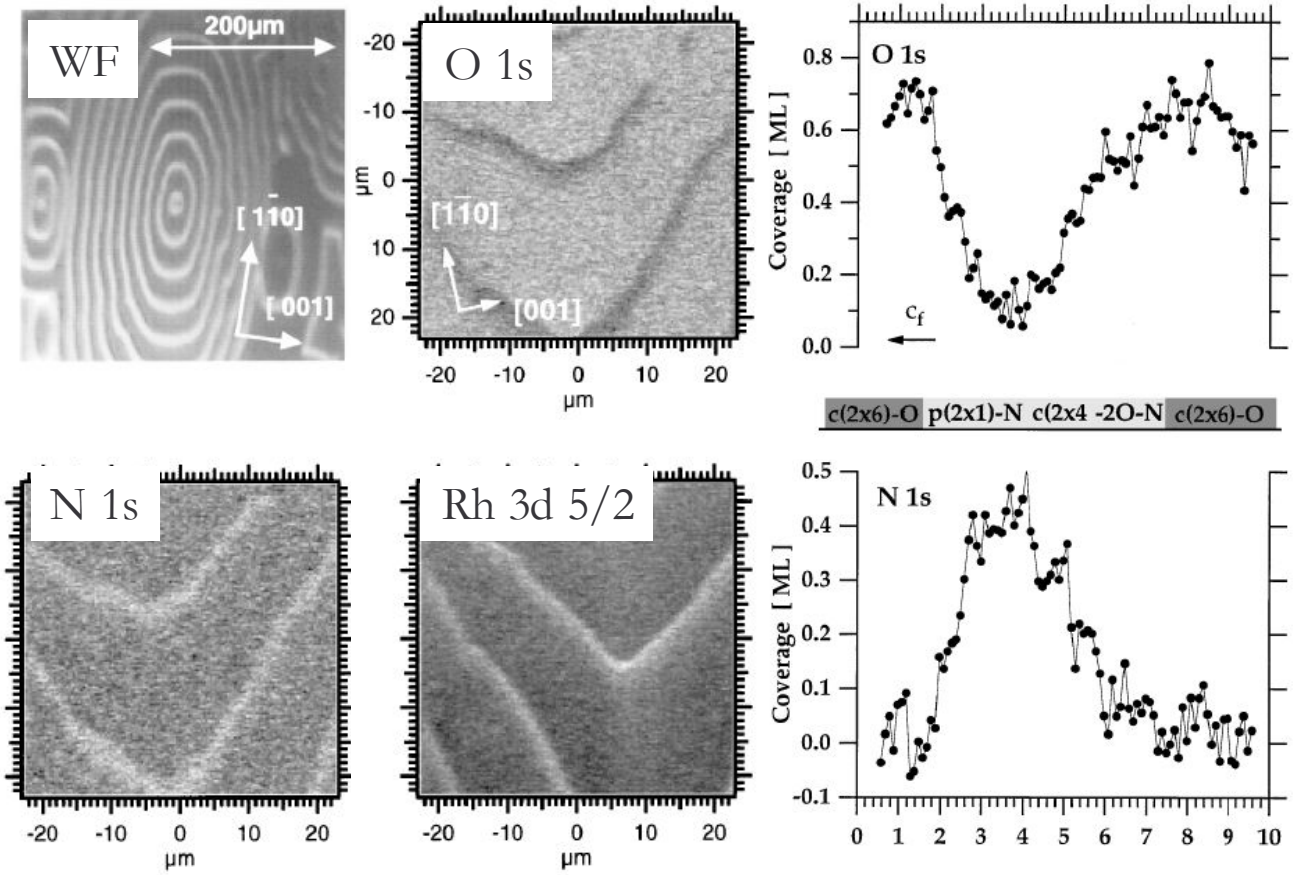

Th. Schmidt et al, Chem. Phys. Lett. 318, 549 (2000)

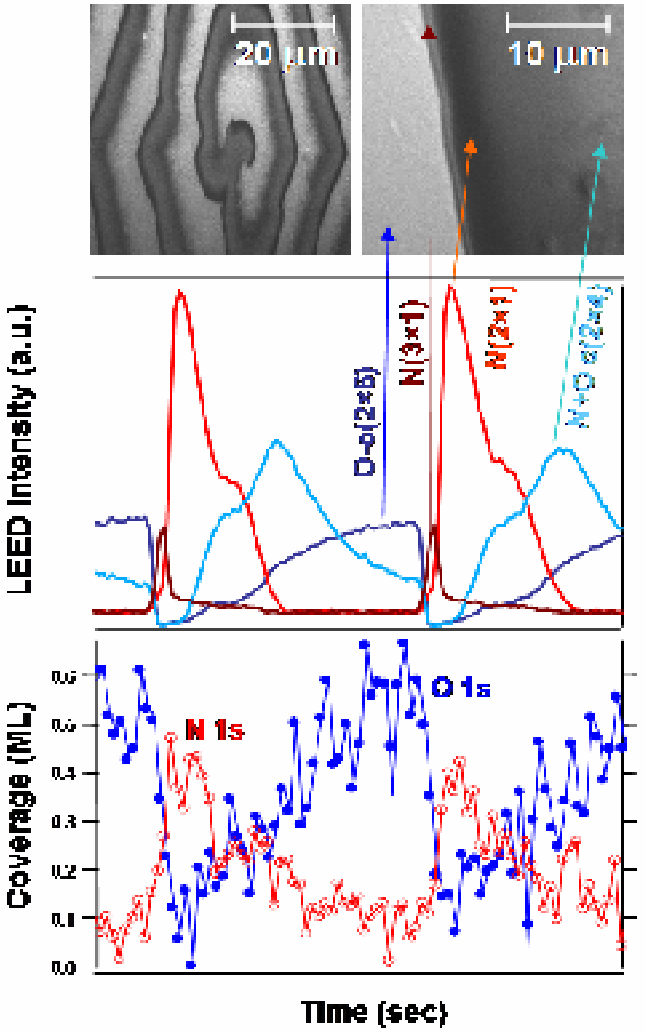

Reaction diffusion patterns: $NO+H_2$ /Rh(110)

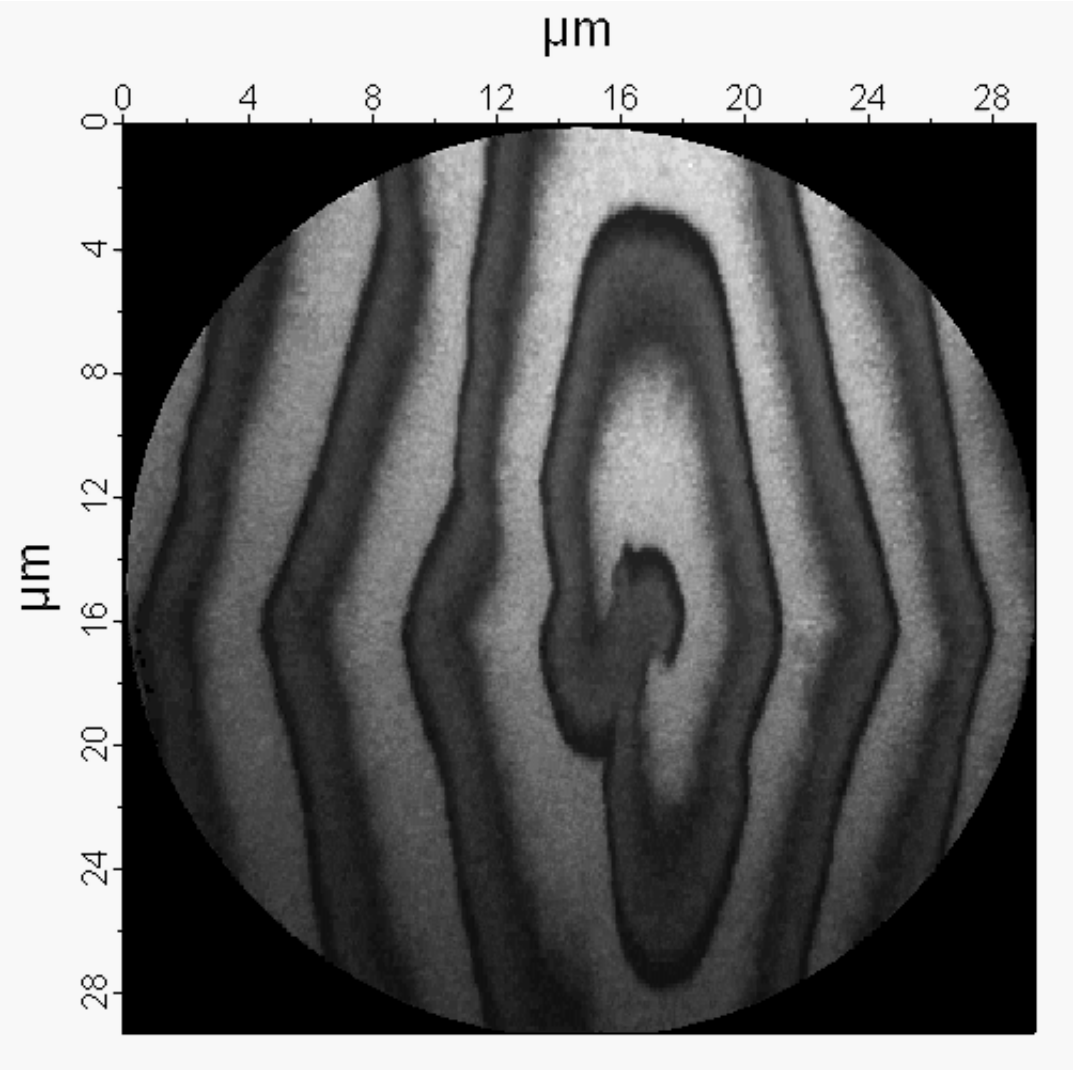

Structure + composition
(LEEM, micro-LEED)

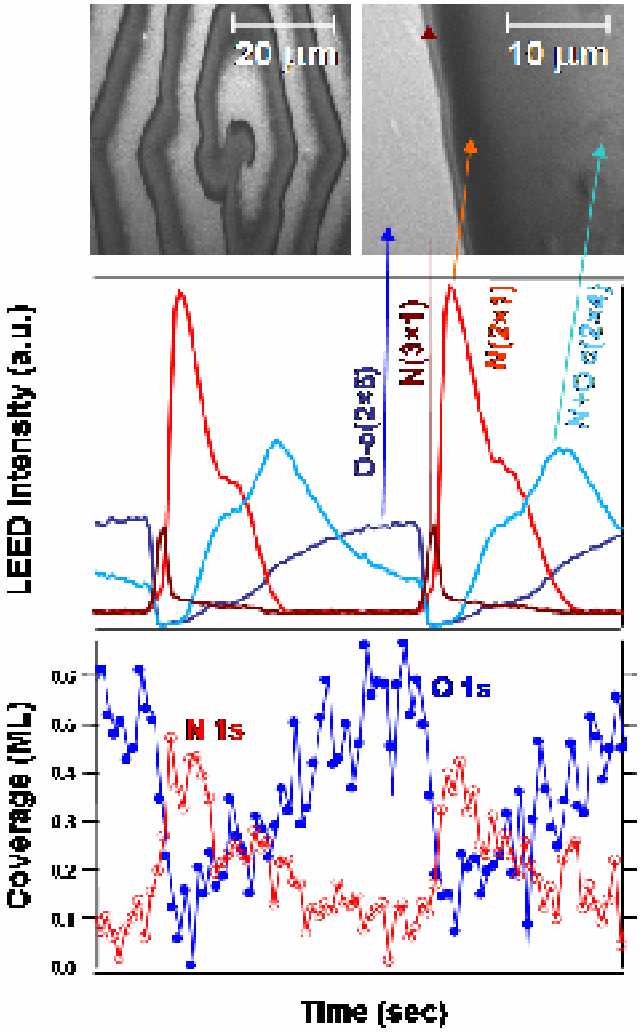

K / O_2+H_2 /Rh(110)

– Mass transport by reaction fronts, K accumulation and depletion

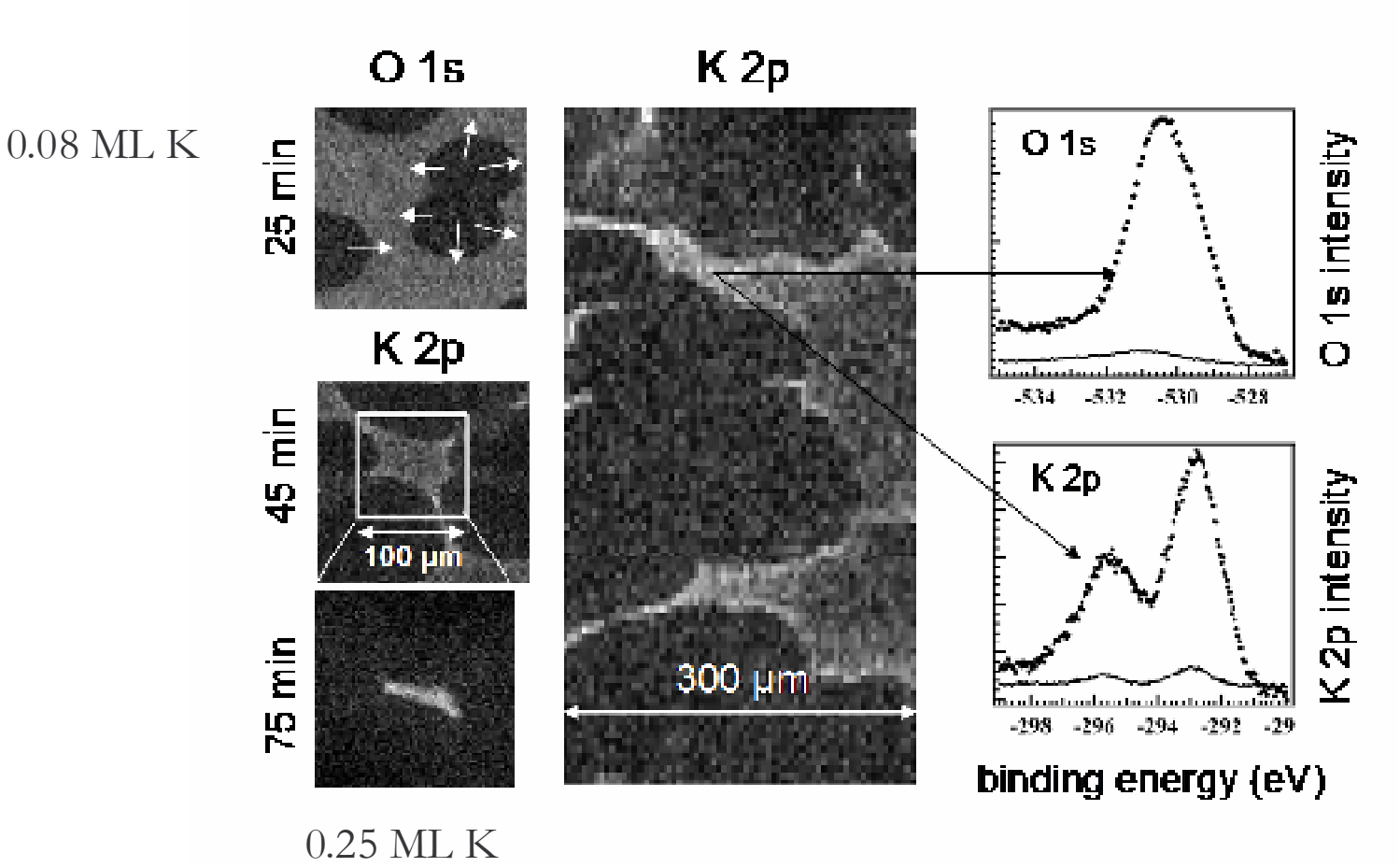

K / NO+H_2 /Rh(110)

– Mass transport by reaction fronts, K accumulation and depletion

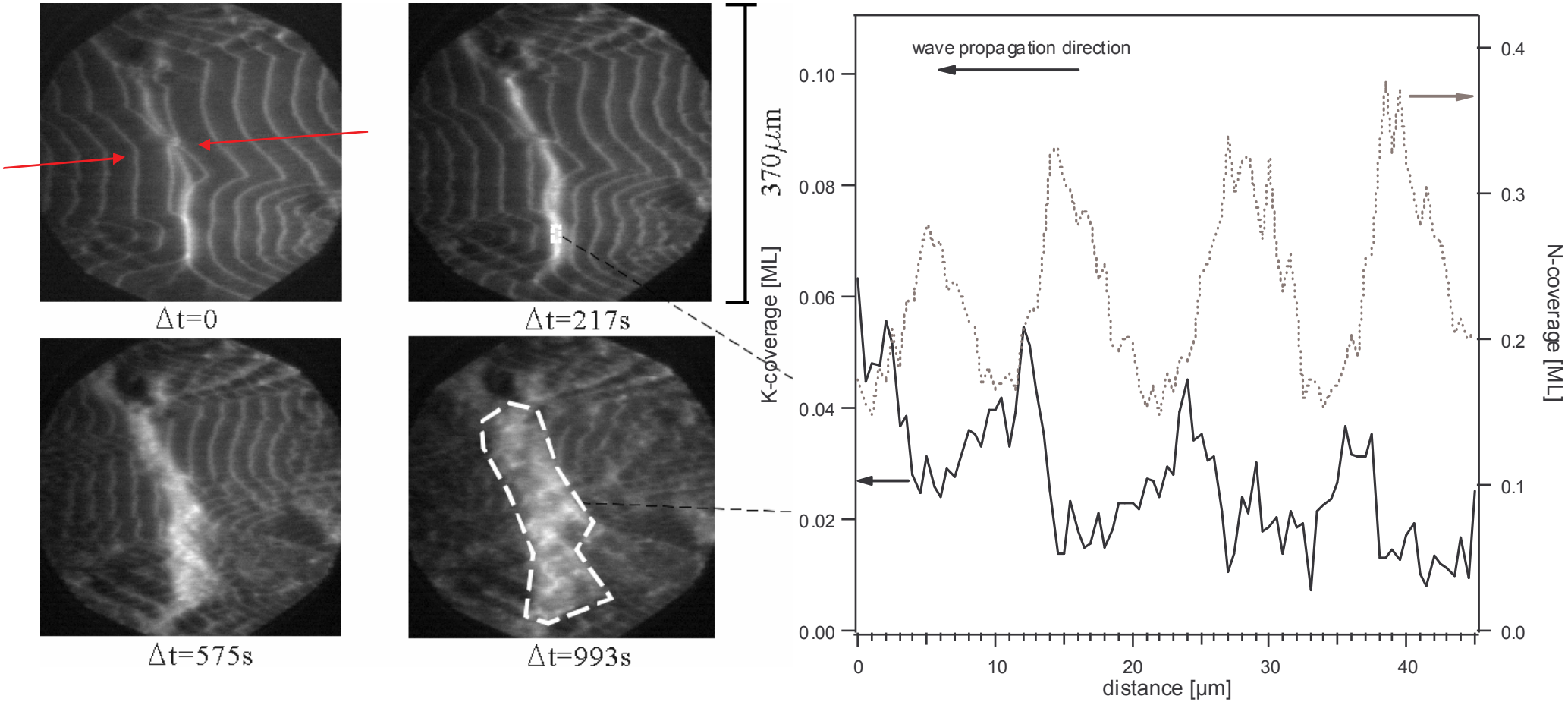

L. Hong, H. Uecker M. Hinz, Qiao Liang, I.G. Kevrekidis, S. Günther, A. Locatelli, and R. Imbihl; submitted to PRE

Au/Rh(110) during H_2+O_2

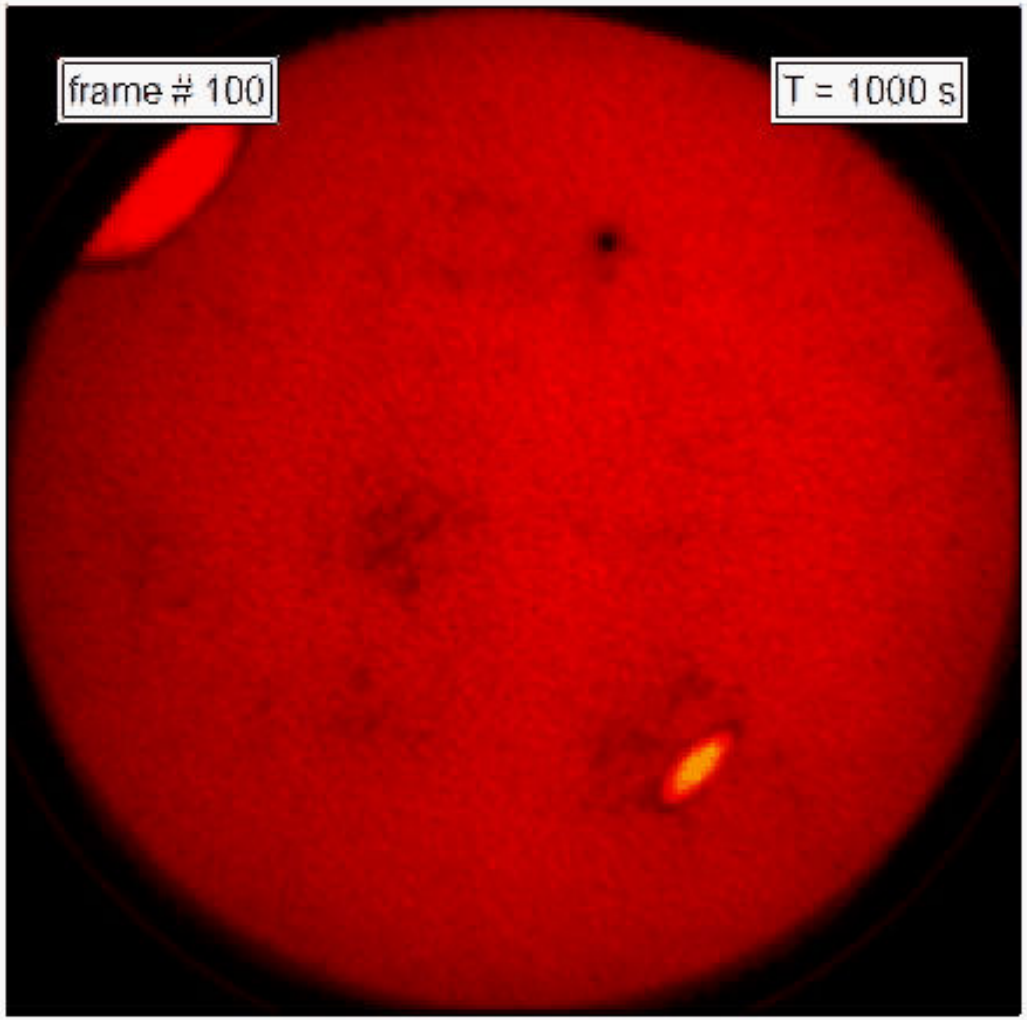

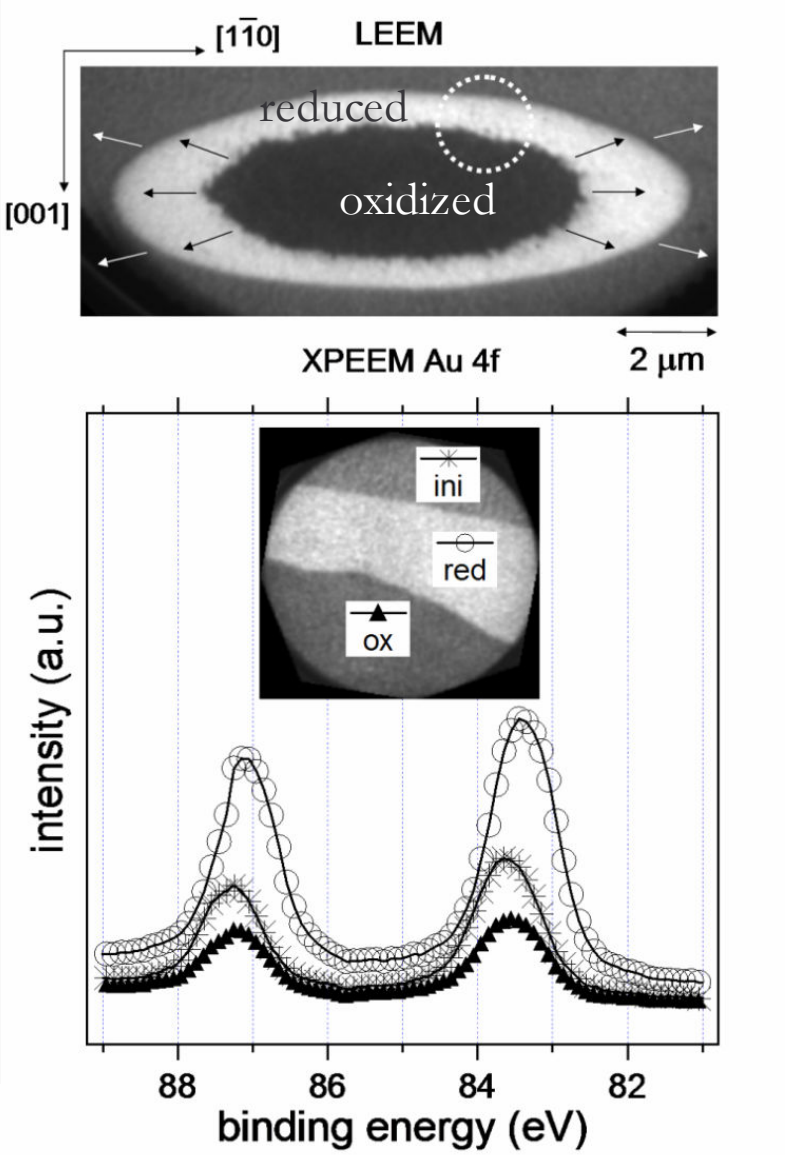

0.5 ML Au; 550 K

Phase separation at stationary state of the reaction

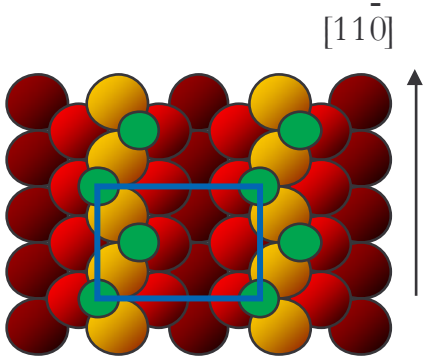

(2x2)p2mg

θ_O = 0.5 ML

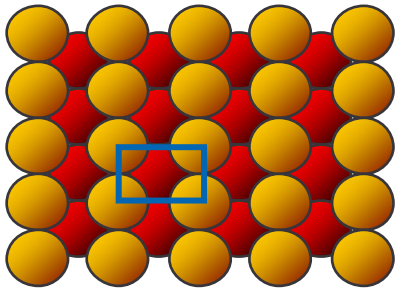

(1x1)

unreconstructed

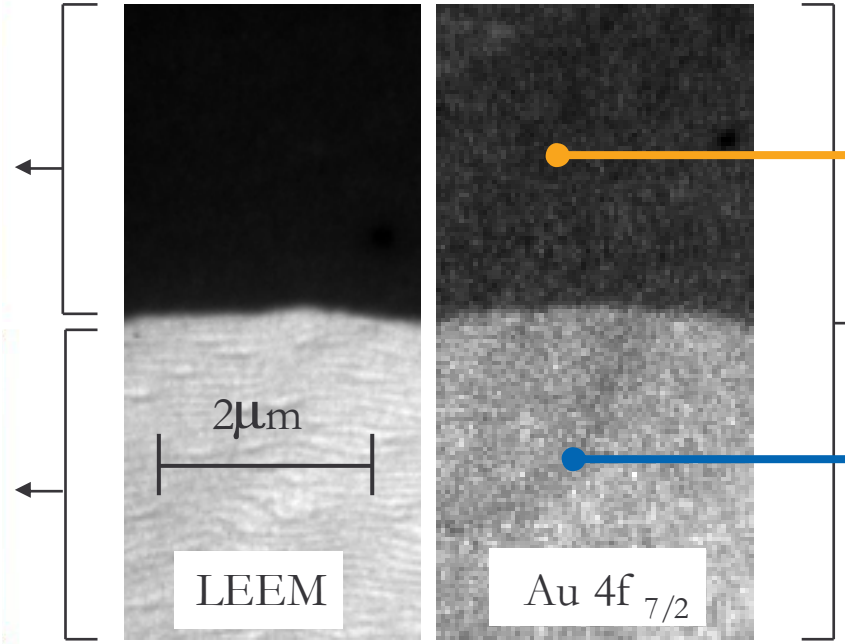

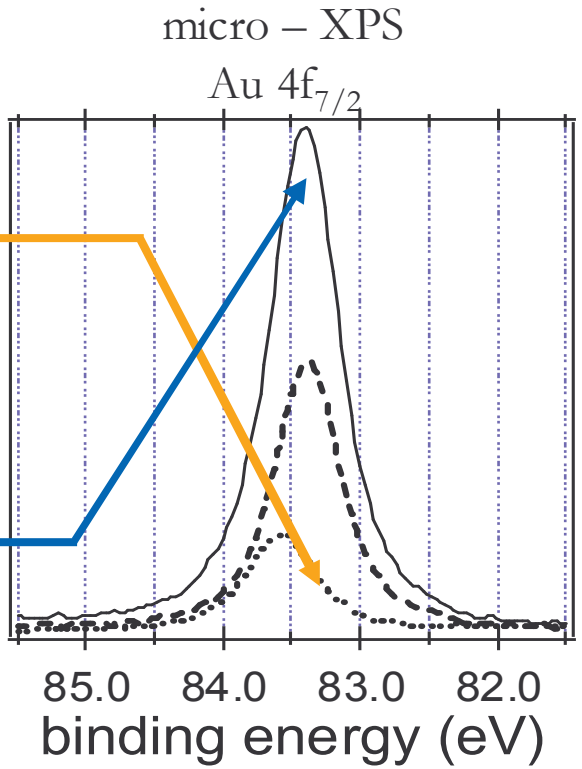

J. AM. CHEM. SOC. 2005, *127*, 2351–2357

Surface Science 566–568 (2004) 1130–1136

Θ_i [Au]= 0.5 ML

homogeneously distributed

Reactivity

- Au+O pattern is preserved under oxidation by destroyed under reduction; oxidized part is the most reactive

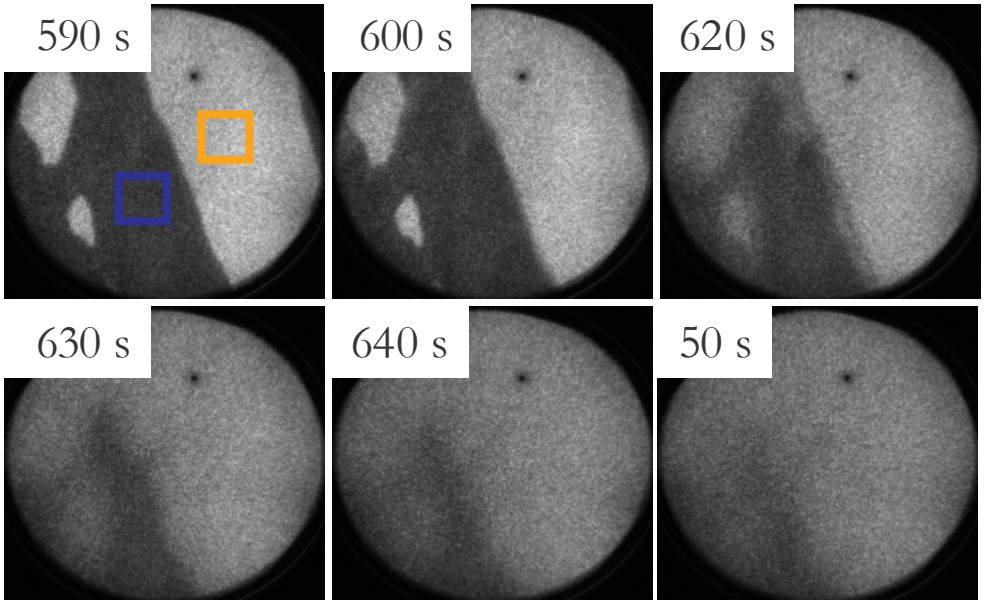

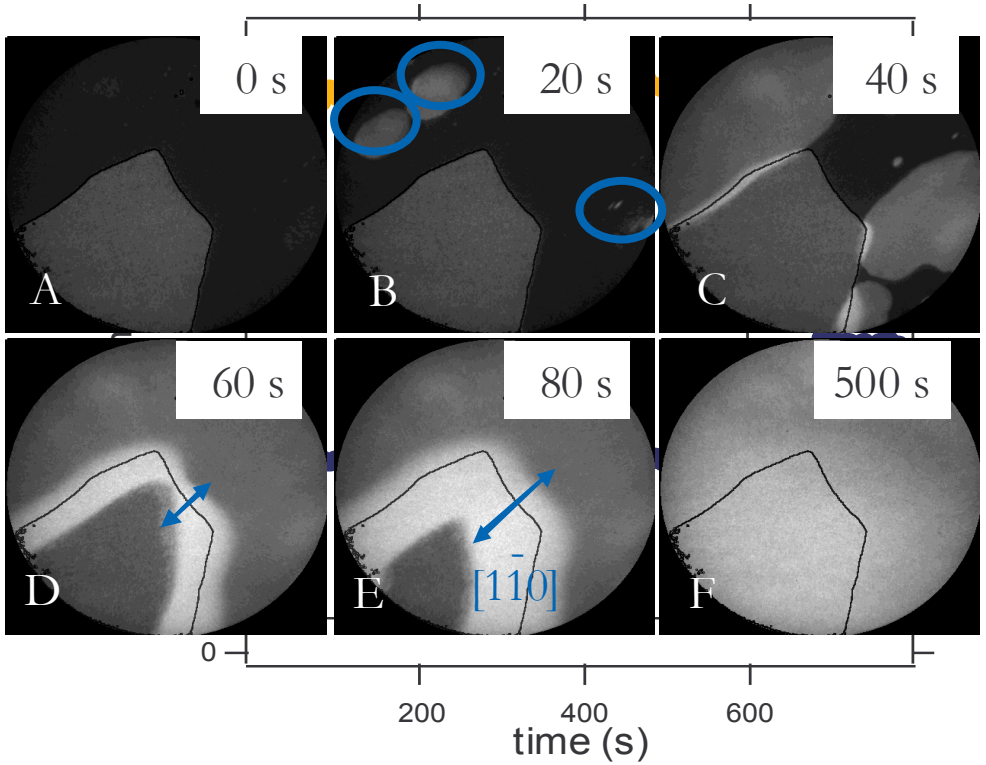

XPEEM Au 4f $_{7/2}$

field of view 10 μm

Energetic origin of phase separation

Mixing energy:

$$E_{mix} = (E_{Au+O}[Q_{Au+O}] - E_{Au}[Q_{Au}] - E_O[Q_O])/N$$

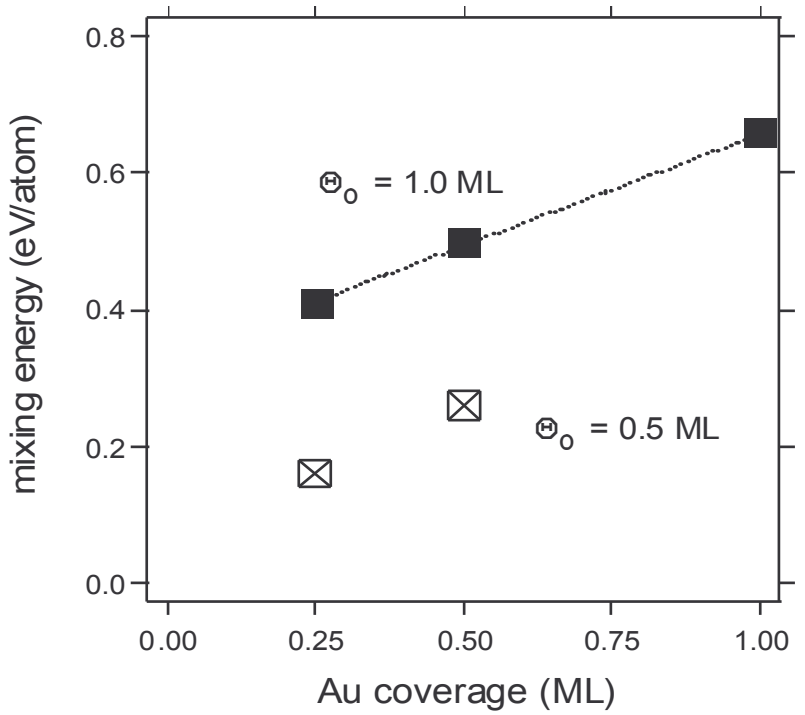

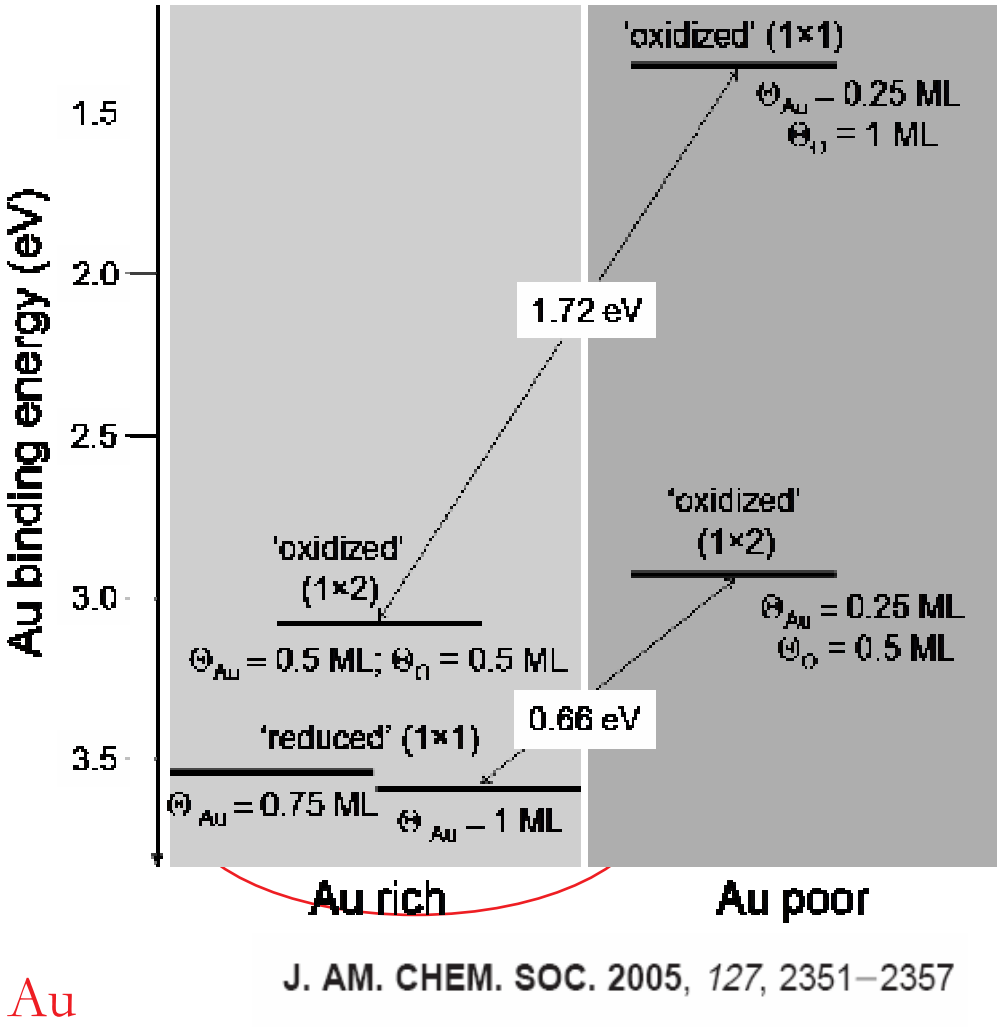

J. AM. CHEM. SOC. 2005, *127*, 2351−2357

The difference in total binding energy between the "mixed" and the separated Au and O phases imposes phase separation

Self-organization during phase separation

Structure formation in phase separating systems

Spinodal decomposition:
development & evolution
of periodic microstructure

PS/PMMA

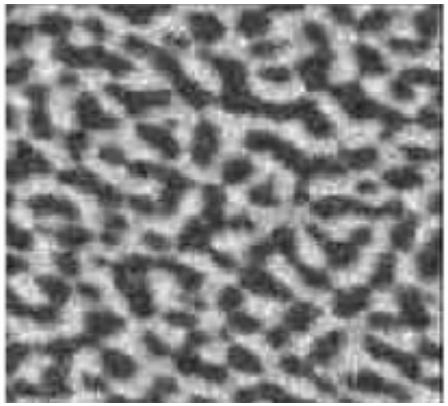

3um

C. Morin et al, J. Electron Spectr.
and Rel. Phenomena 121, 203 (2001)

Phase separation of binary
polymer blends driven
by a photochemical reaction

P(S-*stat*-CMS)/PVME

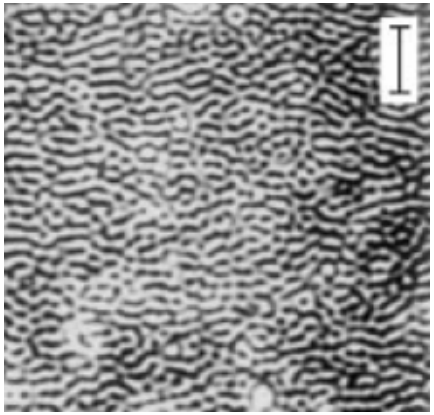

10um

Q. Tran-Cong and A. Harada,
Phys Rev Lett 76,1162 (1996)

stationary or moving
concentration patterns
in reactive adsorbates during
surface chemical reactions

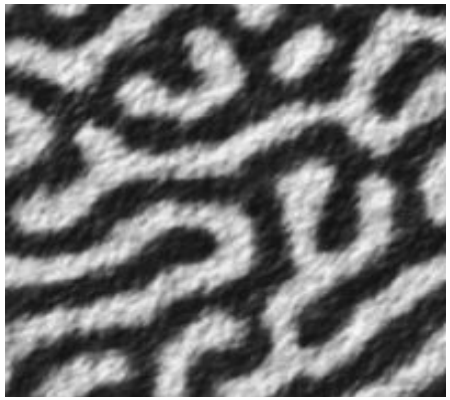

B. Hildebrand et al.;
Phys. Rev. E, 58, 5483 (1998)
Phys. Rev. Lett. 81, 2606 (1998)

Reactive phase separation of metal adspecies

- First experiments with Alkali on Rh(110): formation of O+K rich phases

K/Rh(110) during $H_2 + O_2$ reaction;

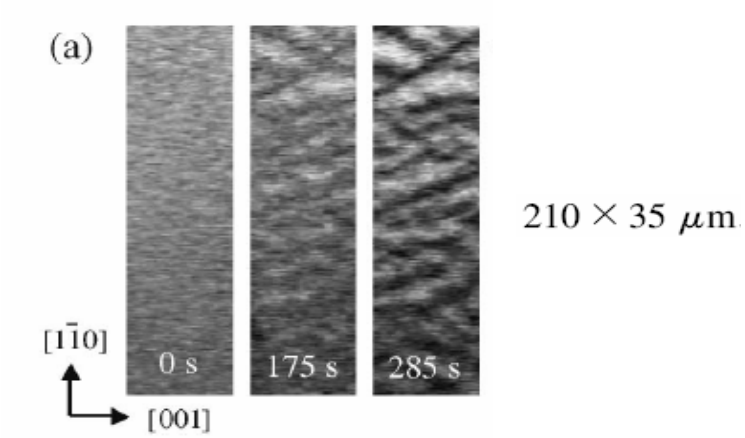

De Decker et al, PRL 92, 198305-1 (2004)

- Numerical simulations predict phase separation.

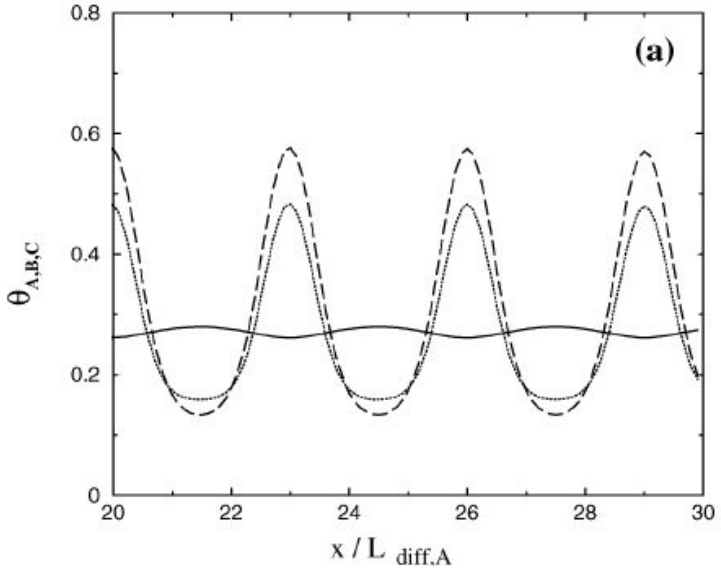

  - Not a Turing pattern! The energetic interactions between adsorbates are responsible for the formation of a pattern and not just an instability of the uniform state due to diffusion.

Surface reorganisation in Au+Pd layers on Rh(110)

LEEM: dynamic phenomena

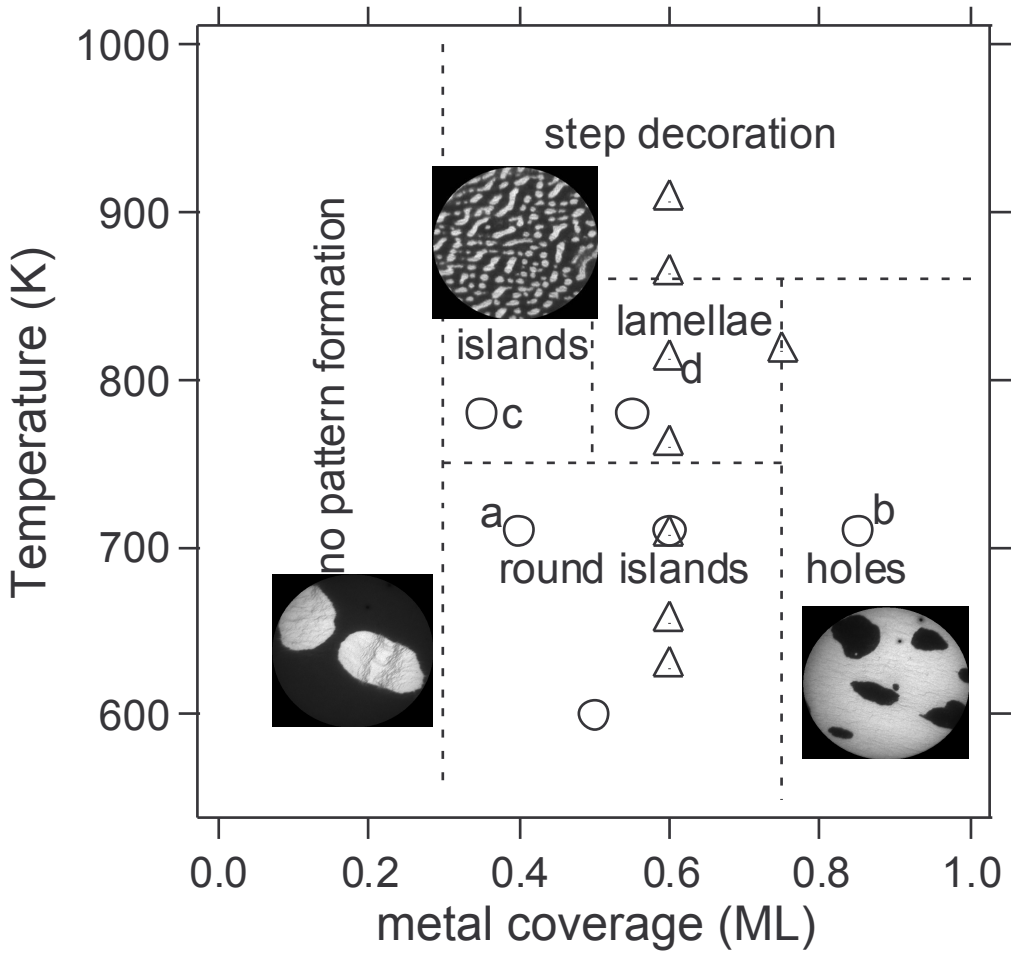

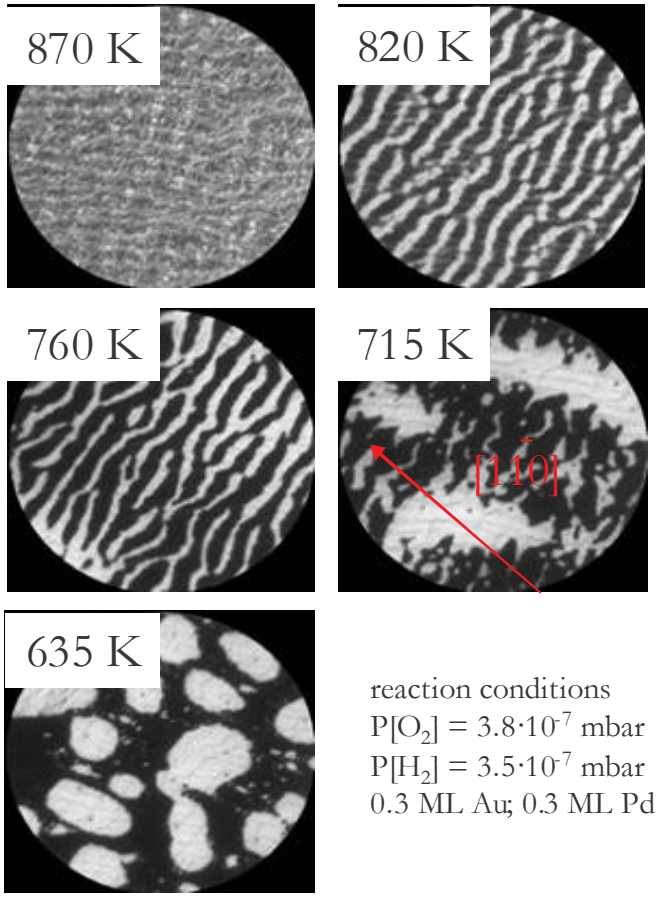

reaction conditions
$P[O_2] = 3.8 \cdot 10^{-7}$ mbar
$P[H_2] = 3.5 \cdot 10^{-7}$ mbar
0.3 ML Au; 0.3 ML Pd

Stripe formation: LEEM investigatoin

- Sub ML Au&Pd is deposited on reduced surface
- Start from homogeneous distribution of Au&Pd
- reaction is started from the uniform state, by increasing the O_2 pressure at fixed H_2 partial pressure
- Formation of lamellae: steady state

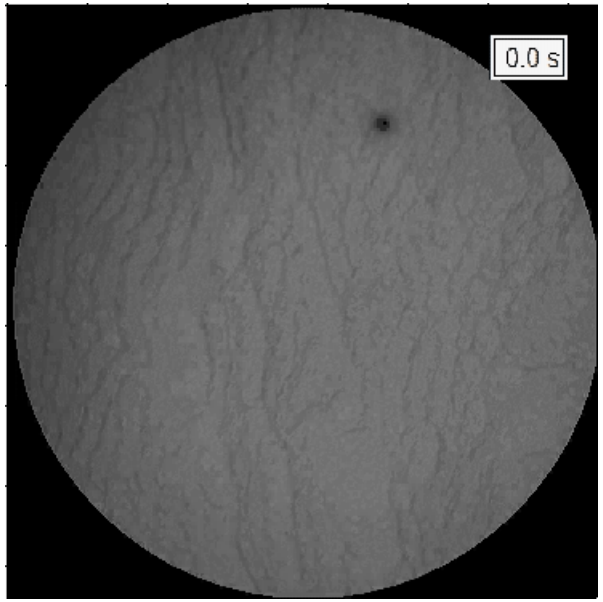

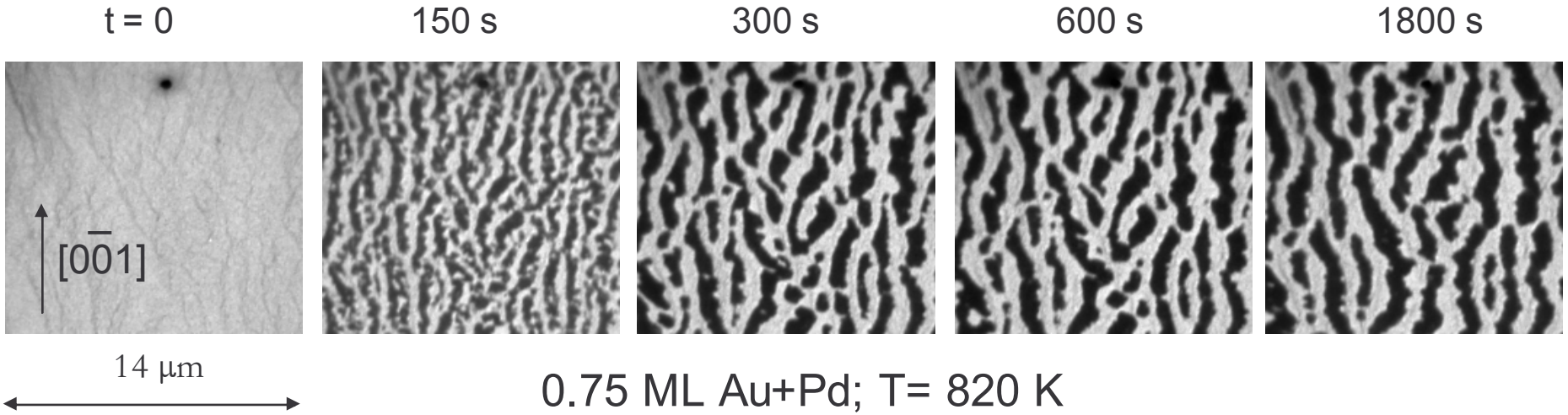

Pattern wavelength dependence on reactants' pressure

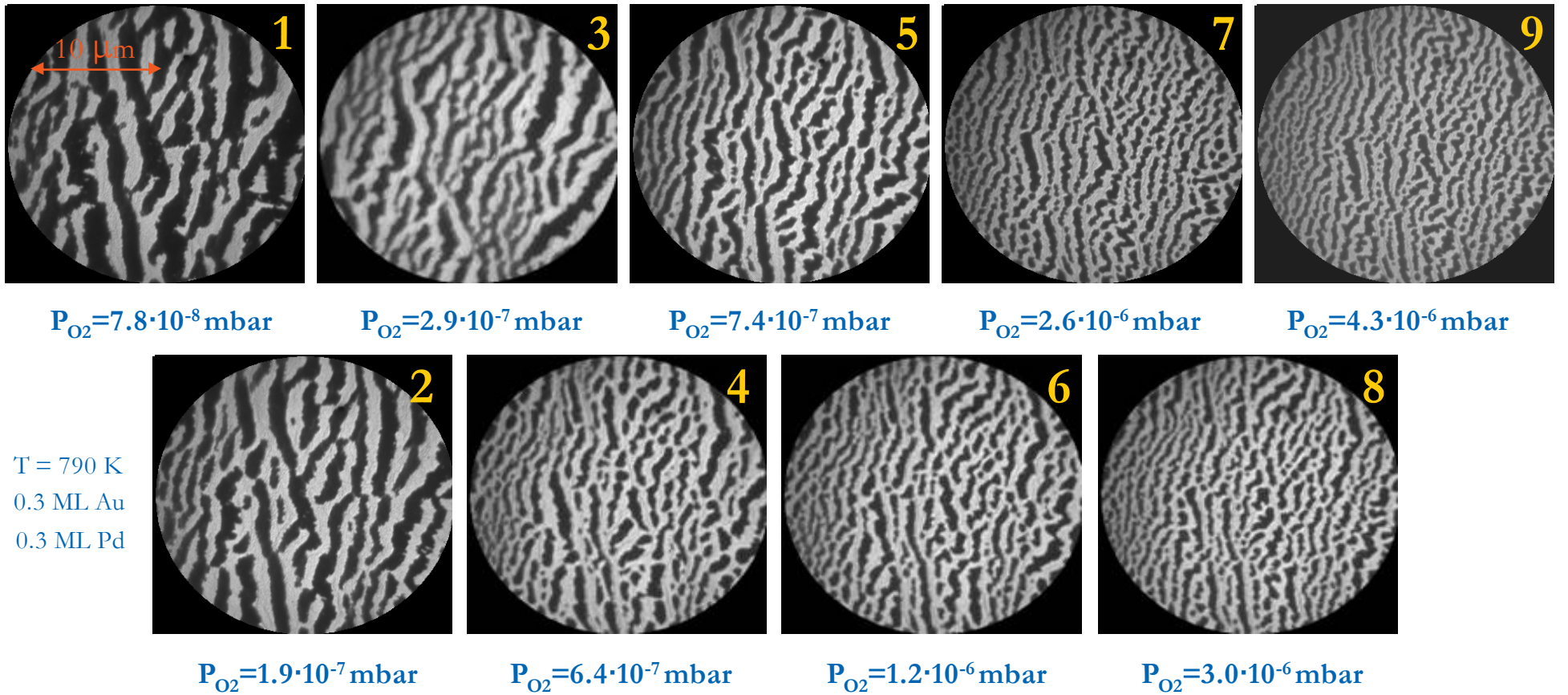

1. The wavelength decreases with increasing reactant pressure
2. Some features of pattern reflect the substrate morphology

Kinetic model

(Y. DeDecker and A.S. Mikhailov, J. Phys. Chem. B 2004, 108, 14759)

A,B molecules from the gas phase; C poison/promoter

$A + *_A \rightarrow A_{ad}$;

$B + *_B \rightarrow B_{ad}$;

$A_{ad} + B_{ad} \rightarrow *_A + *_B + X$; X = product

given D_A,D_B diffusion const., p_A, p_B partial pressure of reactants,

k_A,k_B reaction rate constants and the sticking coefficient for A and B

and provided an attractive/repulsive potential U_{AC} with r_0 (interaction radius)

- **MESOSCOPIC KINETIC EQUATIONS FOR Θ_A Θ_B Θ_C CAN BE DERVIED**
- **INSTABILTY of the UNIFORM STATE → STATIONARY PATTERN**

wavenumber $= \frac{1}{r_0}\left[\frac{2(P_A + \nu_0 b)}{D_A}\right]^{1/4}$

$P_A = k_A p_A$; ν_0 reaction rate const.; $b = \Theta_B$

- Power law of p_A !!!
- The higher p_A → shorter period
- Independent of D_C

Comparison experiment - theory

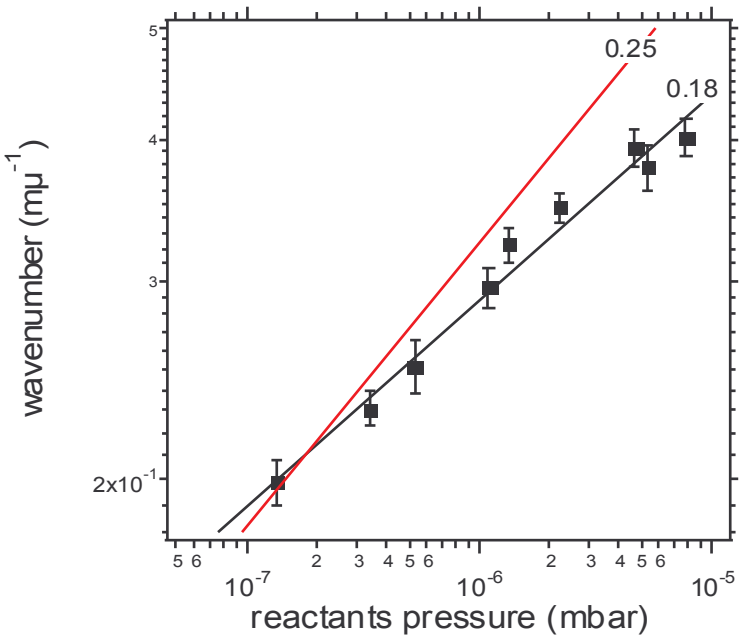

in fair agreement with the CHEMICALLY FROZEN PHASE SEPARATION IN BINARY POLYMER BLENDS DRIVEN BY PHOTOISOMERISATION where power low dependence with exponent 0.2 was measured

T. Otha et al., Macromolecules 31, 6845 (1998).

- **MESOSCOPIC KINETIC EQUATIONS FOR Θ_A Θ_B Θ_C CAN BE DERVIED**
- **APPROXIMATE ANALYTICAL FORMULA FOR PATTERN WAVENUMBER**

$$\text{wavenumber} = \frac{1}{r_0}\left[\frac{2(P_A + v_0 b)}{D_A}\right]^{1/4}$$

- Power law of p_A !!!
- The higher $p_A \rightarrow$ shorter period
- Independent of D_C

$P_A = k_A p_A$; v_0 reaction rate const.; $b = \Theta_B$

Pattern composition: phase separation Pd+Au/O

- Full phase separation at T< 750

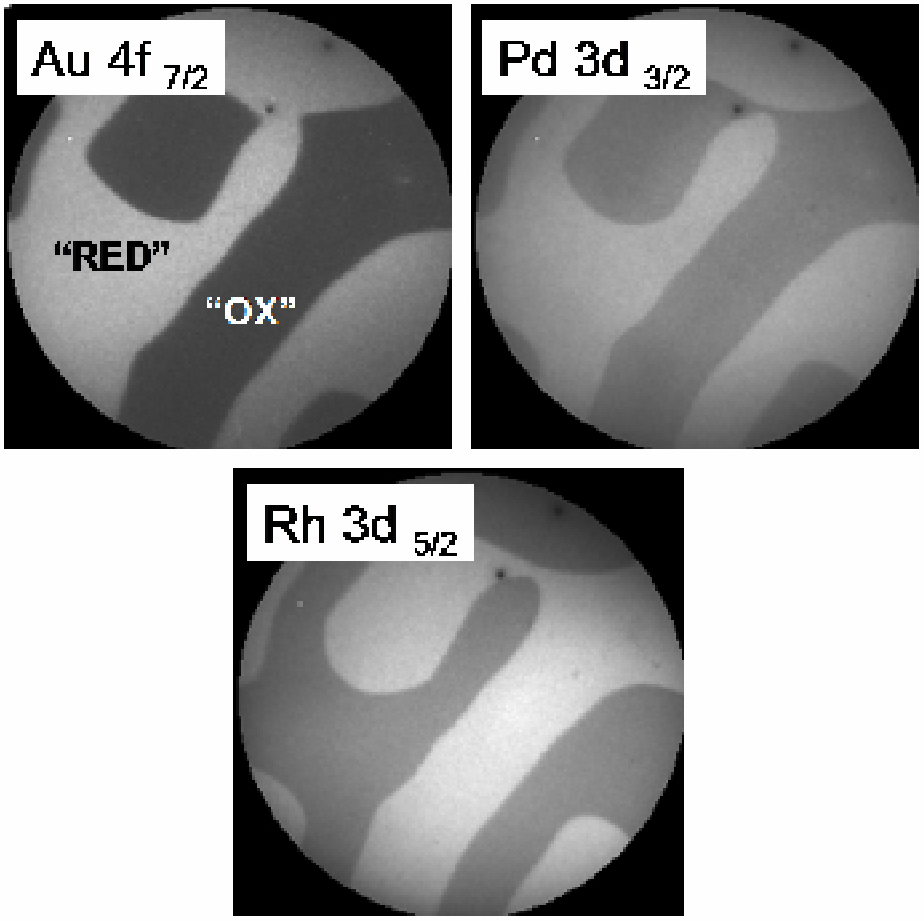

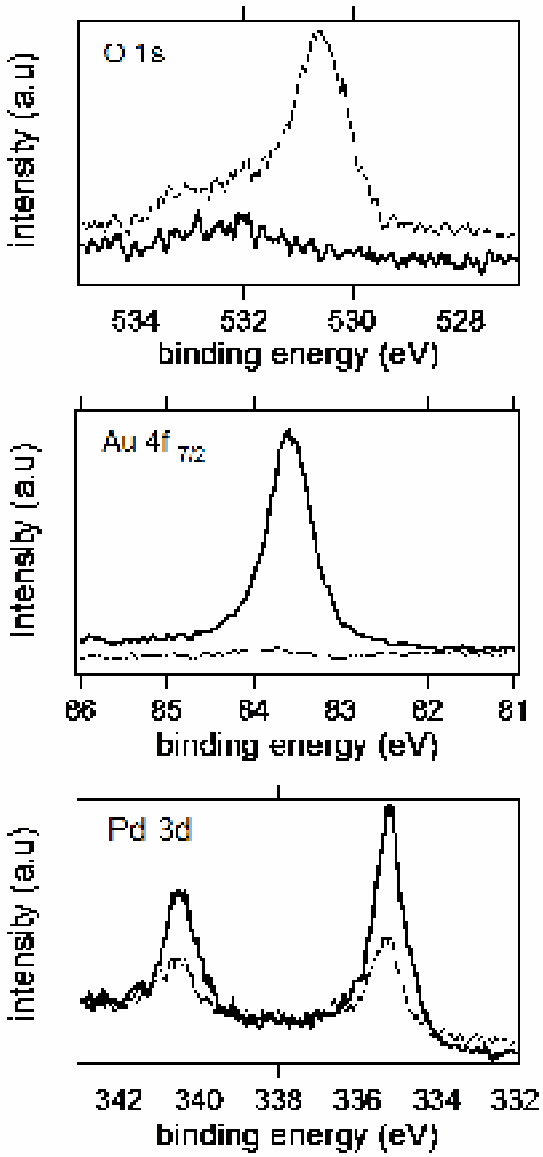

Pattern composition: Pd+Au/O

- Partial phase separation in the striped phase

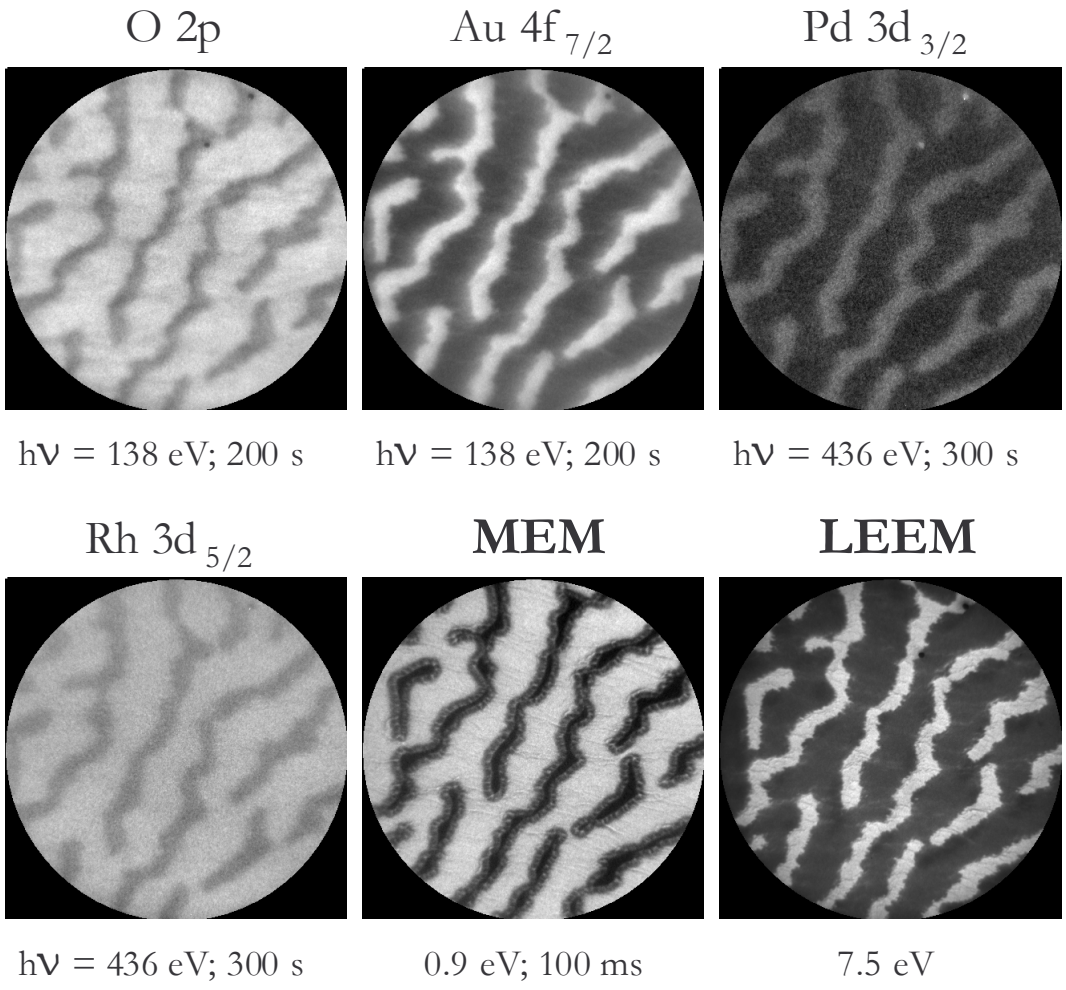

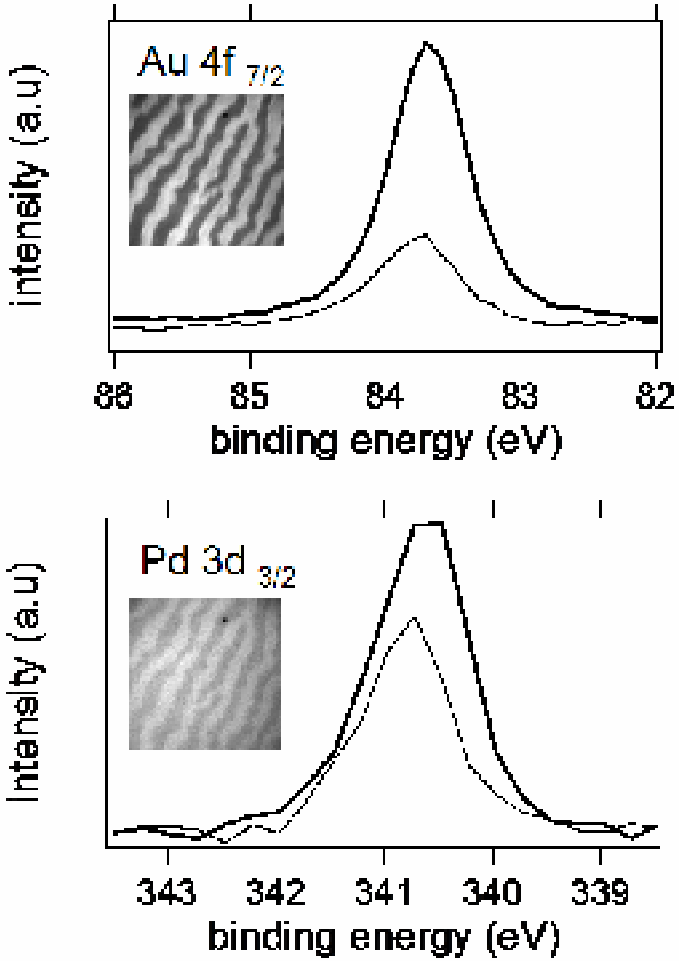

Conclusions

- Mass transport of metal adlayer strongly reorganizes the interfaces: development of "**microstructures**" which may show different catalytic properites.
- The lateral composition of a modified catalyst surface strongly depend on **reaction conditions, but this in turn affects reactivity…**
- The surface reorganisation can be interpreted as a **reactive phase separation**. The pattern **morphology** can be controlled through reaction parameters (P,T) and the coverage of the adspecies.
- Lamellar structures wavelength obeys power low
- Pathway to formation of adaptive microstructures

3.4 Applications of XPEEM

CHEMICAL IMAGING

Applications in biology

Polymer blends

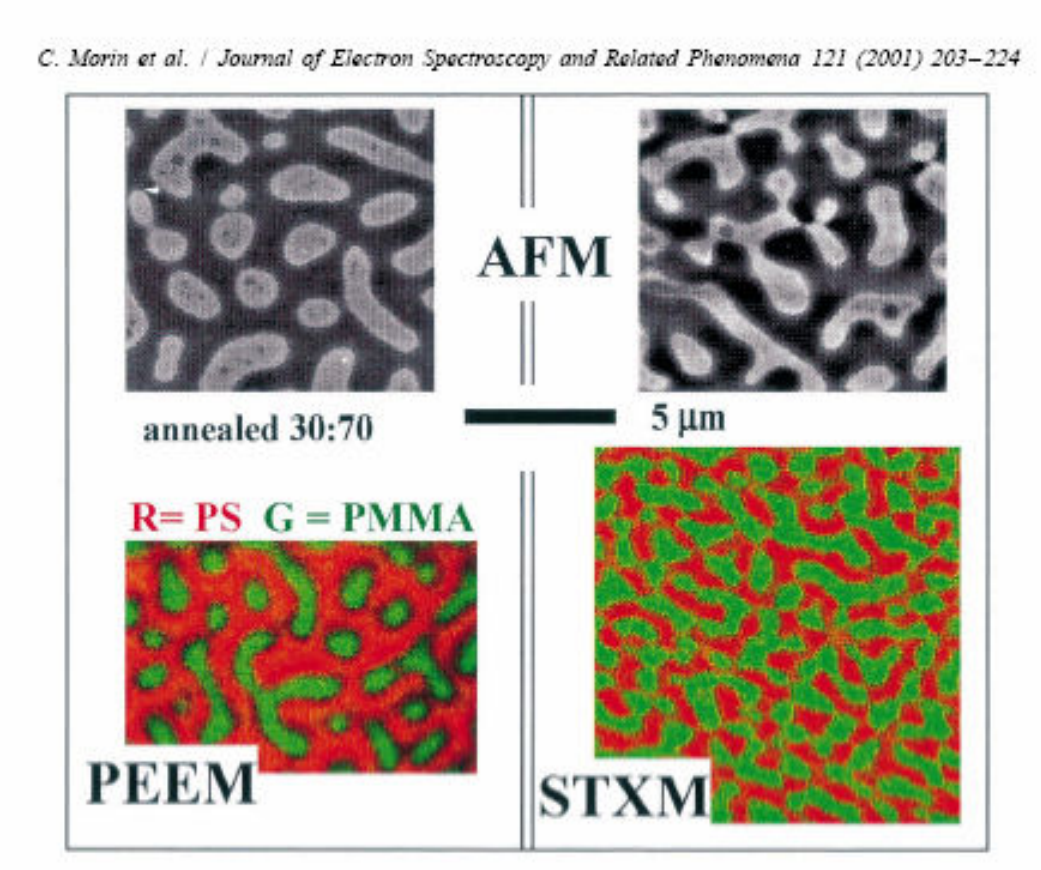

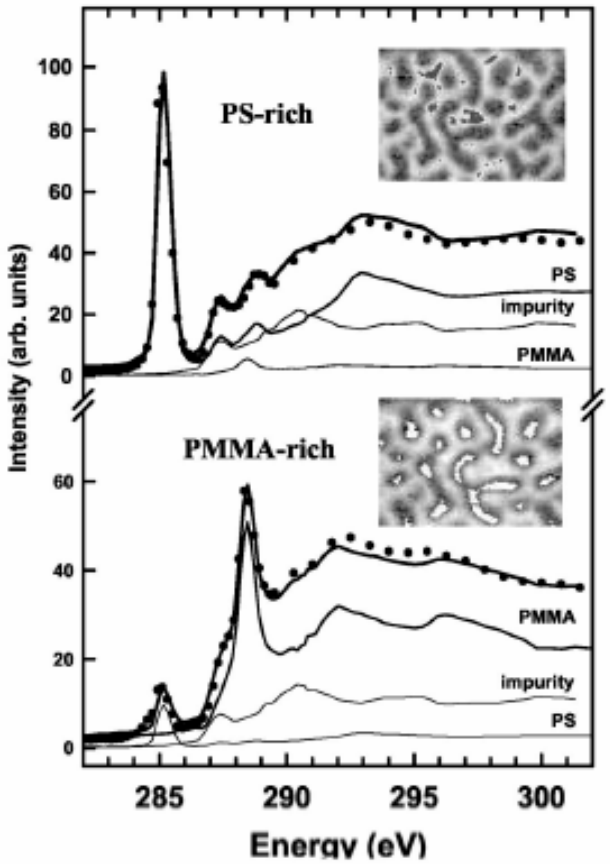

Application in biology

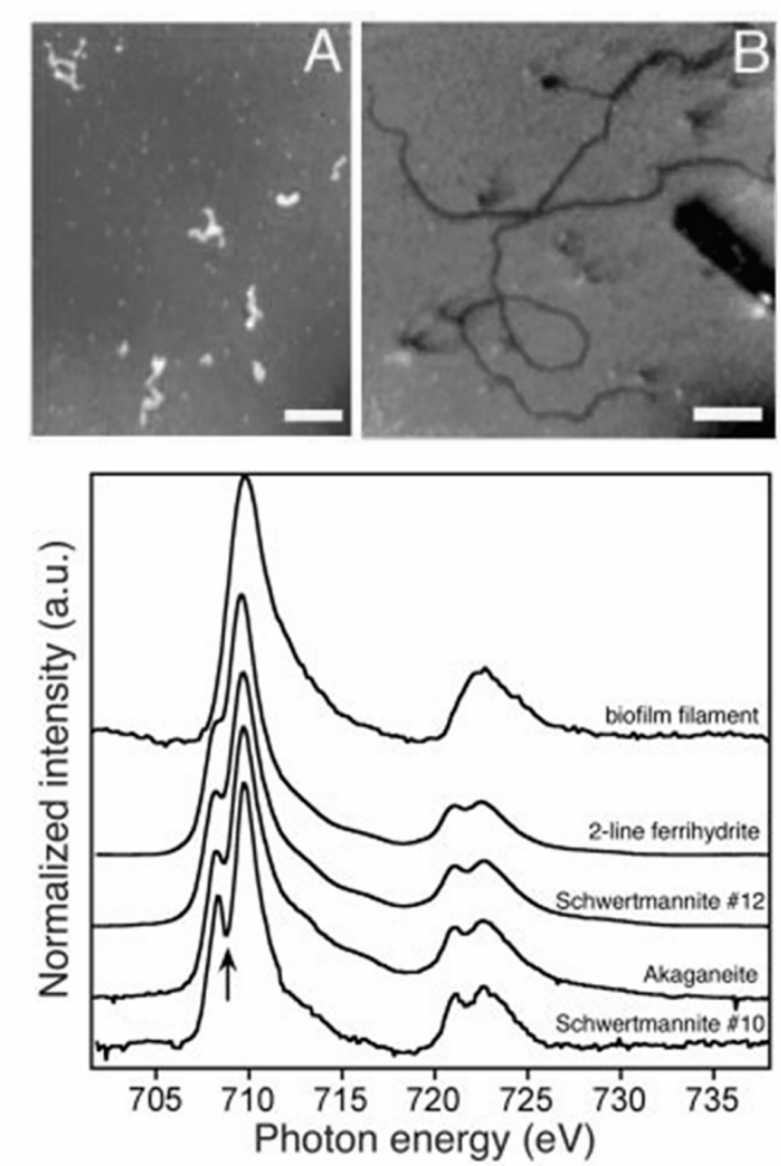

- Bio-mineralization resulting from microbal activity
- X-PEEM images of:
  - (A) non mineralized fibrils from the cloudy water above the biofilm (scale bar, 5 um)
  - (B) mineralized filaments and a sheath from the biofilm (scale bar, 1 um);

- X-PEEM Fe L-edge XANES spectra of the FeOOH mineralized looped filament shown in (B), compared with iron oxyhydroxide standards, arranged (bottom to top) in order of decreasing crystallinity, as measured by x-ray diffraction peak broadening. only fibrils containing polymer strands(polysaccharides) can template akaganeite pseudo-single crystals with aspect ratios of 1000:1

2004 *Science* **303** 1656-1658

4. Applications of XMCD and XMLD PEEM

MAGNETIC IMAGING

Motivations

- Magnetic domains in nanostructures: comparison experiment-theory
- Magnetic domains in thin films: understanding of magnetic state in correlation with structure and morphology
- FM/AFM interfaces; exchange bias; understanding of interfacial spin pinning; understanding of AFM spin structure
- Magnetisation dynamics

XMCD principles

- X-ray magnetic circular dichroism **XMCD** is the dependence of x-ray absorption on the relative orientation of the local magnetization and the polarization vector of the circularly polarized light

- In the case of ferromagnets (Ni, Fe, Co) **3d electrons** determine magnetic properties:
  - $m_s = \langle N_{up} - N_{down} \rangle m_b$ for Co 1.64 m_b
  - $m_o << m_s$ for Co 0.14 m

- We **PROBE** 3d elements by exciting 2p into unfilled 3d states
  - 2p → 3d channel dominant
  - White line intensity proportional to number of holes
  - Sum rules to determine m_s and m_o

XMCD principles

Experimental Confirmation of the X-Ray Magnetic Circular Dichroism Sum Rules for Iron and Cobalt

PRL 75, 152; 1995

C. T. Chen,[1] Y. U. Idzerda,[2] H.-J. Lin,[1,*] N. V. Smith,[1,†] G. Meigs,[1] E. Chaban,[1] G. H. Ho,[3,*] E. Pellegrin,[1] and F. Sette[1,‡]

SUM RULES

$$m_{\text{orb}} = -\frac{4\int_{L_3+L_2}(\mu_+ - \mu_-)\,d\omega}{3\int_{L_3+L_2}(\mu_+ + \mu_-)\,d\omega}(10 - n_{3d}), \quad (1)$$

$$m_{\text{spin}} = -\frac{6\int_{L_3}(\mu_+ - \mu_-)\,d\omega - 4\int_{L_3+L_2}(\mu_+ - \mu_-)\,d\omega}{\int_{L_3+L_2}(\mu_+ + \mu_-)\,d\omega} \times (10 - n_{3d})\left(1 + \frac{7\langle T_z\rangle}{2\langle S_z\rangle}\right)^{-1}, \quad (2)$$

$\langle T_z \rangle$ is the expectation value of the magnetic dipole operator

$\langle S_z \rangle$ is equal to half of m_{spin}

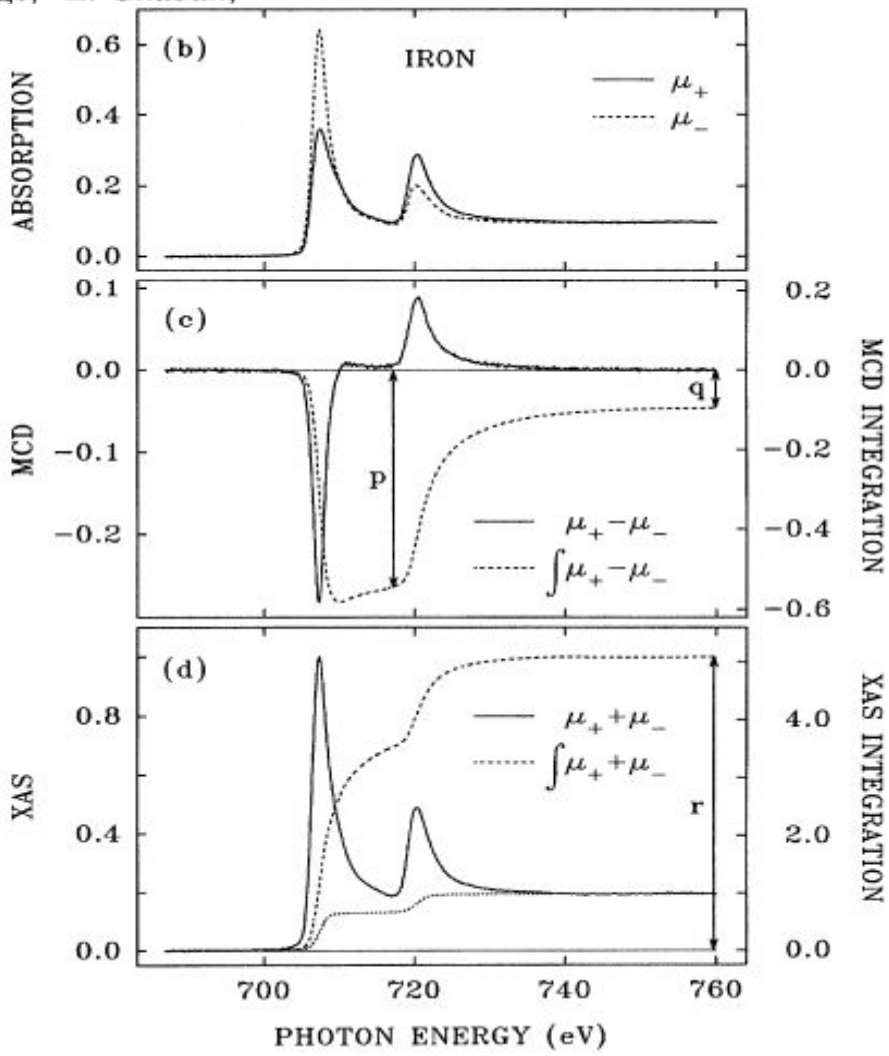

REFERENCES

B. T. Thole, P. Carra, F. Sette, and G. van der Laan, Phys. Rev. Lett. 68, 1943 (1992); P. Carra, B. T. Thole, M. Altarelli, and X.Wang, Phys. Rev. Lett. 70, 694 (1993), J.Stöhr et al, Phys. Rev. Lett. 75 (1995) 3748.

An example: Co/W(110)

XMCD = $(L_2-L_3)/(L_2+L_3)$

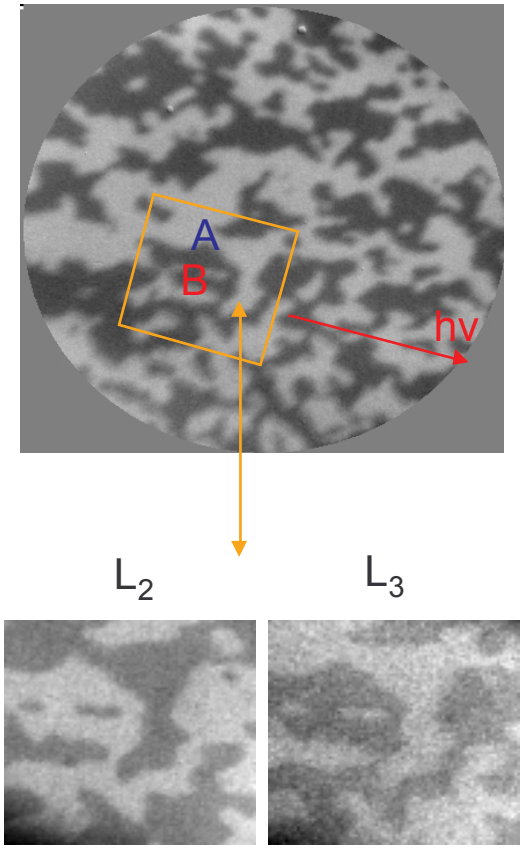

10 ML Co / W{110}

$$m_{spin}=-(6p-4q)*(1-n_d)/r*(1/deg_{CP})$$

$$m_{orb}=-4/3*(1-n_d)*q/r*(1/deg_{CP})$$

n_d[Co] = 7.51; deg_{CP}= degree of circular polarization

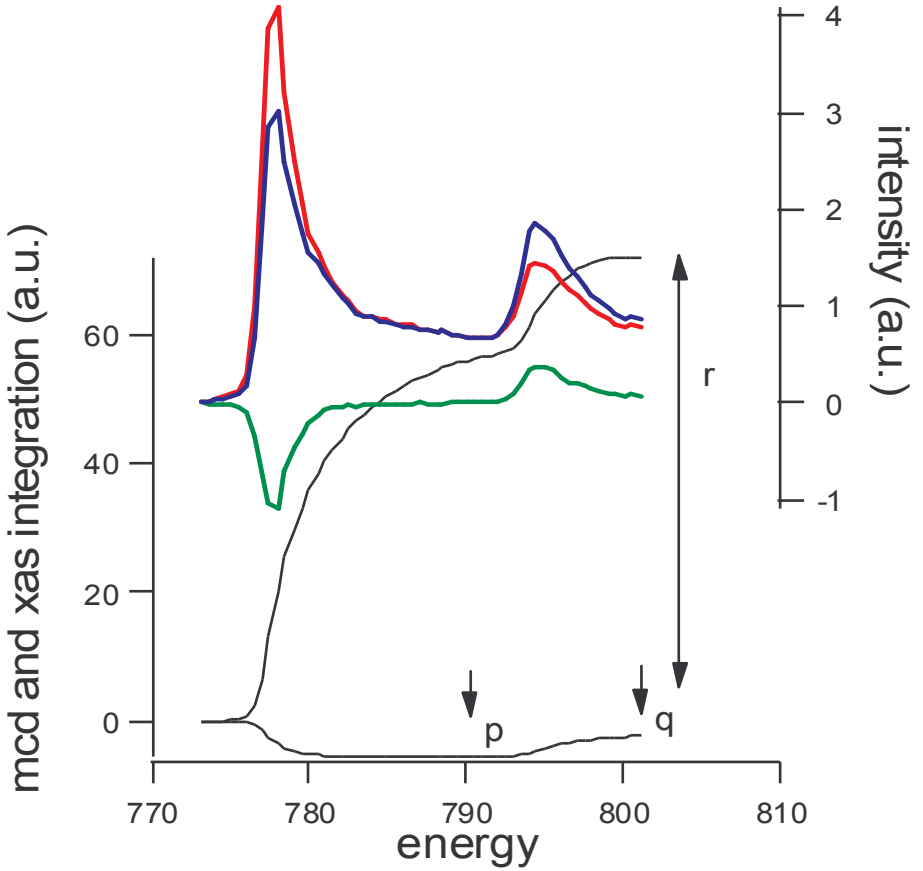

XMLD

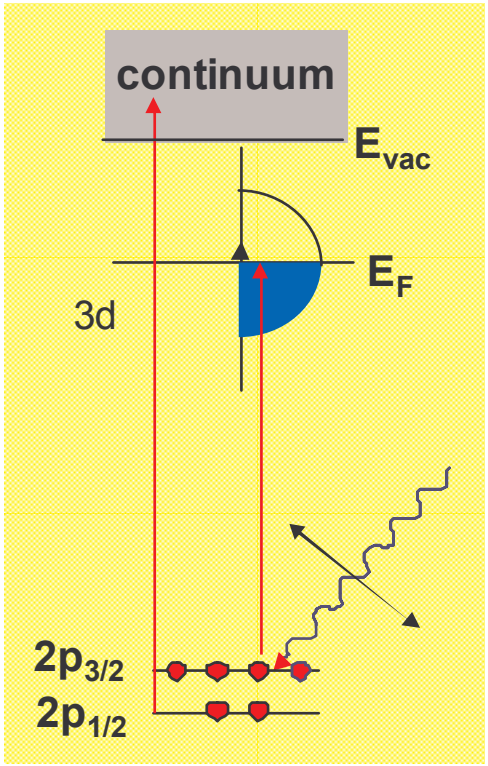

anti-ferromagnetic

absorption intensity at resonance

$$I(\vartheta,\theta,T) = a + b(3\cos^2\vartheta - 1)\langle Q_{zz}\rangle + c(3\cos^2\theta - 1)\langle M^2\rangle_T + d\sum_{i,j}\langle \hat{s}_i \cdot \hat{s}_j\rangle_T$$

Q_{zz} = quadrupole moment of charge, "linear dichroism"

ϑ is the angle of $\vec{E}$ with the crystallographic z axis.

2nd term determines XMLD effect

Θ is the angle between E and magnetic axis A

M reflects long range magnetic order

XMLD at max. for E ∥ A

Examples: XMCD and XMLD

Direct observation of the alignment of ferromagnetic spins by antiferromagnetic spins

F. Nolting*, A. Scholl*, J. Stöhr†, J. W. Seo‡§, J. Fompeyrine§, H. Siegwart§, J.-P. Locquet§, S. Anders*, J. Lüning†, E. E. Fullerton†, M. F. Toney†, M. R. Scheinfein‖ & H. A. Padmore*

Nature, 405 (2000), 767.

Figure 1 Images and local spectra from the antiferromagnetic and ferromagnetic layers for 1.2-nm Co on $LaFeO_3/SrTiO_3(001)$. **a**, Fe L-edge XMLD image; **b**, Co L-edge XMCD image. The contrast in the images arises from antiferromagnetic domains in $LaFeO_3$ (**a**) and ferromagnetic domains in Co (**b**) with in-plane orientations of the antiferromagnetic axis and ferromagnetic spins as indicated below the images. The spectra shown underneath were recorded in the indicated areas and illustrate the origin of the intensity contrast in the PEEM images.

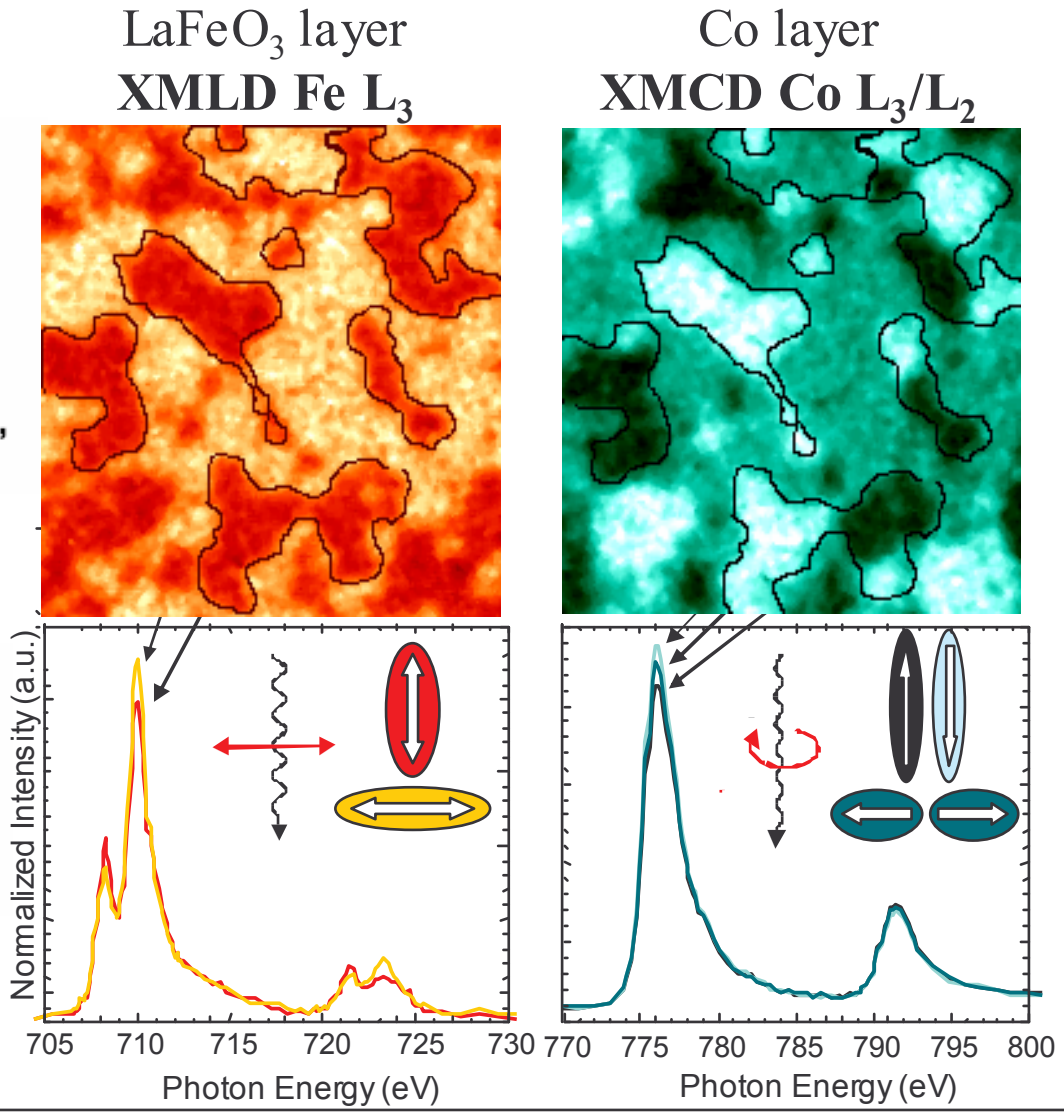

XMCD and XMLD PEEM

- Unique means to obtain spectra from small volumes

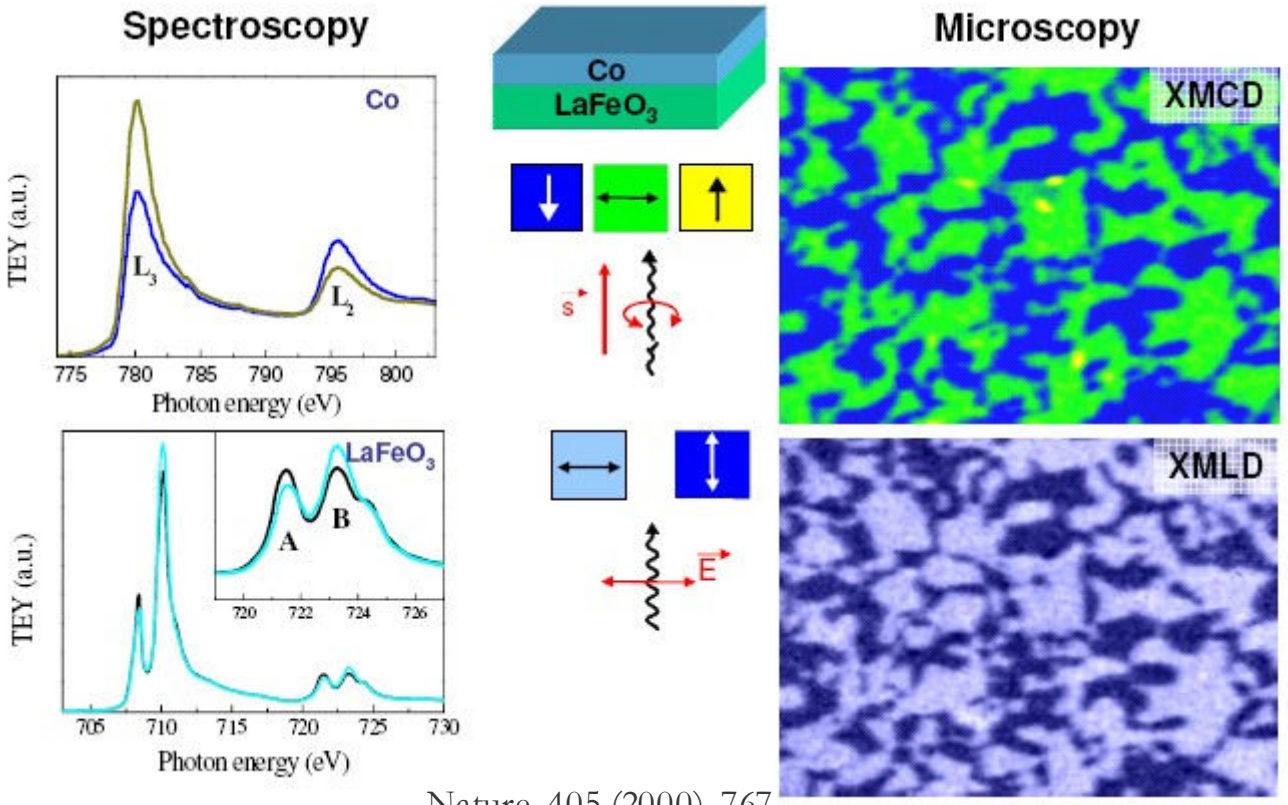

Nature, 405 (2000), 767.

- Parallel and antiparallel alignment of M and helicity determine maximum contrast;
- sum rules available allow obtaining spin and orbital magnetic moments from the spectra
- anisotropic electronic charge distribution, which can be caused either by magnetism or a a lower than cubic symmetry of the unit cell (Magnetostriction, substrate effects, and the lattice type)

ferromagnet/antiferromagnet Co/LaFeO3 bilayer, demonstrating interface exchange coupling between the two materials

MnAs/GaAs(100): epitaxial films

- Two phases coexist at RT
  - Hexagonal α phase (FM)
  - Orthorombic β phase (PM)

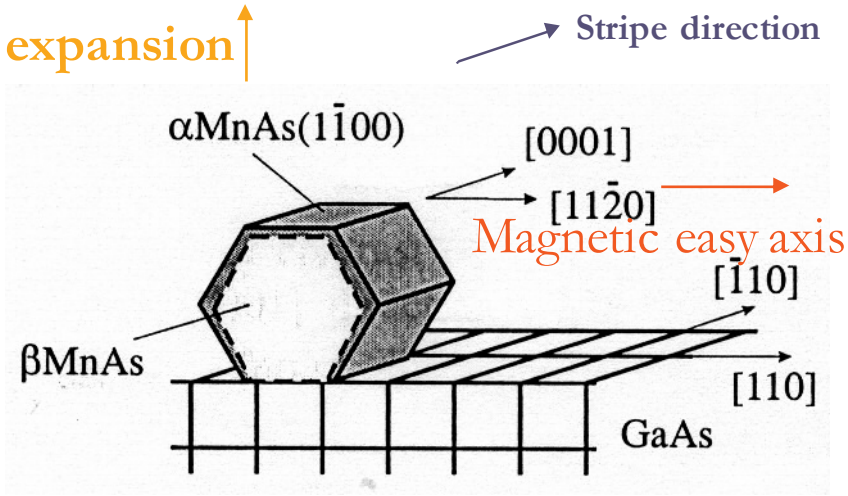

Very large misfit along [0001] direction
→ coincidence lattice

7% misfit along [11-20] direction → strain
Strain relaxation expansion normal to the film

- Stripes along [0001]
- Stripe periodicity depends on film thickness
- Interesting magnetic domain configurations
- First XMCD-PEEM study:

Bauer et al, J. Vac. Sci. Technol. B **20** (2002), p. 2539.

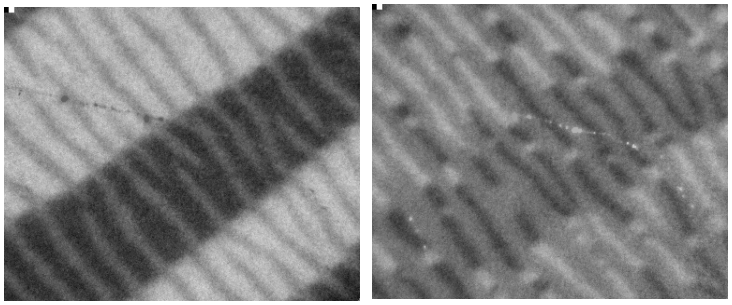

ferromagnetic-paramagnetic phase transition by XMCD-PEEM

215 nm thick MnAs film on GaAs(100) during heating from 10° C to 40° C

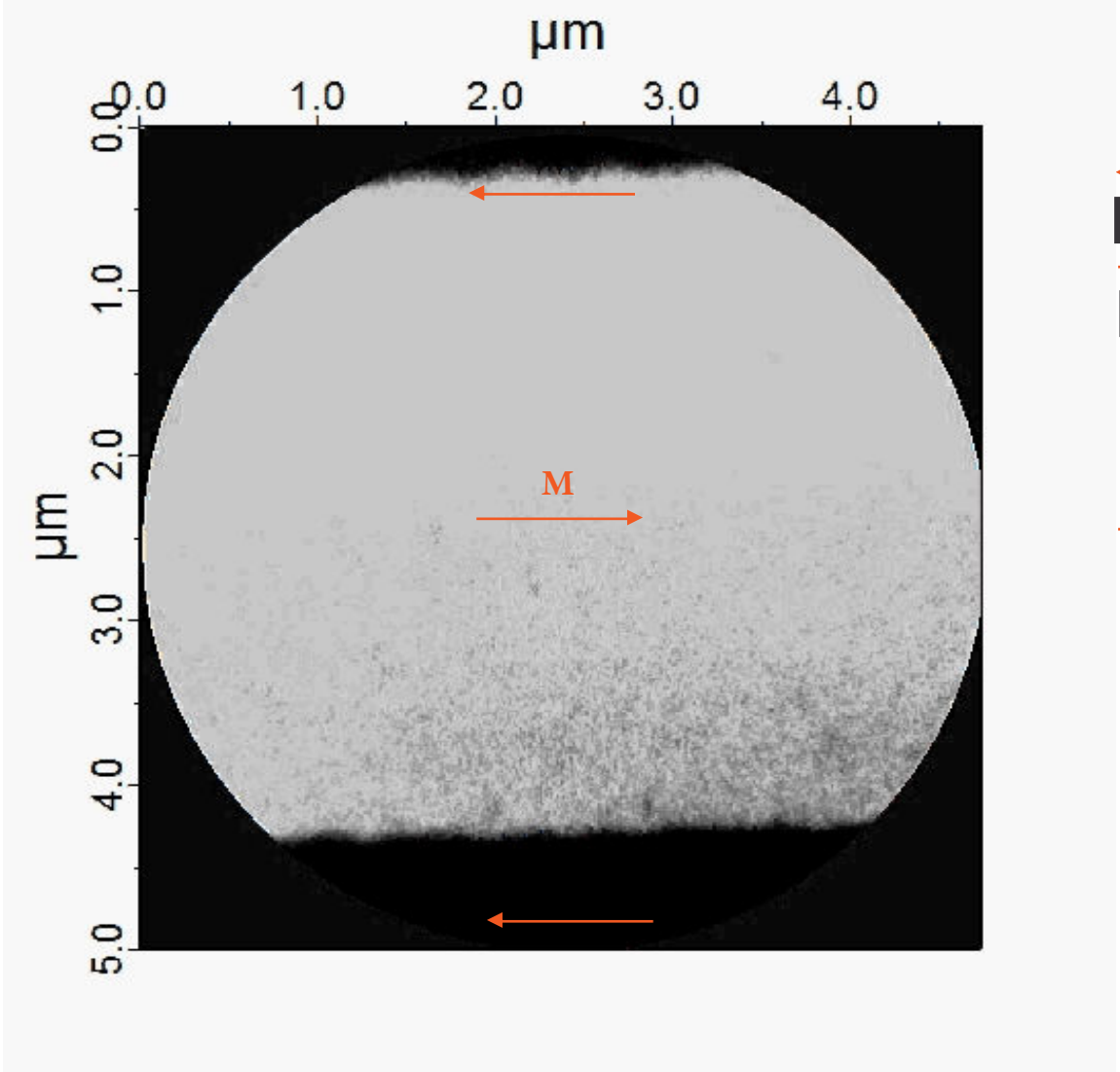

Domain structure dependence on stripe width

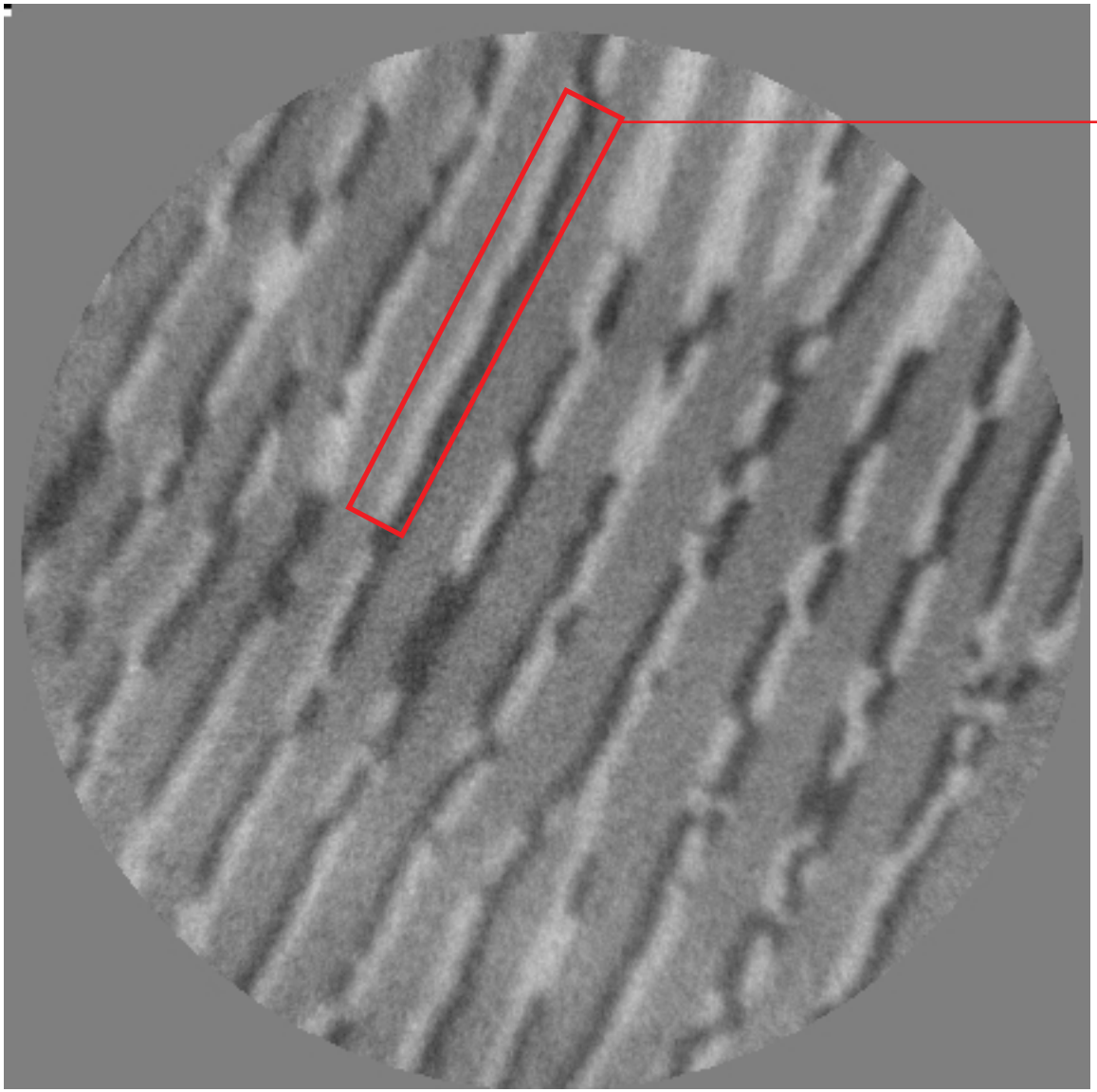

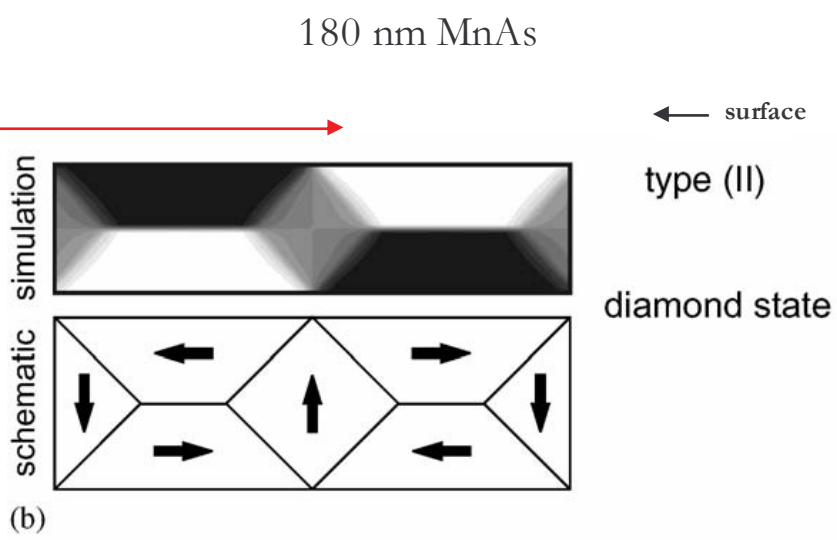

- Straight walls
- Head to head domains
- Cross sectional cut: diamond state

R. Engel-Herbert et al,
J. Magn. Magn. Mater. 305 (2006) 457

Domain structure dependence on stripe width

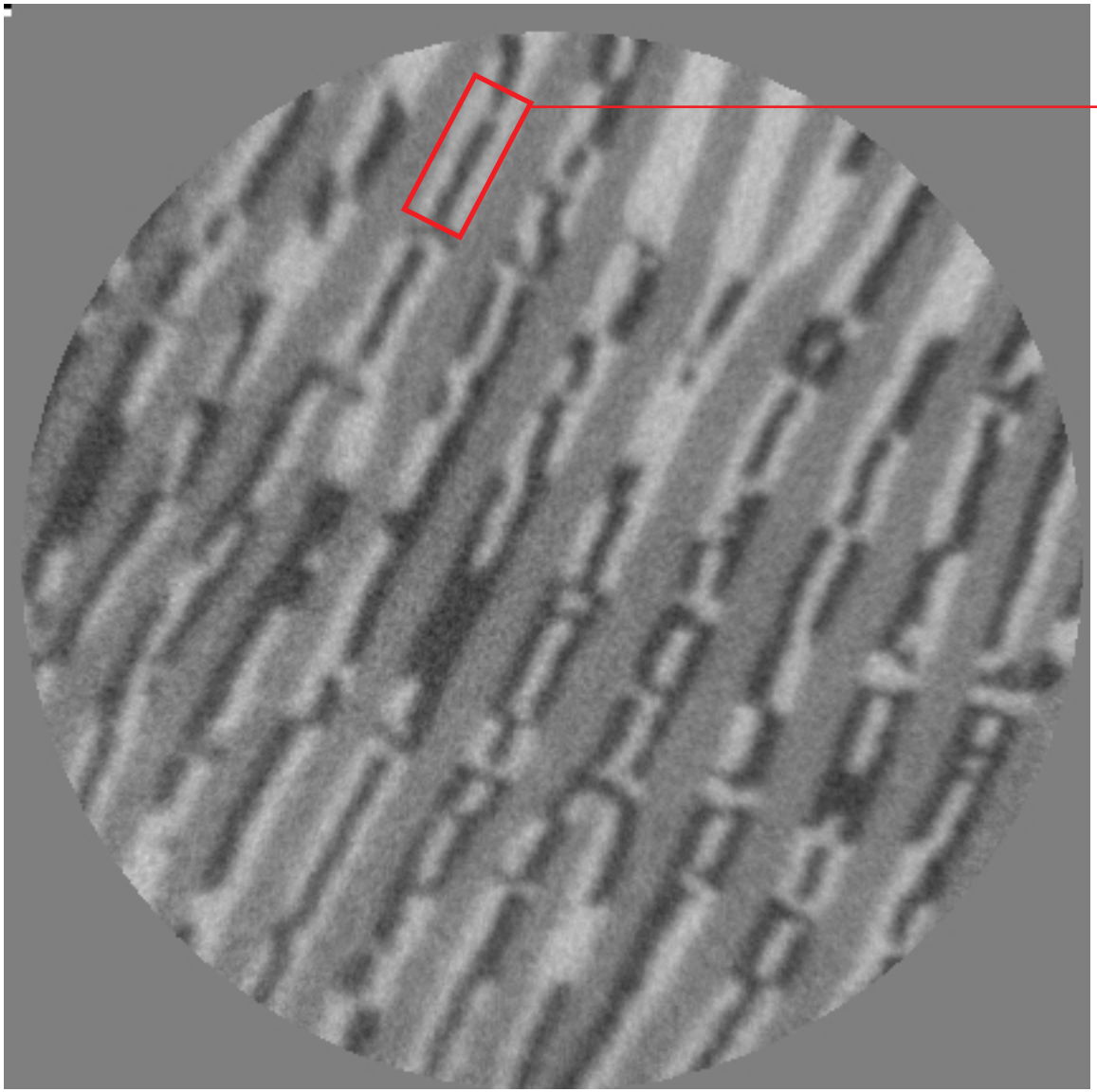

180 nm MnAs

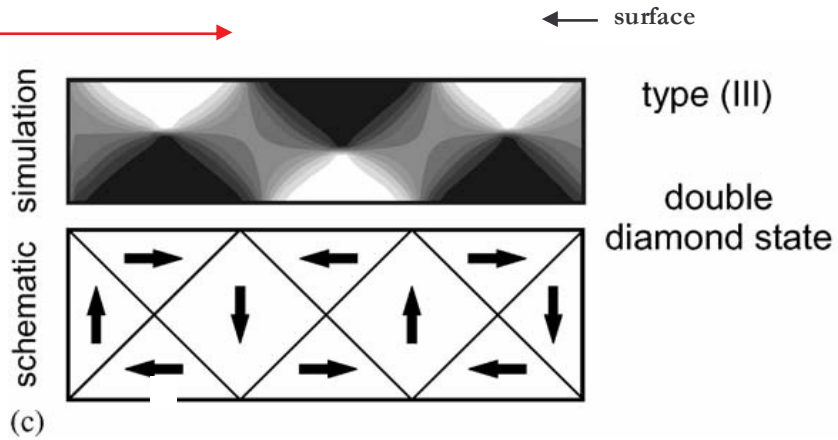

- Straight walls
- Head to head domains
- Cross sectional cut: double diamond state
- Never observed below 150 nm

R. Engel-Herbert et al,
J. Magn. Magn. Mater. 305 (2006) 457

Domain structure dependence on stripe width

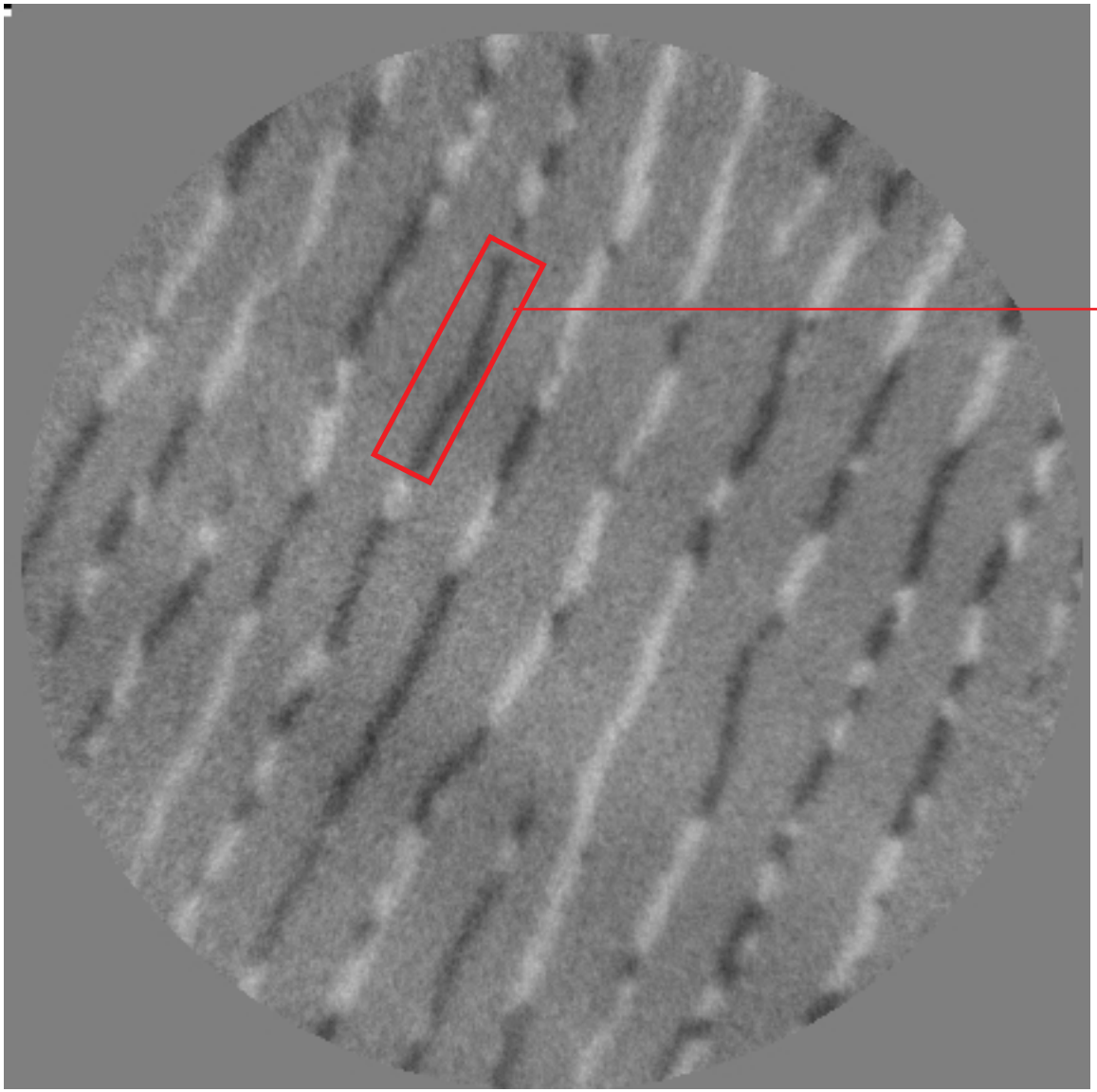

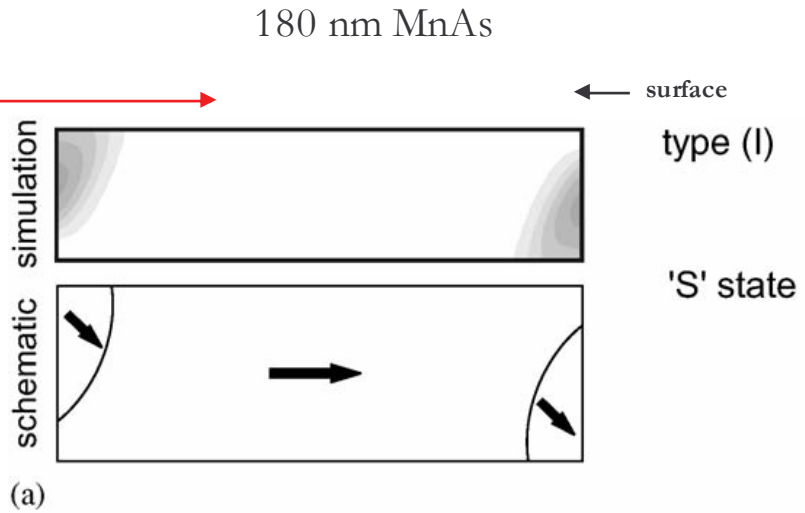

R. Engel-Herbert et al,
J. Magn. Magn. Mater. 305 (2006) 457

References on magnetic imaging

- [4.1] Stöhr J, Padmore H A, Anders S, Stammler T, Scheinfein MR *1998 Surf. Rev. Lett.* **5** 1297.
- [4.2] Feng J and Scholl A 2007 *"Photoemission Microscopy"* in: *Science of Microscopy*, Eds. Hawkes P W, Spence J C H (Springer, Berlin) (also in chapter 4 as 4.2)
- [4.3] Stöhr J and. Siegmann H C 2006 *Magnetism* (Springer, Berlin)

8. Applications of XPEEM

TIME RESOLVED
MAGNETIC IMAGING

Motivation of time resolved magnetic imaging

- Switching processes (magnetisation reversal) in magnetic elements (in spin valves, tunnel junction)
  - Nucleation, DW propagation or both?
  - Effect of surface topography, morphology crystalline structure etc.
  - Domain dynamics in Landau flux closure structures.
- response of vortices, domains, domain walls in Landau closure domains in the precessional regime
- 2 class of processes:
  - Reversible process (stroboscopic technique)
  - Irreversible process (before - after)

Pulse injection experiments

Kläui *et al*, Appl. Phys. Lett. 88, 232507 (2006)

Imaging of magnetization before and after individual 11 μs current pulses with various amplitudes

Curent and future experiments: not only **"before"** ad **"after"** but also **"during"**

Vortex wall motion,
nucleation and annihilation

Vortex wall **velocity**

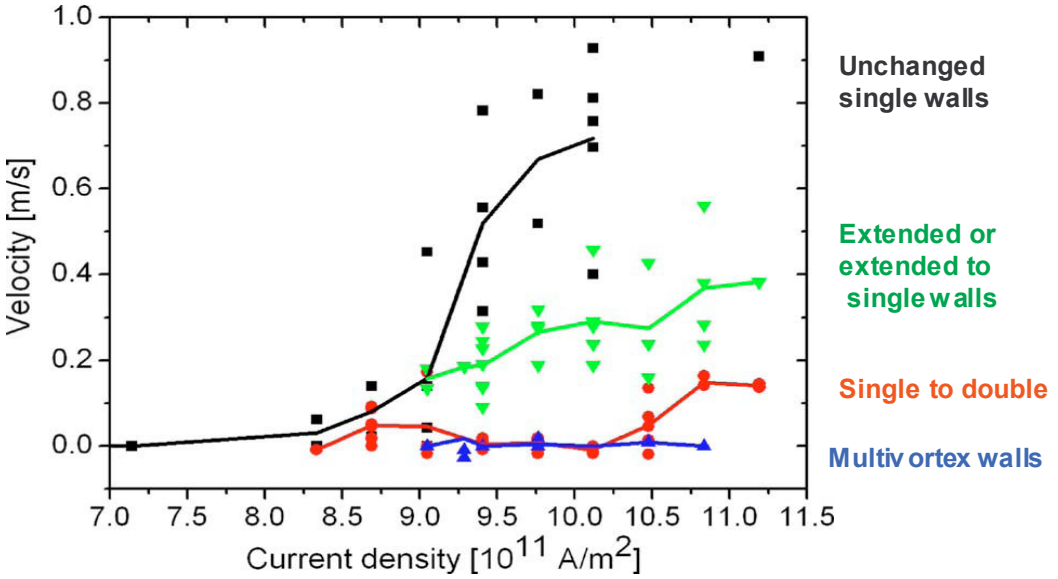

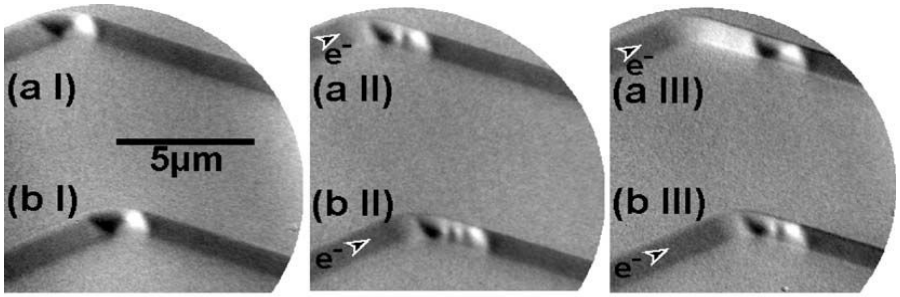

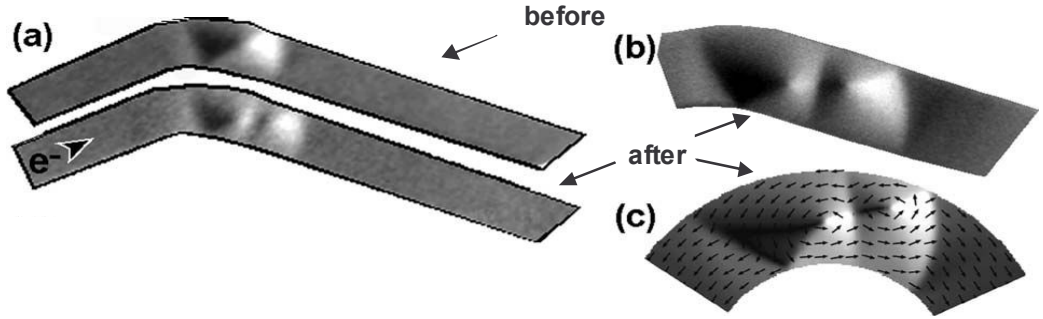

Time resolved PEEM techniques for magnetic imaging

Stroboscopic experiments combine high lateral resolution of PEEM with high time resolution, taking advantage of pulsed nature of synchrotron radiation

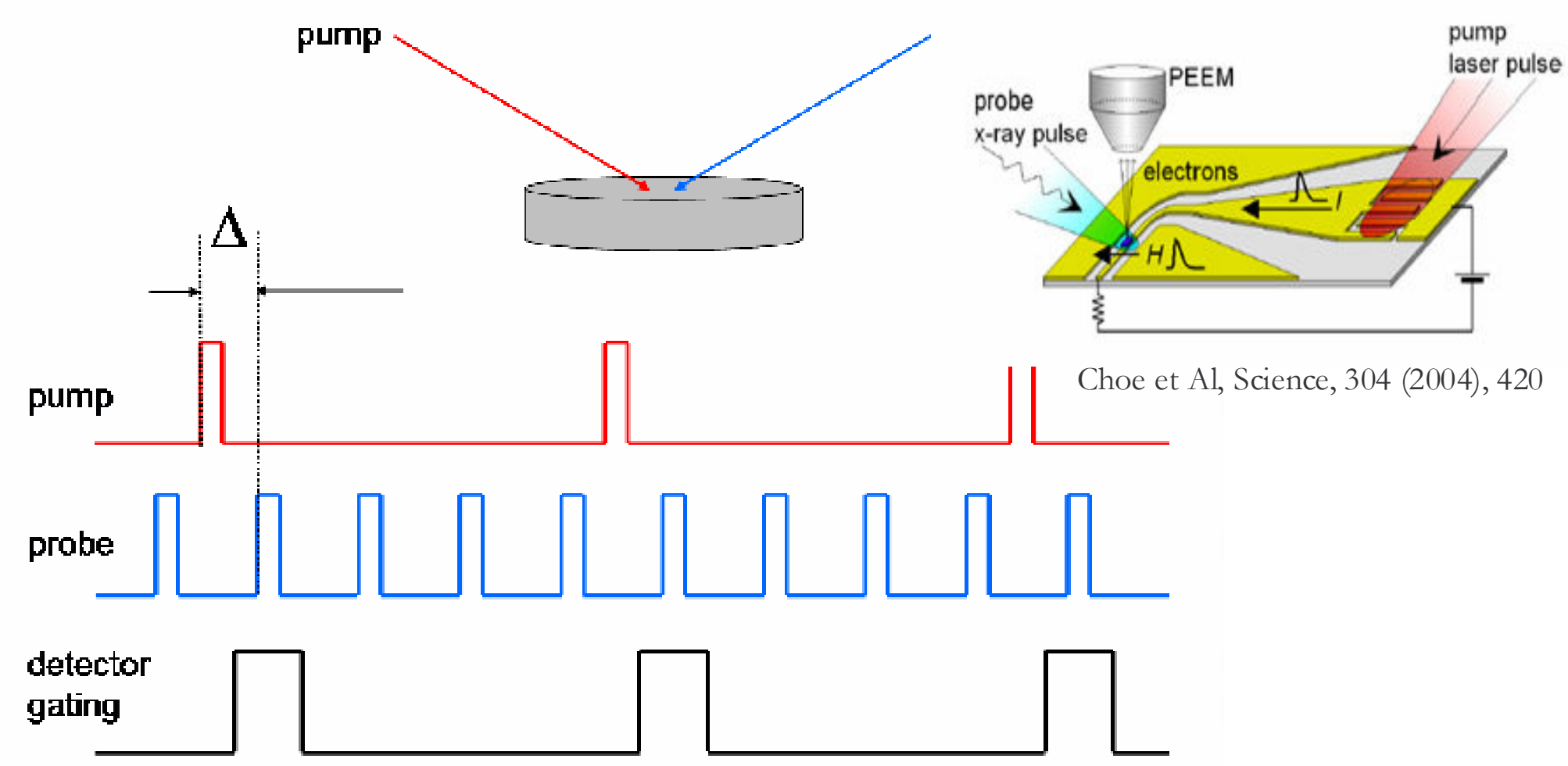

Choe et Al, Science, 304 (2004), 420

Domain dynamics in Py rectangular microstructures

Schneider C M, Krasyuk A, Nepijko S A, Oelsner A, Schönhense A, 2006 *Journal of Magnetism and Magnetic Materials* **304** 6-9.

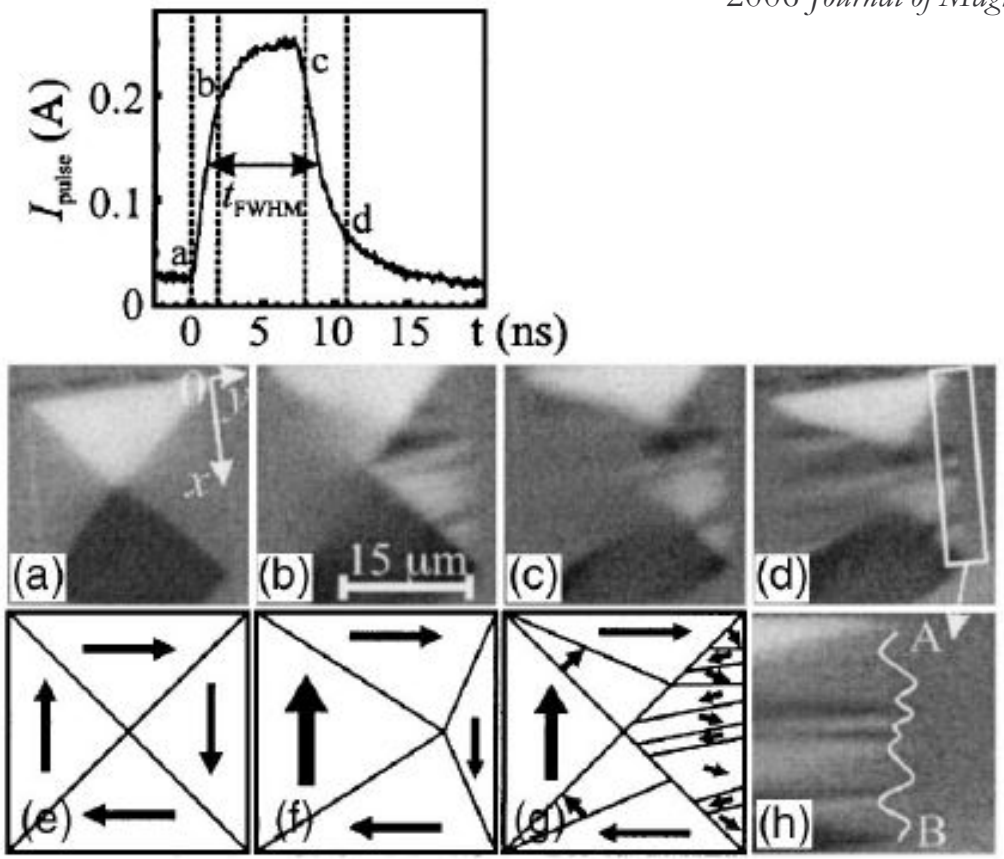

(top) pulse shape of the external field excitation; (a-d) snapshots at selected time intervals;
(e-g) corresponding expected domain configuration in the Landau structure;
(h) aberration induced by Lorentz force due to the stray field of stripe-like domains.
The external field acts in the direction of the x axis.

Magnetic excitations in LFC structures

PRL 94, 217204 (2005)

Quantitative Analysis of Magnetic Excitations in Landau Flux-Closure Structures Using Synchrotron-Radiation Microscopy

J. Raabe,[1,*] C. Quitmann,[1] C. H. Back,[2] F. Nolting,[1] S. Johnson,[1] and C. Buehler[1]

The time dependent magnetization is described by the phenomenological Landau-Lifshitz-Gilbert equation

$$\frac{d}{dt}\vec{M} = -\gamma_0 \vec{M} \times \vec{H}_{\text{eff}} + \frac{\alpha}{M}\left(\vec{M} \times \frac{d}{dt}\vec{M}\right).$$

The first term describes the precession of the magnetization $\vec{M}$ about the total effective field $\vec{H}_{\text{eff}}$. The second term describes the relaxation back into the equilibrium state using the dimensionless damping parameter α.

torque $\vec{T} = -\gamma_0 \vec{M} \times \vec{H}_{\text{eff}}$

xmcd

t_i-t_0

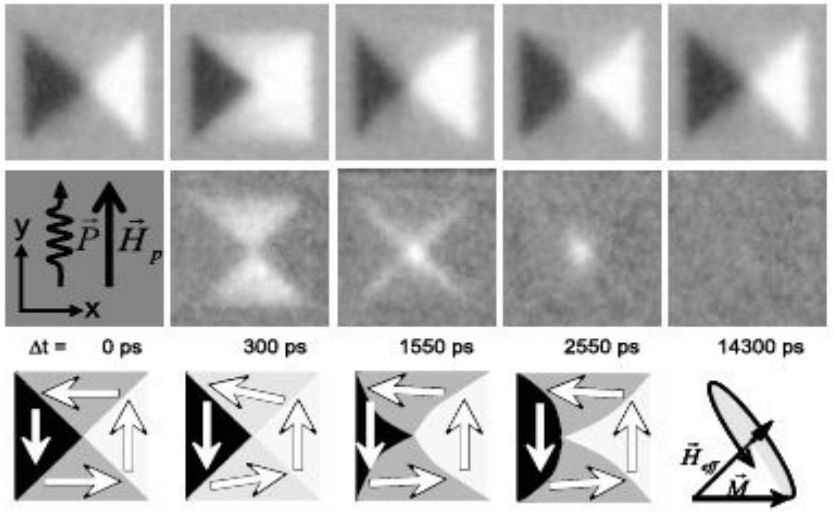

MEASUREMENT OF:

- Vortex displacement (max 750 nm)
- Domain wall displacement and buldging
- Vortex velocity (~ 700 m/s)
- Quantitative time-dependent magnetisation
- Fourier analysis

Magnetic excitations in LFC structures

PRL 94, 217204 (2005)

Quantitative Analysis of Magnetic Excitations in Landau Flux-Closure Structures Using Synchrotron-Radiation Microscopy

J. Raabe,[1,*] C. Quitmann,[1] C. H. Back,[2] F. Nolting,[1] S. Johnson,[1] and C. Buehler[1]

The time dependent magnetization is described by the phenomenological Landau-Lifshitz-Gilbert equation

$$\frac{d}{dt}\vec{M} = -\gamma_0 \vec{M} \times \vec{H}_{\text{eff}} + \frac{\alpha}{M}\left(\vec{M} \times \frac{d}{dt}\vec{M}\right).$$

The first term describes the precession of the magnetization $\vec{M}$ about the total effective field $\vec{H}_{\text{eff}}$. The second term describes the relaxation back into the equilibrium state using the dimensionless damping parameter α.

torque $\vec{T} = -\gamma_0 \vec{M} \times \vec{H}_{\text{eff}}$

xmcd

t_i-t_0

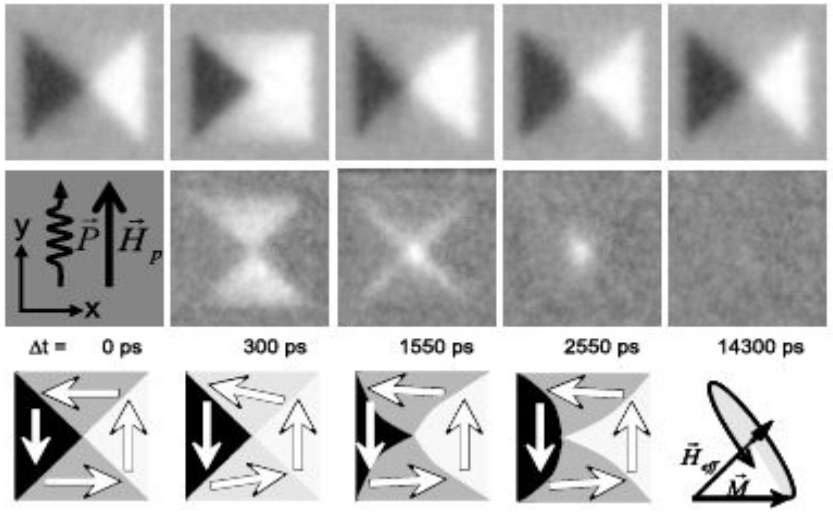

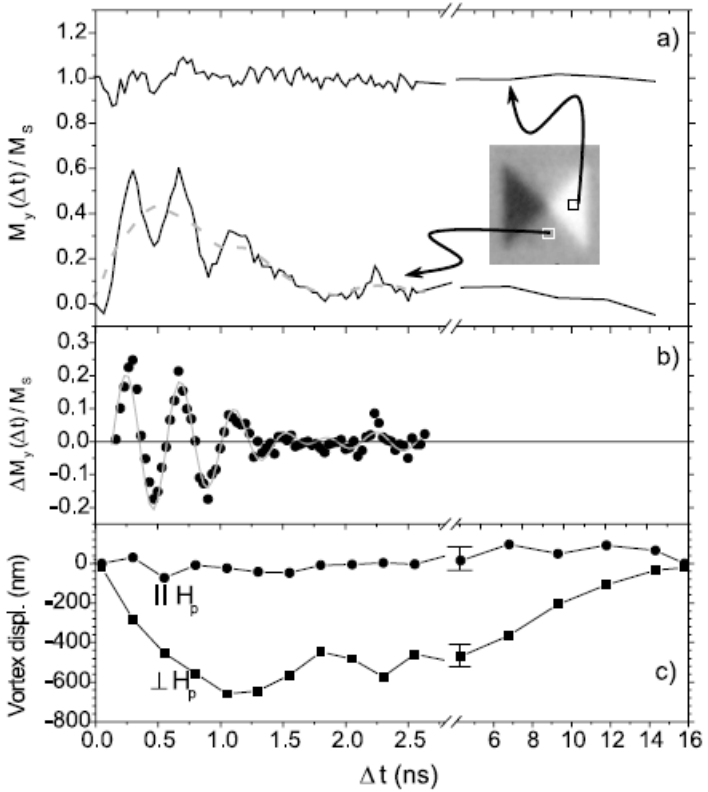

Time resolved XMCD PEEM: summary

- XMCDPEEM gives valuable information on many microscopic aspects of magnetism

- Magnetisation reversal
- Study of precessional regime

- Limitations:

  1. Only the surface-near region can be probed

  2. Only reversible processes can be studied by pump – probe experiments

  3. Spatial and time resolution are still limited

References on time resolved XMCD-PEEM

- [5.1] Choe S-B, Acermann Y, Scholl A, Bauer A, Doran A, Stöhr J and Padmore H A 2004 *Science* **304** 420
- [5.2] Schneider C M, Kuksov A, Krasyuk A, Oelsner A, Neeb D, Nepijko S A, Schönhense G, Mönch I, Kaltofen R, Morais J, de Nadaï C and Brookes N B 2004 *Appl. Phys.Lett.* **85** 2562
- [5.3] Schneider C M, Krasyuk A, Nepijko S A, Oelsner A and Schönhense G 2006 *J. Magn. Magn. Mater.* **304** 6
- [5.4] Krasyuk A, Wegelin F, Nepijko S A, Elmers H J and Schönhense G 2005 *Phys. Rev. Lett.* **95** 207201,
- [5.5] Raabe J, Quitmann C, Back C H, Nolting F, Johnson S, and Buehler C, 2005 *Phys. Rev. Lett.* **94** 217204.
- [5.6] Buess M, Raabe J, Perzlmaier K, Back C H and Quitmann C 2006 *Phys. Rev. B* **74** 100404
- [5.7] Kuch W, Vogel J, Camarero J, Fukumoto K, Pennec Y, Pizzini S, Bonfim M and Kirschner J 2004 *Appl. Phys. Lett.* **85** 440
- [5.8] Vogel J, Kuch W, Hertel R, Camarero J, Fukumoto K, Romanens F, Pizzini S, Bonfim M, Petroff F, Fontaine A and Kirschner J 2005 *Phys. Rev. B* **72** 220402
- [5.9] Fukumoto K, Kuch W, Vogel J, Romanens F, Pizzini S, Camarero J, Bonfim M and Kirschner J 2006 *Phys. Rev. Lett.* **96** 097204
- [5.10] Pennec Y, Camarero J, Toussaint J C, Pizzini S, Bonfim M, Petroff F, Kuch W, Offi F, Fukumoto K, Nguyen Van Dau F and Vogel J 2004 *Phys. Rev. B* **69** 180402

Conclusions

Spectromicroscopy with the XPEEM microscope

- XPEEM
  - » Chemical maps
  - » Chemical state (core level shifts)
  - » High versatility
  - » Limitation: size (< 40 nm) and flux: aberration corrected?
- LEEM, micro-LEED
  - » Structure
  - » Study of dynamic processes
- XMCD and XMLD PEEM
  - » Magnetic state in nanostructures and thin films
  - » Element sensitivity
  - » Thin films and buried interfaces
  - » High lateral and time resolution